INFORMATION TO USERS

This manuscript has been reproduced from the microfilm master. UMI films the text directly from the original or copy submitted. Thus, some thesis and dissertation copies are in typewriter face, while others may be from any type of computer printer.

The quality of this reproduction is dependent upon the quality of the copy submitted. Broken or indistinct print, colored or poor quality illustrations and photographs, print bleedthrough, substandard margins, and improper alignment can adversely affect reproduction.

In the unlikely event that the author did not send UMI a complete manuscript and there are missing pages, these will be noted. Also, if unauthorized copyright material had to be removed, a note will indicate the deletion.

Oversize materials (e.g., maps, drawings, charts) are reproduced by sectioning the original, beginning at the upper left-hand corner and continuing from left to right in equal sections with small overlaps. Each original is also photographed in one exposure and is included in reduced form at the back of the book.

Photographs included in the original manuscript have been reproduced xerographically in this copy. Higher quality 6" x 9" black and white photographic prints are available for any photographs or illustrations appearing in this copy for an additional charge. Contact UMI directly to order.

UMI

A Bell & Howell Information Company
300 North Zeeb Road, Ann Arbor MI 48106-1346 USA
313/761-4700 800/521-0600

PERFORMANCE OF MULTILEVEL CODES IN CONTEXT WITH CARRIERLESS AMPLITUDE AND PHASE MODULATION (CAP) IN A HIGH-BIT RATE DISTRIBUTION ENVIRONMENT

by

RAJESH FAGERIA

A dissertation submitted to the Graduate Faculty in Computer Science in partial fulfillment of the requirements for the degree of Doctor of Philosophy, The City University of New York.

1997

This manuscript has been read and accepted for the Graduate Faculty in Computer Science in satisfaction of the dissertation requirement for the degree of Doctor of Philosophy.

Jan 29, 1997
Date

Chair of Examining Committee

Jan 30, 1997
Date

Executive Officer

Professor Michael E. Kress

Professor Charles Giardina

Dr. Victor B. Lawrence

Supervisory Committee

THE CITY UNIVERSITY OF NEW YORK

Abstract

PERFORMANCE OF MULTILEVEL CODES IN CONTEXT WITH CARRIERLESS AMPLITUDE AND PHASE MODULATION (CAP) IN A HIGH-BIT RATE DISTRIBUTION ENVIRONMENT

by

RAJESH FAGERIA

Advisor: Professor Syed Ahamed

The systematic replacement of bandwidth inefficient codes (AMI, Manchester, HDBk, etc.) with more efficient codes is a fact to be noticed, since the introduction of new services (video on demand, telecommuting, teleconferencing, internet services, multimedia, etc.) requires such a need. As fiber is replacing the copper layer (distribution plant) with transmission rates ranging from 51.84 Mbits/s to 4.98 Gbits/s, the last connection to made (customer premises) is still a complicated and not viable option. Only codes with truly bandwidth efficient capabilities will be able to handle the integration of optical and cable capacities.

Shannon formula attests that if a strong S/N can be maintained than increased transmission capacities can be achieved for limited bandwidth. To achieve this goal, the present research introduces an efficient coding mechanism that look upon the characteristics of multilevel encoding (M levels) of symbols in one or two dimensions using efficient spectral shaping.

Premises distribution system (PDS) is studied, and analysis is done with existing code structures, with particular emphasis given onto multilevel (ML) and carrierless amplitude and phase (CAP) types of coding structures. As the work evolved into maturity, new loop configuration were made available with parameters assessed.

Contributions of this work are oriented toward the objective to allow the integration and transmission of information scattered over the network with efficient line codes that will provide high bit rate for a given bandwidth or alternatively, for a fixed bit rate reduce the bandwidth required. A final step toward completion of task, it kept in mind the goals and boundaries of a micro-model, while instigating itself into a unique synthesis of analysis, experience and perspective for the fields of networking, information processing and telecommunications.

Acknowledgment

To Mom and Dad for giving me moral support and to Anjeet, Savita and Neera, for giving support I needed to continue to the end.

To my advisor and mentor Professor Syed V. Ahamed for his continuous guidance and encouragement throughout the course of this work.

To Ann, Mary, Prof. Charles Giardina and Prof. Mike Kress at College of Staten Island /CUNY for providing both support and facilities.

To Dr. Victor Lawrence at Bell Laboratories for providing both support and facilities.

To all of you, thanks.

Table of Contents

Tables

Table of Figures

"As a net is made up of a series of ties, so everything in this world is connected by a series of ties. If anyone thinks that the mesh of a net is an independent, isolated thing, he is mistaken. It is called a net because it is made up of a series of interconnected meshes, and each mesh has its place and responsibility in relation to the other meshes."

- Gautama Buddha/563-483 B.C.

CHAPTER 1

1. Introduction

What is it that can be so pervasive and yet so mysterious? Information, of course. Influence of noisy channels has defined it as something quantifiable that could be collected, moved, and processed. But as the intellectual culture progresses, the word has become equivocal, pseudoscientific, hard to grasp "scythe of time."

Driving the changes is the computer's ability to reduce all conventional information forms into one big digital body of one's and zero's, called bits. These bits can be engineered to represent complex expression of text, video,

images, and voice into cross-linked and meaningful objects, all of it cross-indexed and able to respond instantly to society's desires.

As the computer model has moved from central processor (mainframe), which used to calculate, store and send data, to a distributed system, information has gained new powers with the advent of this new architecture. It can be accessed and processed more easily as it becomes localized and specific to the domain.

The network has merged into a collective identity and it has assumed the self-containment of the computer. As channel capacity and diversity of the net increases with fiber optics, schemes for compressing more data into copper lines, wireless transmission, satellites and information highways, amazing amount of data is now at our disposal. New techniques are emerging for managing this flood of information. "Ubiquitous systems" are now in place. Their resources are unlimited and gains from them will derive a better understanding of subject matters as well the whole part of information, which is knowledge.

To access domains of knowledge a path is taken, which can be misleading to the signal sent and received, if it is a raw signal. For this purpose the signal is transformed into an entity, which is self complementary and coded such

that as it traverses through the path it becomes immune to the imbalance imposed by the path.

As the transmitter transmits the signal, the channel introduces impairments that will corrupt the signal. Control over information being transmitted is gained only if a suitable coding mechanism is applied. Several line codes are analyzed; among them, alternate mark inversion (AMI), Manchester, high density bipolar (HDBn), mBnT, two binary one quaternary (2B1Q), class IV partial response (PR-4) , etc..

With transmitter complexity increased, coding is combined with modulation, and some joint coding and modulation schemes are presented. They include multilevel pulse amplitude modulation (m-PAM), quadrature amplitude modulation (QAM) and carrierless amplitude and phase modulation (CAP).

CHAPTER 2

2. Digital Transmission System

The existing telephone network basically comprises of source and destination (S/D) which can be a user or a machine, local exchange (LE) and trunk exchange (TE). The user and local exchange are usually connected by a 2-wire facility and then the local exchange is connected to trunk exchange through a 4-wire facility. Fiber has been introduced at the last stage, but this is only true where the network has matured.

As signals arrive from several users, the local exchange convert them into digital format through Pulse Code Modulation (PCM), Adaptive Differential Pulse Code Modulation (ADPCM), Delta Modulation, Adaptive Differential Delta Modulation and other analog to digital (A/D) modulation techniques.

Now several signals are combined in the local exchange through time division multiplexing (TDM), statistical time division multiplexing (STDM), wavelength division multiplexing (WDM) and other multiplexing schemes and sent to the trunk exchange. At this point the reverse process takes place,

as signals arrive at the opposite local exchange they are demultiplexed and demodulated into their original format.

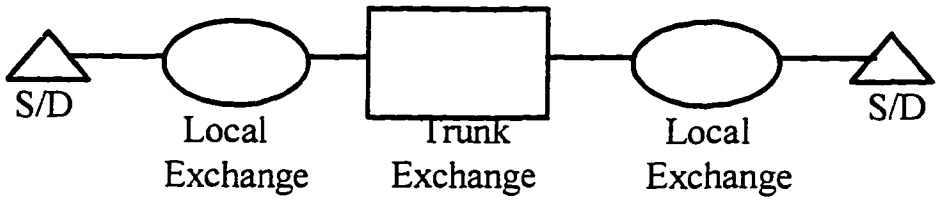

Figure 2.1 Basic Communication System.

2.1. Communication Hierarchies

In telephone circuits each voice channel has a frequency range of 0 to 4 KHz. To make sure that no information is lost and the original signal can be exactly reconstructed, it is sampled at twice the Nyquist frequency. Each channel therefore, is sampled at a rate of 8000 samples/s (8 KHz) and encoded with 8 bits/sample.

Hence, the transmission rate per channel becomes:

$$8000 \text{ Samples/s} \times 8 \text{ Bits/Sample} = 64 \text{ Kb/s}$$

In the time division multiplexing and pulse code modulation (TDM-PCM) hierarchy of 30 or 24 channels additional information is added, which constitute framing and signaling. For the European or CCITT recommendation of 30 channel PCM system the frame constitute of 30 TDM channels plus a channel for signaling and another for framing (synchronization) and maintenance, with each channel using an 8-bit time slot. Therefore the total capacity is:

$$(30 + 2) \times 64 \text{ Kb/s} = 2.048 \text{ Mb/s}$$

This is the basic rate for the European digital hierarchy (EDH) system, which is carried out as E-1 rate. Further, when data signals carries four multiplexed E-1 signals it is known as E-2 rate. As it expands into higher order of multiplexing the rates known are E-3, E-4 and E-5, where for E-5 the effective data rate is 565.148 Mb/s. More details of this hierarchy are given in figure 2.2.

For the US and Canadian T1 PCM system the frame constitute of 24 channels plus 1 frame synchronization bit. The channel subsequently is encoded with 8 bits/sample.

Hence, the total capacity is:

Frame = encoding and signaling bits per sample x number of channels + frame synchronization bit

= 8 bits/sample x 24 channels + 1 bit

= 193 bits

Capacity = sampling rate x frame length

= 8000 samples/s x 193 bits

= 1.544 Mb/s

The capacity of 1.544 Mb/s represents one digital service level 1 or DS1 channel of the TDM hierarchy (figure 2.2). Even though there are 193 bits/frame for both voice channel and data channel the bits in the framing format has different configuration. For voice channels, 8-bit PCM samples are used on five of six frames and on every sixth frame each channel contain 7-bit PCM samples with the eighth bit used as signaling bit.

The data channel frame has 23 channel positions for data and the twenty-fourth channel position is reserved as a synchronization byte which allow a

faster reframing if a frame error occurs. Within each data channel byte, every sample is encoded as 7 bits/sample and the eighth bit is added as a control bit to further verify if the channel for that frame has user data or transmission control data. When only 7 bits/sample are considered the trans-mission capacity of the channel becomes 56Kb/s, since each frame is repeated 8000 times per second (8000 samples/s x 7 bits/sample).

Lower data rate are also provided by using a scheme called subrate multiplexing where only 6 bits/sample are used and therefore a total capacity of 48 Kb/s (6 bits/sample x 8000 samples/s) is achieved. This rate can accomodate multiplexed channels of 2.4 Kb/s, 4.8 Kb/s and 9.6 Kb/s.

The DS1 format can also be used for transmission of voice and data at the same time. In this case, all the 24 channels are utilized and no synchronization byte is provided.

When two of the DS1 channels are put together they form a DS1C channel. The signal for DS1C channel is carried out on a T1C line. It has a capacity to transmit data rate at 3.152 Mb/s. As the hierarchy goes higher four of the DS1 channels are multiplexed to form a DS2 channel, which is equivalent to a total capacity of 6.312 Mb/s. Still higher, as it continues, when seven DS2 channels are grouped together they form one DS3 channel, with data rate of

44.736 Mb/s. At last when six DS3 channels are multiplexed together they make one DS4 channel with total transmission capacity of 274.176 Mb/s.

The transmission facility carrying the four hierarchical levels DS1, DS2, DS3 and DS4 are called T1, T2, T3 and T4 lines.

2.2. Elements of Encoding and Decoding Systems

Digitization of analog waveform is relevant to time discretization (sampling), amplitude discretization (quantizing) and encoding of these discretization levels. As parameters of analysis, time discretization and amplitude discretization are information-preserving and information-lossy respectively by definition [13].

As the process of digital representation of analog waveforms takes place, it introduces some coding distortions, e.g., aliasing, quantization error, etc.. The objective of an encoder is to achieve zero distortion level or up to an acceptable level with minimum encoding rate.

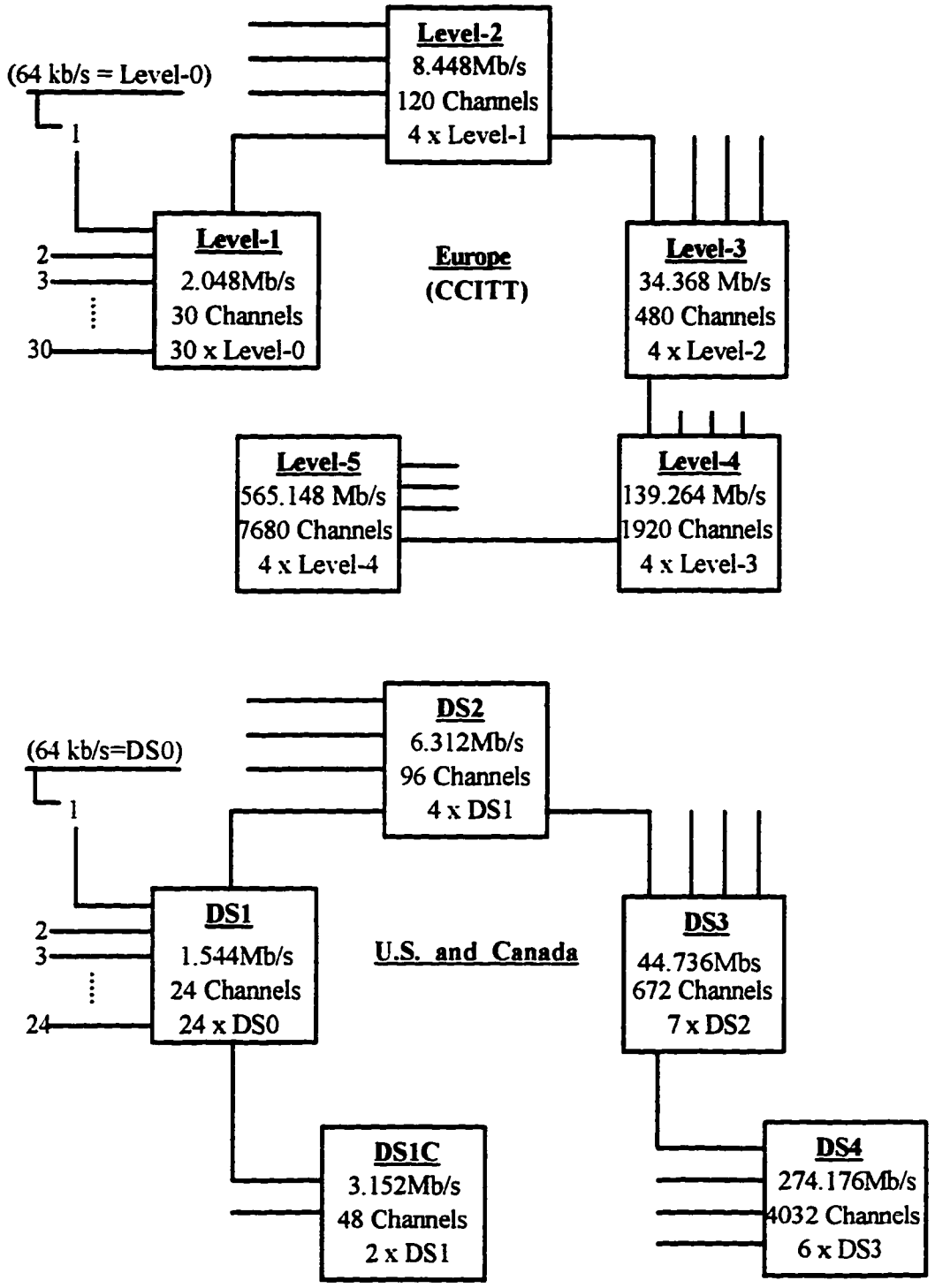

Figure 2.2 TDM hierarchies.

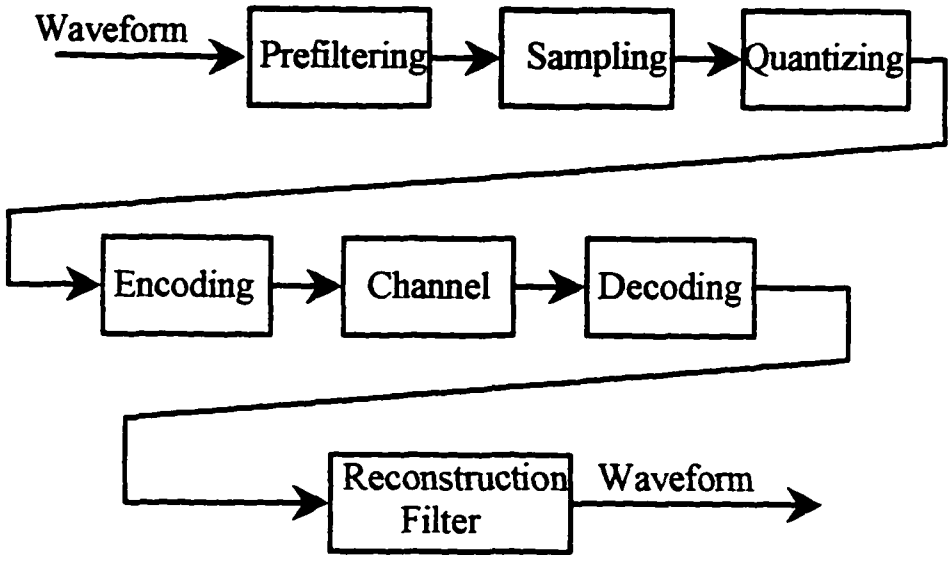

Figure 2.3 End-to-end digital conversion.

The intricacy of encoder has prompted a division of the device into several stages, where each stage has a different set of functions associated to it (figure 2.4).

In source coding, the objective is to eliminate or reduce, redundancy and irrelevency as to provide an efficient representation of the source output. The outcome of source coding is condensed information, increased throughput and reduced transmission bandwidth, which translates in fitting more

information into a slice of spectrum. Also for security purposes, the bit stream is encrypted at this stage.

Information at the output of the source encoder has a very high point of randomness [1], since a reduction of redundancy had occurred. All of this translates into higher entropy level, or more information per message. Sources usually have a direct relationship with entropy level and a maximum representation of information by a source is only feasible if a high measure of entropy is affiliated to it.

The role of channel coding is to add controlled redundancy into the bit stream such that the noise parameter can be identified and minimized at the opposite end of the channel encoder, at the channel decoder. As a result, basic functionality of channel encoder is to provide error control and error detection. Retransmitting the signal if an error has occurred, which is generally detected at the channel decoder.

The line coder now maps the incoming signal from the channel encoder, which is in digital format, into another suitable form also of digital nature. The mapping is one-to-one [14], and can be done as bit to symbol mapping or binary block to symbol mapping.

---

[1] Randomization of information is usually done with a scrambler.

Also the line coder determines what kind of code is suitable for the physical medium used by the channel. This stage has the important task of pulse shaping the binary signal into a line signal with frequency spectrum appropriate for transmission over the channel. It also provides bit synchronization that support in recuperating the signal by the receiving clock.

The modulator takes input from the encoder and translates them into analog signal, since an analog physical medium is being used for transmission. It operates by mapping shifts in amplitude, frequency, or phase of a carrier wave from the output of the encoder. The most common mapping mechanism used by analog to digital conversion are amplitude-shift-keying (ASK), frequency-shift-keying (FSK), phase-shift-keying (PSK) and quadrature amplitude modulation (QAM).

After transmission through the channel, which may include one or more repeaters the demodulator receives the signal and according to the an appropriate decision threshold, translates the received analog waveform back to binary digits. Several functions are performed by the demodulator, most of them are regenerative functions and include, amplifying, equalizing, timing recovery, etc.. The digital signal is handled from this point on by the de-

coder, which will work in reverse functionality of the encoder to get back the original signal transmitted.

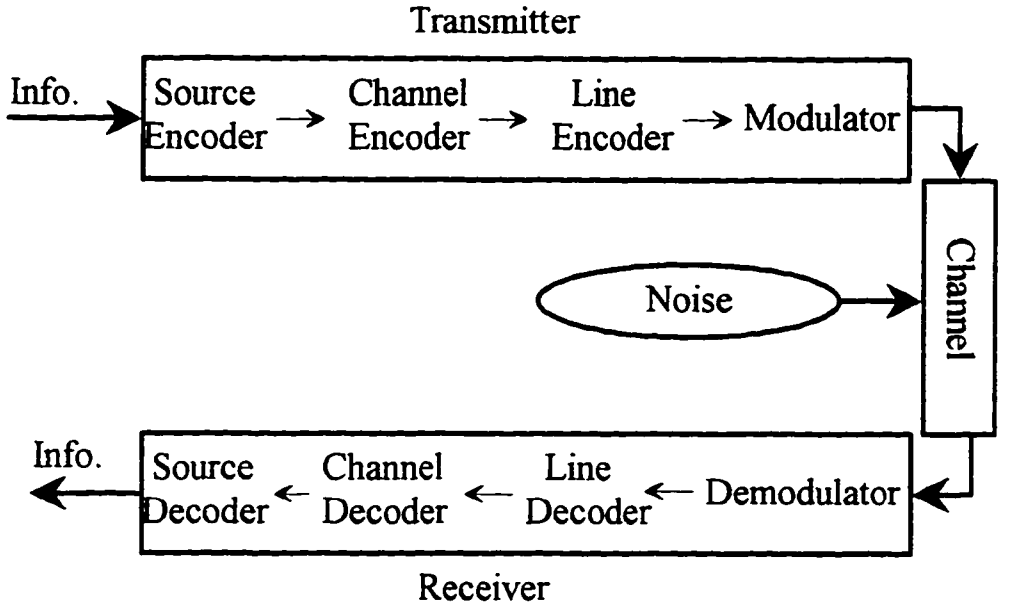

Figure 2.4. Digital communication system with encoding and decoding elements.

CHAPTER 3

3. Coding Fundamentals

As binary data signal is transmitted over a noisy channel, with significant bit error rate (BER), a suitable coding mechanism can be used to significantly reduce the error rate that is assimilated by the signal.

Two broad classes of channel coding techniques named block codes and convolutional codes can address the problem with significant precision. In block coding, the signal containing binary data is partitioned into blocks of p bits, where p is the size of the block. Each such block is then mapped into a group of n bits code word by an encoder (usually n is bigger than p), which is then transmitted in a signal format. For example, an encoder can be constructed by the pair (n, p) = (5, 3), meaning that information from the source is taken 3 blocks at a time and stored, then shifted five times (n=5), or also signifying that code words of five bits are formed. The last added bits are usually for parity check and are structured by taking the modulo-2 sum (exclusive-or gates) of certain blocks.

Hence, every n bits code word transmitted over the channel contains a block of p bits, and therefore the bit rate per code word or symbol is:

$$B_r = p/n \quad \text{bits per code symbol}$$

A common noisy channel modeling can be done through the Gaussian channel model, where each bit is viewed as a square pulse of certain amplitude and prune to additive noise. The noise factor in the signal is considered uniform across the whole range of frequencies.

As a result of noise, the channel introduce errors in the data stream and the received n-bits block can be any of 2^n possible code words. Subsequently there are 2^p different inputs that can be transmitted (each block of p bits carry one code word), and since 2^p is smaller than 2^n, the number of possible received code words 2^n is much larger than the number of inputs 2^p. On the arrival of the signal at the receiver, the decoder makes decision on what was the most likely code word that was transmitted, and from there the p-bit block is identified. This is one possible method for error detection and correction.

Another method for detecting and correcting errors is given by Hamming distance. The distance is the minimum number of digits that differ in two

encoded words. To detect ε digits in error the code's Hamming distance (d) should have the property of $d \geq \varepsilon + 1$. As for error correction, to correct e digits in error the code should have $d \geq 2\varepsilon + 1$ (i.e., a code with $d = 3$ can detect 2 digits in error and correct 1 error).

The other coding scheme is convolutional coding. As bits arrive they are fed into a K-stage shift register and shifted by q bits at a time. Every block of K bits stored in the register is mapped by the encoder into block of n bits code word, using modulo-2 sum operation. Hence, with each shift of the register q bits are inserted and n bits code words are transmitted. For example, in a 7 stage shift register, data can be shifted one bit at a time and using four modulo-2 adders the encoder can be described as having the following properties: $K = 7$, $q = 1$ and $n = 4$.

In figure 3.1, information bits are inserted through the bottom and as they enter the register they are shifted upward one or more bits at a time (i.e., if one shift then $q = 1$). In the process of being shifted the first bit is utilized by the modulo-2 adders and after it arrives to the top of the register it is discarded. The output of the adders is dependent on any of the K storage modules, therefore K is defined as the constraint length of the encoder. It should be noted also that a particular block of bits remains in the register for K/q shifts, and thus influence the values of nK/q code words.

The bit rate for q bits shifted into the register at a time is,

$$B_r = q/n \quad \text{bits per code word}$$

This can be better visualized when q = 1, where 1 bit is shifted into the register at a time and the code word carries an average of 1/n bits, and consequently $B_r = 1/n$.

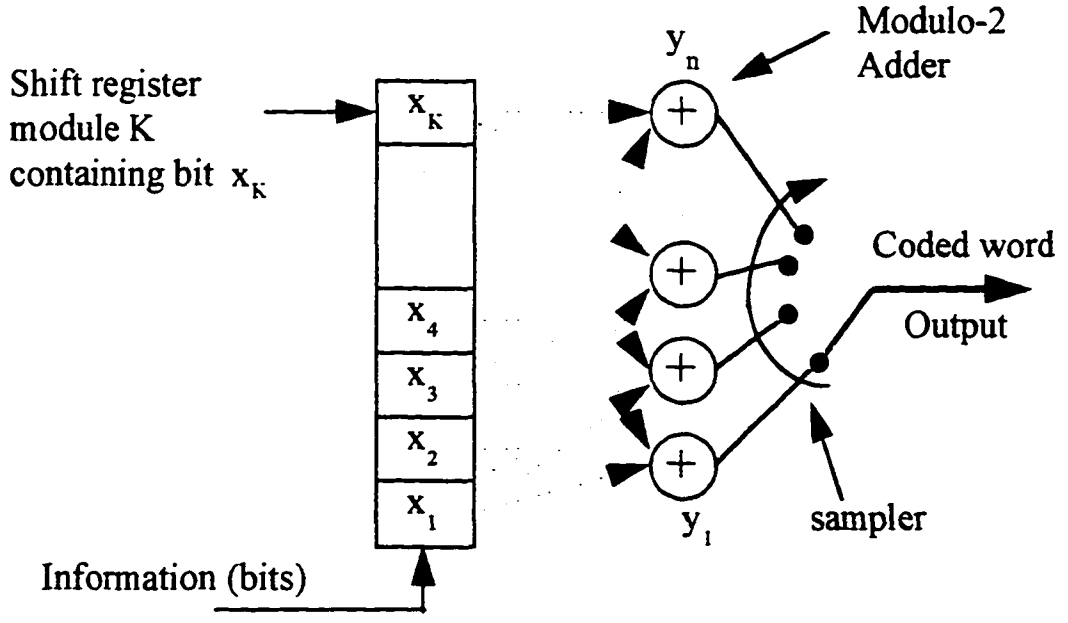

Figure 3.1 Convolution encoder.

An example for the convolutional encoder is the 1/2 rate encoder given in figure 3.2 . The encoder output is a sequence of 2 bits for every bit that it receives from the input. Initially the register has zeroes as storage contents and after the last input bit arrives a stream of zeroes is used again to dislodge the last data bits entered.

An instance of the example given is when the input of 1110 is inserted from the bottom of the register; as the first bit arrives into slot one of the register the output of y_1 is one and the output of y_2 is one. Subsequent in the sequence, the second bit comes in and the first bit is shifted up one slot; the output of y_1 is still one but the output of y_2 becomes zero, since modulo-2 addition of 1 and 1 is 0.

When the whole input is exhausted, the final output sequence is:

Output -> 11 10 11 00 01 00 00

Input -> 1 1 1 0 0 0 0

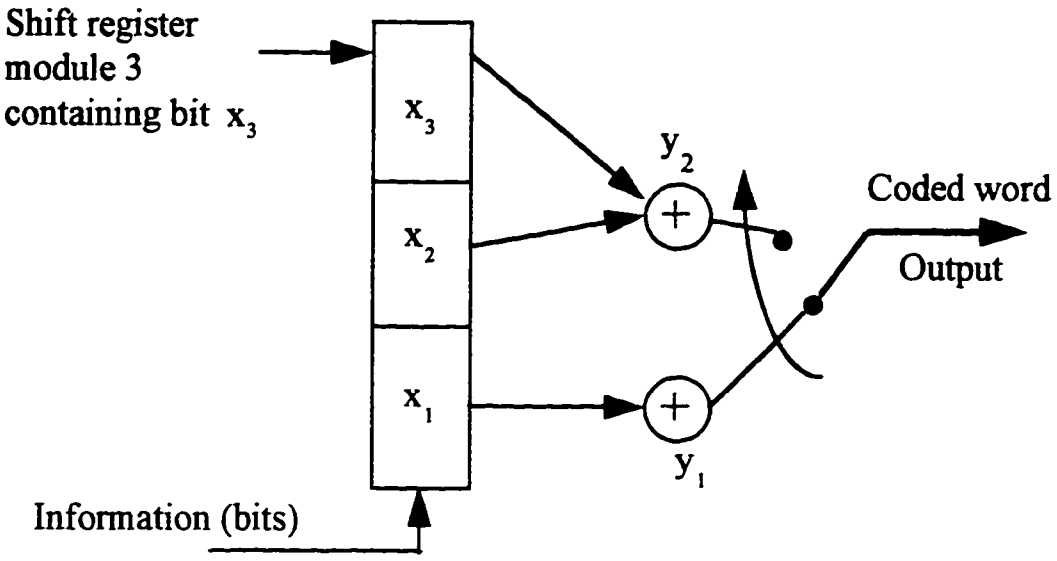

Figure 3.2 Half rate convolution encoder with K = 3, q = 1.

Unlike for block codes, in convolutional codes, past information bits exert an influence on the code word used to represent a present information data. Therefore, the output consist of the contents of shift register storage slots with a combination of some input information data (i.e., the shift register can be represented by a code generating polynomial).

The encoder of figure 3.2 can also be represented through a tree diagram, trellis diagram or a state diagram. In a tree diagram (figure 3.3) the first incoming bit from the input determines whether to follow the upper path or

the lower path. In the example of figure 3.2, the first bit of the sequence is one, hence the lower path is taken and the output given is 11. Subsequently, the second input is 1 and therefore the lower path is taken again and the output is given as 10. Similarly, other inputs and outputs are represented through a dotted line in the graph of figure 3.3. The line thereupon portray the encoder computation for that specific sequence of input.

Some of the characteristics seen in the tree are that, at every dividing point the two paths yield complimentary outputs; after three levels of splitting the top half of the tree is identical to the bottom half (K = 3). And for last, the encoder of bit rate q/n and constraint length K has 2^q branches fanning out from each node of the tree (e.g., q = 1, two branches comes out of each node).

In a tree diagram, as each node spawn new branches it becomes a burden to structure the tree for long input sequences. A better method is the trellis diagram (figure 3.4). The trellis take advantage of the repetitiveness encountered in the tree diagram by using a finite number of states, which are determined by the constraint limit K.

Decoding for block codes and convolutional codes is quite different. For block codes the algebraic structure of the constraints among the code words is very

useful in the decoding process. Examples of good block codes with defined decoding algorithms are the Bose-Chaudhuri-Hocquenghem (BCH) codes given in [29] and [30].

Variant from block coding, the optimal decoding procedure for convolutional codes requires a memory that can store the whole sequence of received information. The performance aspect of a convolutional code improves as the complexity allowed for the decoder is increased. Examples of such complexity include memory allocation and the capacity of the decoder to backtrack a sequence when it finds itself at a wrong path in the tree. For the last example the decoder has the capacity to change the decoded information until the correct sequence is found (sequential decoding).

several methods of decoding convolutional codes have been developed, including by means of probabilistic techniques such as the sequential decoding algorithm by Wozencraft and the maximum likelihood technique by Viterbi known as the Viterbi algorithm [29][30]. Viterbi decoding for fairly smaller constraint lengths is attainable and fast decoding can be achieved in a reasonable time complexity. For a large constraint length K, the probability error is significantly reduced (BER better than 10^{-9}), but the computational complexity start taking its toll as K is increased.

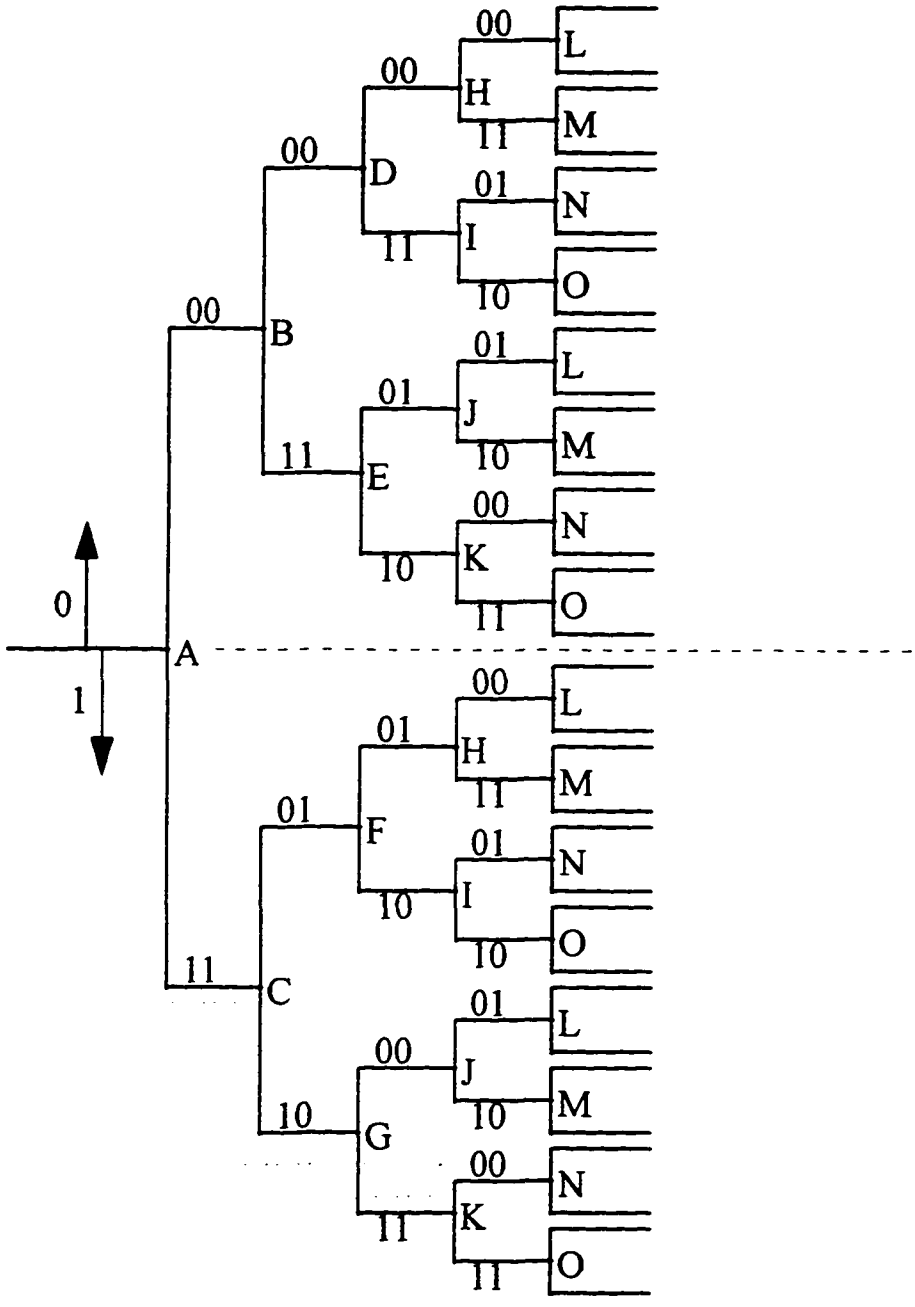

Figure 3.3 Tree representation of the half rate convolution encoder.

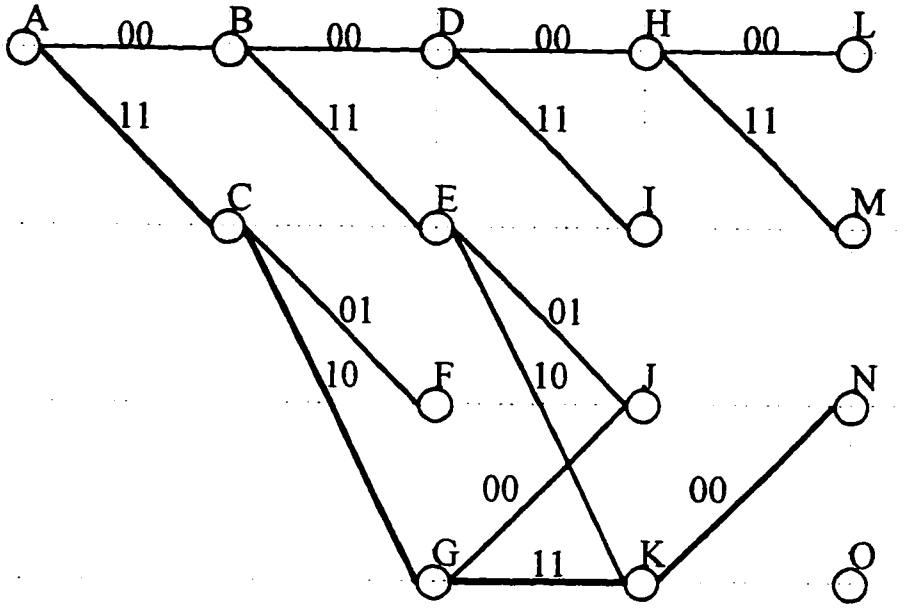

Figure 3.4 Trellis representation of the half rate convolution encoder.

Until now a limited study of codes has been tackled, which involved the addition of redundancy to the code directly in the digital sequence. Now codes will be explored with intricacies involving real-time operation of the decoder. Henceforth, codes will be looked at the channel level taking into considerations impairments, where signal distortion and interferences are the major sources of degradation, besides the additive noise factor. In relevance to the topic, spectral properties of the codes will be considered, with the objective of shaping the spectrum of the transmitted signal. The codes that will be analyzed are called line codes.

3.1. Limitations of Conventional Coding Techniques

The simplest representation of binary information is through presence of a specific voltage for logic one and absence of voltage for logic zero. This is the purest form of digital representation. It is satisfactory for limited purposes, but when transmission of logical data through a medium is considered, there is a need to enhance and formulate the pure binary stream into a representation that will suit the specific needs of the channel.

3.2. Line Code Selection

The channel needs are fulfilled and enhanced by choosing a specific line code for transmission. In selecting the code, the nature of line repeaters and signal regenerators should be taken in consideration, such that a minimum bit error rate is achieved at the receiver.

Desirable line codes characteristics are outlined with one or more of the following considerations:

(1) Need to avoid direct current (DC) or zero frequency component in the transmitted signal spectrum. An answer to the problem can be found in achieving zero mean voltage by balancing the code.

(2) Ease of synchronization. The solution is to maintain a frequency component at the clock rate, such that the clock can maintain pace with the signal being transmitted. To maintain such rate of synchronization, there should be an avoidance of long string of code with same signs.

(3) Ideal code is one that can have infinitesimal bandwidth and infinite transmission rate, that is, a code that can have embedded compression

and has very small alphabet of symbols. Each symbol would be characterized by a level of voltage or a sign.

(4) Provide automatic error detection and some sort of error correction. As a condition, this is not as necessary as the others that are referred above, since error detection and correction are already part of channel encoder. But, if a possibility arises in embedding such characteristics into the code, the encoder and decoder circuits complexity will be reduced.

3.3. Line Codes

When a signal is transmitted over a communications channel, it is distorted to some degree and signal loss occurs throughout the medium of transmission. The received signal, therefore, differs from the original transmitted signal in considerable amount. Signal recovery is done by usage of robust coding, equalization techniques and other signal recovering means.

Digital technology compared to analog, is immune to some of the losses that affect the analog domain. The signal at any instant represents a number in signal level format rather than an analog waveform. It is unambiguous when only two levels (binary 1 and 0) of distinction are present.

Figure 3.5 Digital transmitter and receiver with two binary levels.

A signal produced by a node consist of a stream of pulses that represent information coded into binary form. There are two different types of digital signals They are either, Baseband or Bandpass signals.

A Baseband signal has signal power distribution around direct current (DC). While, a Bandpass signal has signal power distribution around frequency range far from DC. Baseband signals can be: Unipolar, Polar and Bipolar signals.

3.3.1. Unipolar, Polar and Bipolar Codes

Unipolar signal is the simplest of all three. The presence of voltage represents logic one and the absence represents a logic zero. Polar signal waveform differs from the unipolar in that opposite polarity of voltages,

represent the binary logic of ones and zeros. For example, +3 Volts and -3 Volts can be used to represent 1 and 0. The decision threshold in this case is zero Volt (figure 3.6).

If the waveform of the received signal is between zero and positive full amplitude at the sampling instant, it will be restored as logic 1. If it is between zero and negative full amplitude it will be restored as a logic 0.

The polar waveform signal is basically used in transmission of non-synchronous digital signals. As one of the simplest form of coding and relatively primitive in usage, it eliminates some of the residual DC problem. It has a disadvantage, that most of its signal energy contents are concentrated around zero frequency.

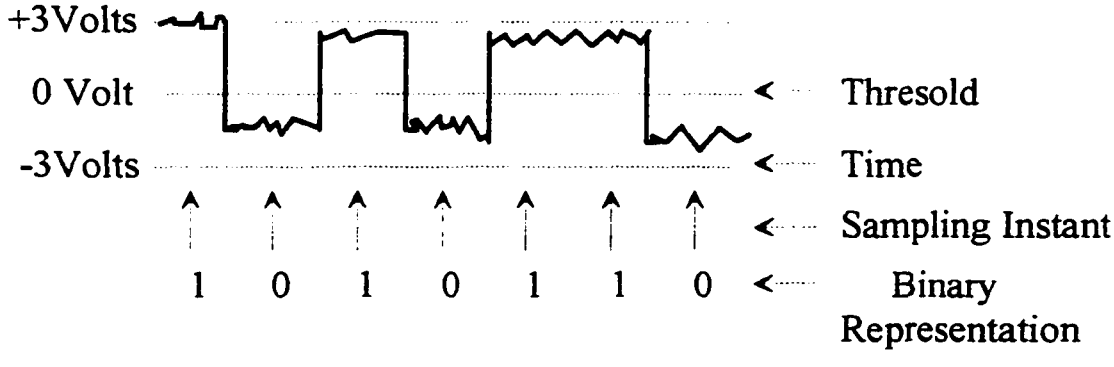

Figure 3.6 Polar Waveform.

A more advanced coding scheme is that used in T1 carrier system. This scheme, called bipolar or alternate mark inversion (AMI) signal is also called ternary line code, since it has three levels of representation (+V, 0V, -V). It has alternate polarity for voltages assigned to logical one's (figure 3.7). For transmission of successive binary one's the two opposite voltages must be alternated. This virtually eliminates the DC component and therefore eliminating the signal interference with repeaters along the route. Since, repeaters are powered with DC component.

AMI code has some inherent error detection attributes, where a single bit error can be monitored if two successive pulse of same polarity occurs. This violates the alternate-mark property of the code.

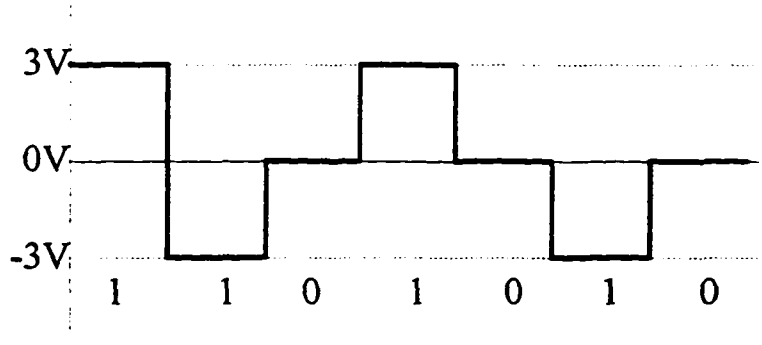

Figure 3.7 Alternate mark inversion waveform.

Unipolar and Bipolar signals can be implemented by either Return-to-Zero (RZ) or Non-Return-to-Zero (NRZ), within a time slot (figure 3.8). The time slot represents a bit. The Return-to-Zero signal returns the voltage to zero level within each time slot. This reduces the margins of sampling time variation compared to NRZ. As the receivers timing recovery circuitry is clocked by the transitions of the incoming signal, this technique improves receiver clock synchronization, since transitions from 0 to 1 and 1 to 0 have been increased.

The disadvantage of RZ is that a break in connection can be interpreted as a string of zeros and also a long string of zeros can allow the receiving clock to slip sync.

NRZ format has a waveform signal with constant amplitude or voltage in each time slot and returns to zero voltage only when there are logical zeros present. An NRZ waveform is 100 percent duty cycle pulse train, since a one is represented by a pulse that has a duration for the whole symbol interval. On the other hand a RZ waveform has duty cycle of approximately 80 percent, since the pulse train for high voltage covers only about that range.

3.3.2. Diphase Code

Another code that has received considerable acceptance is diphase code, which is also called Manchester, biphase, twinned binary or split phase code. As referred in the different names that it takes, it provides signal voltage transitions at least once for every bit representation, whether it be a one or a zero. Hence, it provides strong timing information and therefore easy clock recovery. Another advantage is that it eliminates the DC or baseline wander problem since there exist both positive and negative polarity for every bit. The Manchester coding scheme is used in the most widely accepted local area network protocol, Ethernet.

However, with all the desirable characteristics of the code, the main disadvantage of the code is that it occupies twice the bandwidth utilized by the bipolar code. An example of diphase waveform for a given bit stream is presented in figure 3.9a.

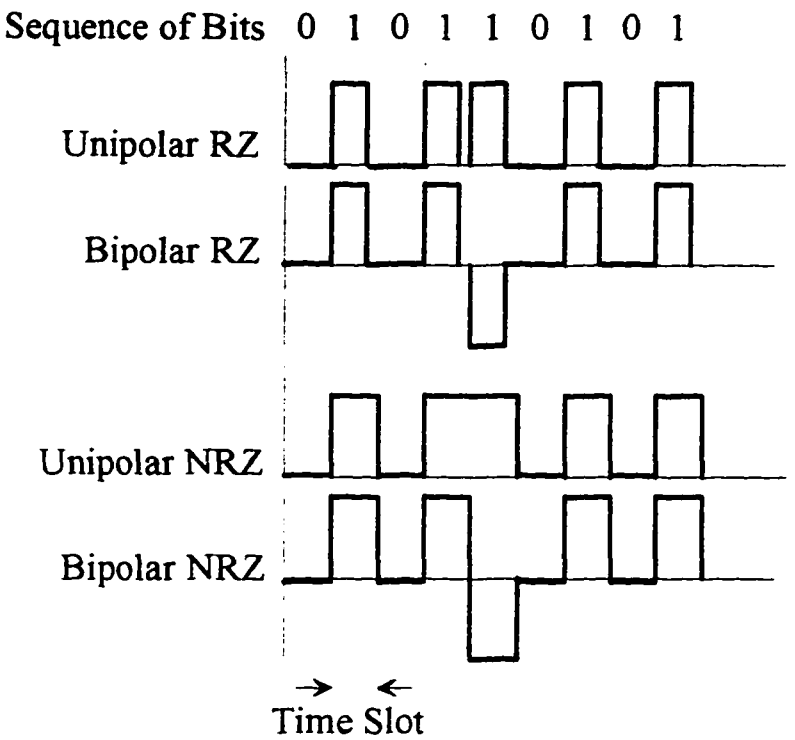

Figure 3.8 RZ and NRZ waveforms for unipolar and bipolar signals.

3.3.3. Differentially Encoded Diphase Code

This code has similar characteristics as the diphase code, differentiating itself only at the transitions. Each data bit is encoded as having transition in the center of the bit interval, while each zero is distinguished from a logic one by also being encoded with a transition at the starting edge of the bit interval (figure 3.9b).

Differential diphase and biphase code are collectively known as Manchester group of codes. Like the biphase, Differential diphase also simplifies the clock recovery process at the regenerator and requires a large bandwidth for transmission compared to the bipolar code. It is used in balanced subscriber cable pairs (local loops) at bit rates of the order of 64 kb/s [1].

3.3.4. High Density Bipolar (HDBk) Codes

These are modified version of AMI code and classified in the family of non-alphabetic block codes. Input stream containing long sequence of zeroes is encoded and blocks of maximum one, two, three and up to k zeroes are made, that is, HDB1, HDB2, HDB3 and HDBk respectively.

High density bipolar codes cover the most serious shortcoming in AMI code, which is, lack of timing information for signals with long string of zeroes. The basic concept behind high density bipolar codes is that when a sequence of more than m+1 zeroes occur, this sequence is substituted by the code words "000...0V" or "A00...0V," where "A" means a normal alternating AMI pulse, while "V" means a substitution mark pulse that violates the AMI rule.

In the first code word "000...0V", the symbol "V" violates the alternate-mark rule, since it is necessary to distinguish in the coded bit stream, input data sequences that are alike the one created by the substitution mark pulse. For example, the two sequences "000...01" and "000...0V" become the same type of signal if the "V" rule is not applied.

As the "V" rule is defined, another problem arises if the coded bit stream consist of sequences that have very long strings of zeroes and therefore the output would become ".....000..0V000..0V000..0V.....". The result would be that the coded bit stream would contain low frequency energy (many zero levels in the sequence) down to zero frequency. The solution is to use both code words and choose the one with objective of keeping number of " A's " between consecutive " V's " odd [12].

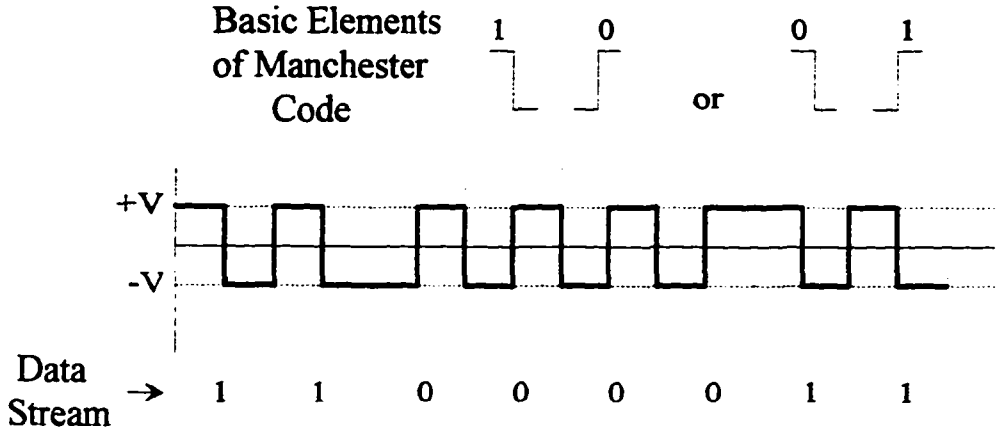

a. Diphase

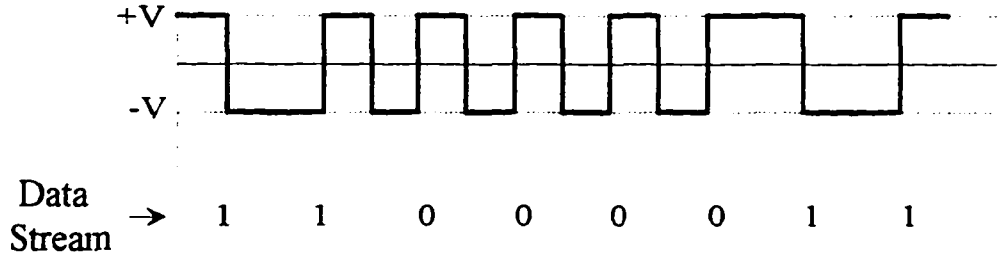

b. Differentially Encoded Diphase

Figure 3.9 Examples of Manchester group codes.

Another way to solve the same problem of small spectrum for low frequency energy is much like the first solution, the code word "A00...0V" should be used when an even number of ones occurs since the last special sequence, otherwise "000...0V" should be used.

A performance breaking code in the HDBk family of codes is the HDB3 (High Density Bipolar with a maximum of three zeroes) code. It has a better power density spectrum and also can handle more appropriately the synchronization problem of the data receiving clock in comparison to the bipolar code. Also, this code is constantly specified for use at the primary multiplex output and higher order multiplexers up to the 34 Mbit/s multiplexer output [1]. An example of HDB3 waveform for a given bit stream is presented in figure 3.10 .

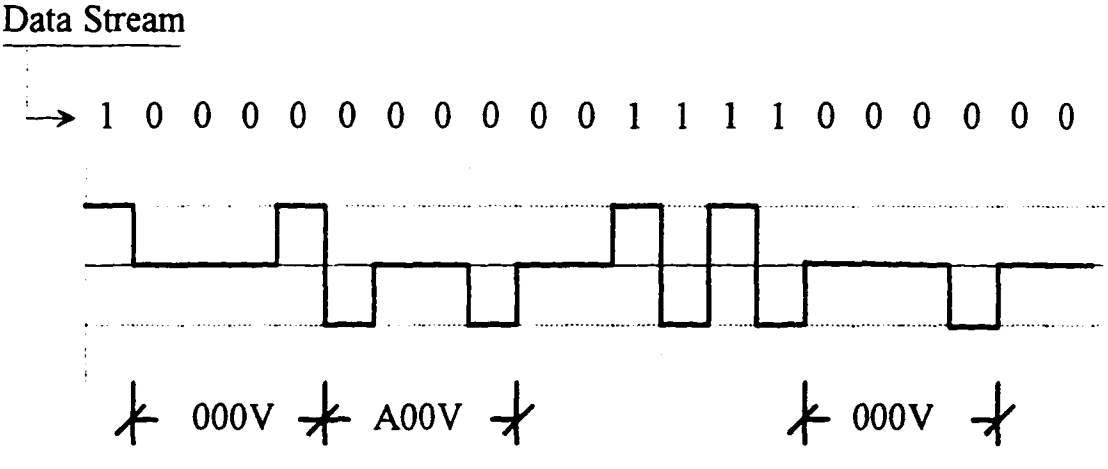

Figure 3.10 HDB3 code waveform for an arbitrary data sequence containing large sequences of zeroes.

3.3.5. mBnT Codes

As the need arises to make more efficient use of the bandwidth available, the pseudoternary (two binary digits are mapped into three levels of code) codes give a relatively meager performance. The transmission capability of these codes is on average 1 bit/symbol, which is far less than the real capacity or upper bound of 1.6 bit/symbol that can be offered, since they have three levels of transmission.

A new class of codes called alphabetic codes is introduced. These codes reduce the redundancy, present in the AMI class type codes and map blocks of binary data bits into blocks of multilevel (for mBnT case, ternary) symbols. The mBnT code can define itself as to map blocks of "m" binary data bits into blocks of "n" ternary channel symbols.

The most prominent code of the family is the 4B3T code, where four binary data bits are replaced by three ternary levels. There are 16 (2^4) possible combinations for blocks of 4 bits that are mapped into 27 (3^3) different combinations of ternary symbols. A total mapping of $C_{27,16}$ different ways. As the degree of freedom in choosing the right sequences is reasonably big, the right choice for a sequence will solely depend on the code selection criteria defined in section 3.2 (line code selection). However, finding the

smallest digital sum (DS) of the ternary sequence is another selection criterion, where a method of mode change is applied when the sum reaches a set threshold.

As higher groupings are made, 5B4T (five binary four ternary), 7B5T (2^7 blocks for 3^5 ternary symbols), 8B6T, 10B7T, generally increased efficiency can be achieved. This is due to the fact that, enlargement in binary block size lowers the baud rate and therefore a smaller spectrum is utilized by the bit rate. At the same token, noise level is reduced in selected channels due to smaller bandwidth. But, on the counterpart, as redundancy is decreased there is a lesser control over the overall statistics of the code, which are, timing recovery, number of bits transmitted per signal level, power spectrum, etc.. Also loss due to ISI becomes visible, since the codes start to exhibit low frequency cutoff effects and therefore control of baseline wander or DC is lagged.

3.3.6. Two Binary in One Quaternary (2B1Q) Code

2B1Q encoder utilizes four two bits combinations (01, 10, 11 and 00) to be mapped onto four voltage levels (+3, +1, -1, -3) or four symbols. Each symbol therefore represents a group of two bits (figure 3.11). The code has zero frequency spectral energy (baseband) and operates at twice the data rate of bipolar code, due to the 2 bits/symbol combination.

There is no level or voltage representation for zero in this code as compared to the bipolar code. Most of the energy in the signal is concentrated toward the higher end of the frequency spectrum rather than at one half of the spectrum as it is in the bipolar code. It is defined as the standard code for integrated services digital network (ISDN) basic rate transmission.

In 2B1Q code the bandwidth efficiency has been improved by a factor of two, considering polar code as the reference. The binary encoder is substituted by a multilevel encoder and hence a more powerful way of improving efficiency is contemplated here.

Now additional efficiency can be achieved through usage of better shaping filters. The derivation of the transfer function for the 2B1Q code is given in appendix C.

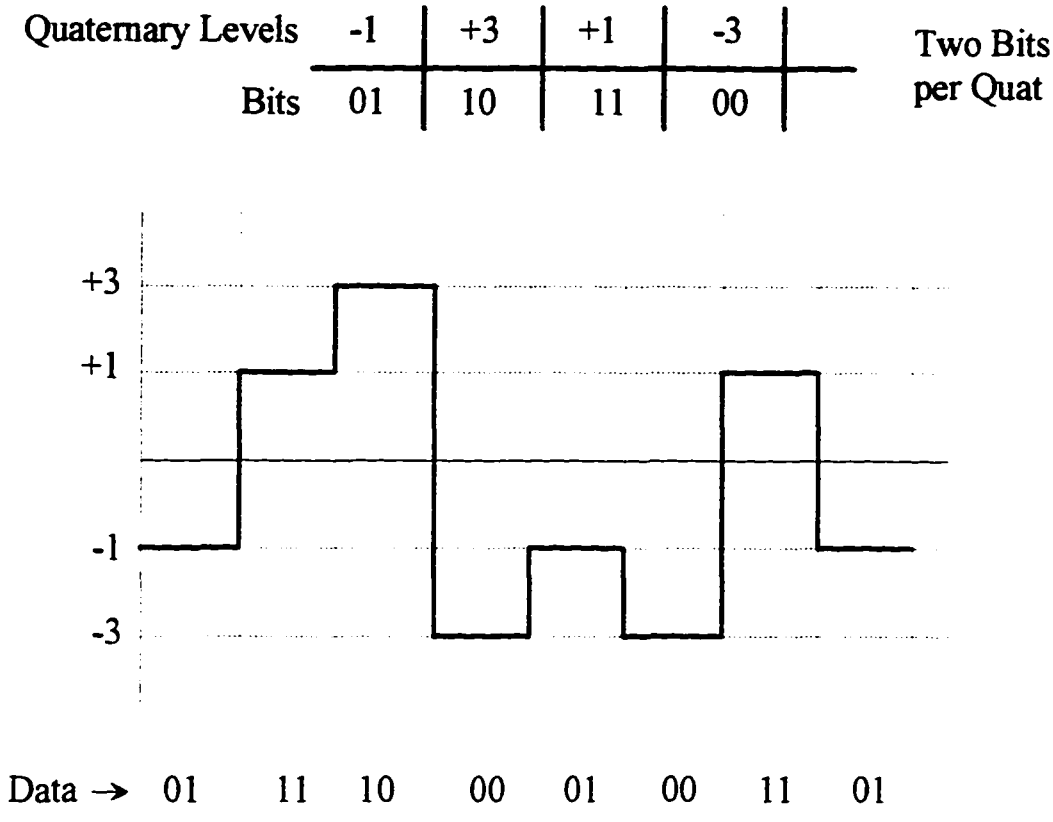

Figure 3.11 2B1Q waveform.

3.3.7. Partial Response Class-4 (PR-4) Code

Also referred to as modified duobinary code, it is obtained by subtracting pulses or symbols, spaced at two symbol periods (2T) apart. The output voltage of the transmitter therefore will assume three different new values, which are proportional to -2A, 0 and +2A, given that the initial voltage values or symbol values are -A and +A. An example of a PR-4 signal is shown in figure 3.12 .

The main advantage of the PR-4 code is that it shifts the spectral components of the polar form away from the origin (because of delay that has been introduced). Therefore the power spectral density becomes zero at the origin (passband characteristics).

In its simplest form, PR-4 coding of a binary sequence $\{x_i\}$ is accomplished by transmitting the sum $y_i = x_i + x_{i-1}$. Other differing methods also exists where modulo-2 addition is considered.

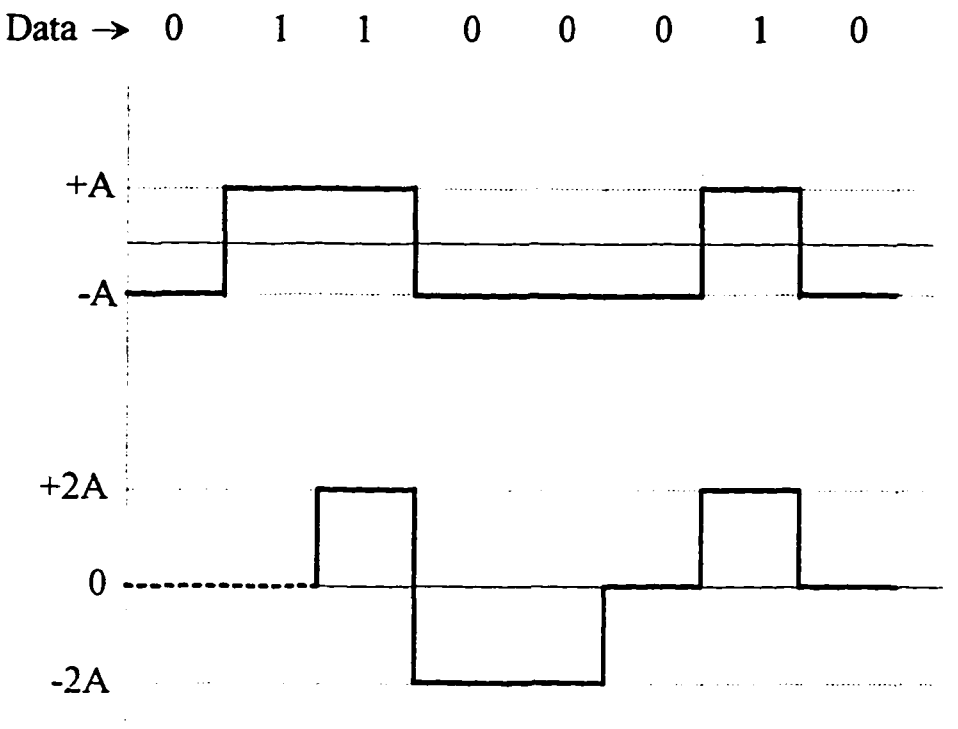

Figure 3.12 Partial response class-4 (PR-4) Waveform.

3.3.8. Transfer Function of the Shaping Filters

The transmitter is a sequence of encoder and shaping filter. The transfer function S(f) of the shaping filters can be obtained by taking the Fourier transform of the individual impulse response s(t) of the Polar, Manchester, and 2B1Q codes.

Scrambled sequence of bits are mapped into rectangular pulse shaped symbols and fed to the shaping filter. The symbol rate is inverse of the symbol period and for Polar codes it is equal to bit rate, 1/T (figure 3.13). The transfer function for Polar codes can be given as, $S(f) = \sin(\pi fT)/\pi f$. This is baseband spectrum, since it has no zero frequency components at DC (figure 3.14). From S(f), the effective bandwidth utilized is $W = 1/T$, which is also same as the bit rate.

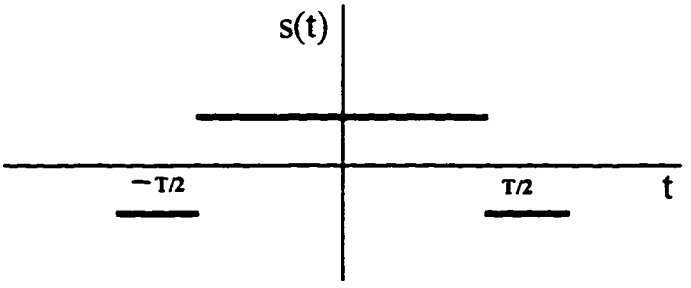

Figure 3.13 Impulse response for a Polar code.

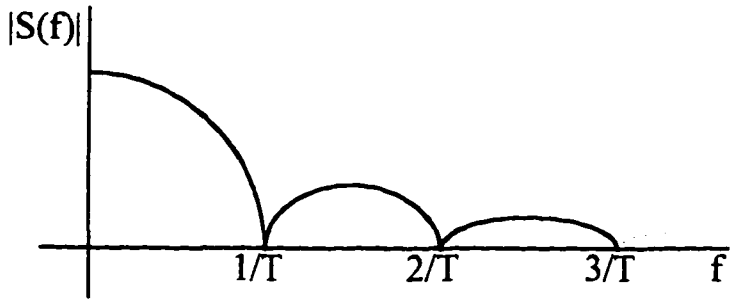

Figure 3.14 Transfer function response of a Polar transmitter.

Transfer function for the Manchester code is also derived from its impulse response and it is given as, $S(f) = [\cos(\pi fT) - 1] / j\pi f$, which has a passband spectrum (null at DC). The effective bandwidth utilized is $W = 2/T$, which is twice the bit rate, $B_r = 1/T$. Also, as a comparison, the Polar code uses half the bandwidth required by the Manchester code.

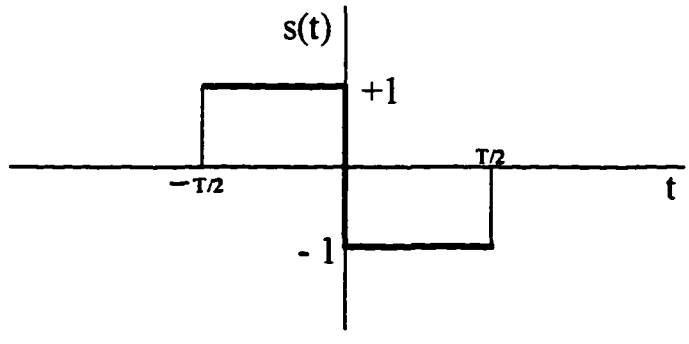

Figure 3.15 Impulse response for a Manchester code.

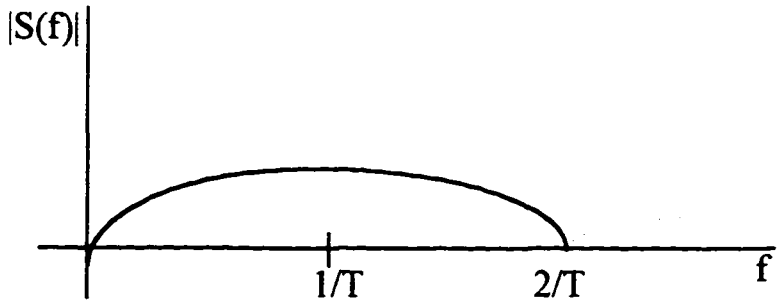

Figure 3.16 Transfer function response of a Manchester transmitter.

The 2B1Q code requires a different encoder than the previously discussed codes, in that, it starts taking into account the multilevel characteristics of the code. The impulse response used for 2B1Q line code's shaping filter has the same shape as the Polar code's pulse with the added factor that it has twice the duration (2T), compared to the polar pulse. The transfer function is given as, $S(f) = [\sin(2\pi fT)] / \sqrt{2}\pi f$, which has a baseband spectrum (no null at DC). The effective bandwidth utilized is $W=1/2T$ due to the multilevel nature of the code. This is half the bandwidth utilized by the Polar code for a fixed bit rate, $B_r = 1/T$. If it is desired to use the same bandwidth as of the polar code then the bit rate is doubled ($B_{r\_2B1Q} = 2/T$). A more detailed description of the transfer function derivation is given in appendix C.

CHAPTER 4

4. Combined Modulation and Coding Techniques

As the goal of attaining better efficiency and increased throughput by usage of more robust codes, two parameters are to be looked which will determine the upper bounds that can be reached; they are multilevel encoding and efficient spectral shaping.

As data rate is increased, a criterion should be developed such that it would maintain an acceptable error rate and also eliminate Nyquist rate phenomena (resulting from intersymbol interference), which constrain the limits to a maximum of 2W elements/second for a channel of W bandwidth.

The solution is to perform multilevel encoding of the symbols in two (or more) dimensions. A multilevel encoding (M levels) can achieve $2W \log_2 M$ or higher bit rate with an acceptable error rate. Thus, changing the Nyquist limit.

As multilevel encoding is introduced, the presence of noise can corrupt one or more bits. With increased data rate, as a result of compaction of bits per

signal, more bits are affected by a given pattern of noise. Thus, at a given noise level, the higher the data rate, the higher the error rate. To get around the problem is to strenghten the signal such that it will improve the ability to correctly receive data in presence of noise. Basically, the S/N ratio has to be refined for Shannon's formula (equation 4.1).

$$C = W \log_2(1 + \frac{S}{N}) \qquad (4.1)$$

The capacity in bits per second for a band-limited voiceband channel (C), is defined through the parameters W, S and N. S is the waveform signal power given in Watts and applied to an ideal low-pass filter whose bandwidth is W Hz. N (Watts), is the channel noise uniformly distributed (Gaussian noise) over the passband.

As seen, Shannon formula attests that a maximum channel capacity, in bits per second, can be attained if the S/N ratio is increased with same length as the information rate. This can be secured by usage of efficient spectral shaping.

Constraint from basic information theory [17]; if input data rate for a band-limited channel is less than Shannon's theoretical limit C (equation 4.1), a

code can be generated for which the error rate approaches zero as the message length reaches a maximum bound. On the other hand, if the data input rate is higher than the value of C, the error rate cannot be lowered below a threshold point. Therefore the codes that will be reflected upon, have the burden to achieve certain rates for a given bit error rate (BER) as the threshold point.

As an example, consider a voice channel with S/N ratio of 30 dB (ratio of 1000:1) and a bandwidth of 3100 Hz. Shannon's channel capacity (C) is therefore approximately 31 kbps. To achieve higher rates a bit error rate is to be introduced and signal shaping has to be considered to work around that particular error rate.

4.1. Quadrature Amplitude Modulation (QAM)

Quadrature Amplitude Modulation is a combined amplitude and phase modulation scheme. Data is transmitted in polar coordinate format, where the phasor (x,y) consist of a real and imaginary axis. Data is grouped into symbols, where each symbol is a combination of phase and amplitude. A 2^n point constellation can be used to send n bits/symbol.

A 64 point constellation in a QAM environment has 64 symbols, where each symbol is represented by 6 bits ($64 = 2^6$). When these symbols are transmitted, each symbol represents a specific signal level (different signal levels). The transmission frequency is same for all symbols, the only thing that varies from symbol to symbol is the amplitude and phase. When a train of bits comes, they are grouped into blocks of six and transmitted on same frequency but with different amplitude and phase.

4.2. Carrierless Amplitude and Phase (CAP) Modulation

Carrierless Amplitude and Phase Modulation is in its simplest form QAM with suppressed carrier. It is a bandwidth efficient two dimensional passband line code.

A 16 point constellation in a CAP environment has 16 two-dimensional symbols, where each symbol is represented by 4 bits ($16 = 2^4$). The symbols are encoded by using Gray coding techniques. CAP constellations for 16, 32 and 64 points are shown in figure 4.3 and 4.4.

Components of a canonical QAM modulator are shown below.

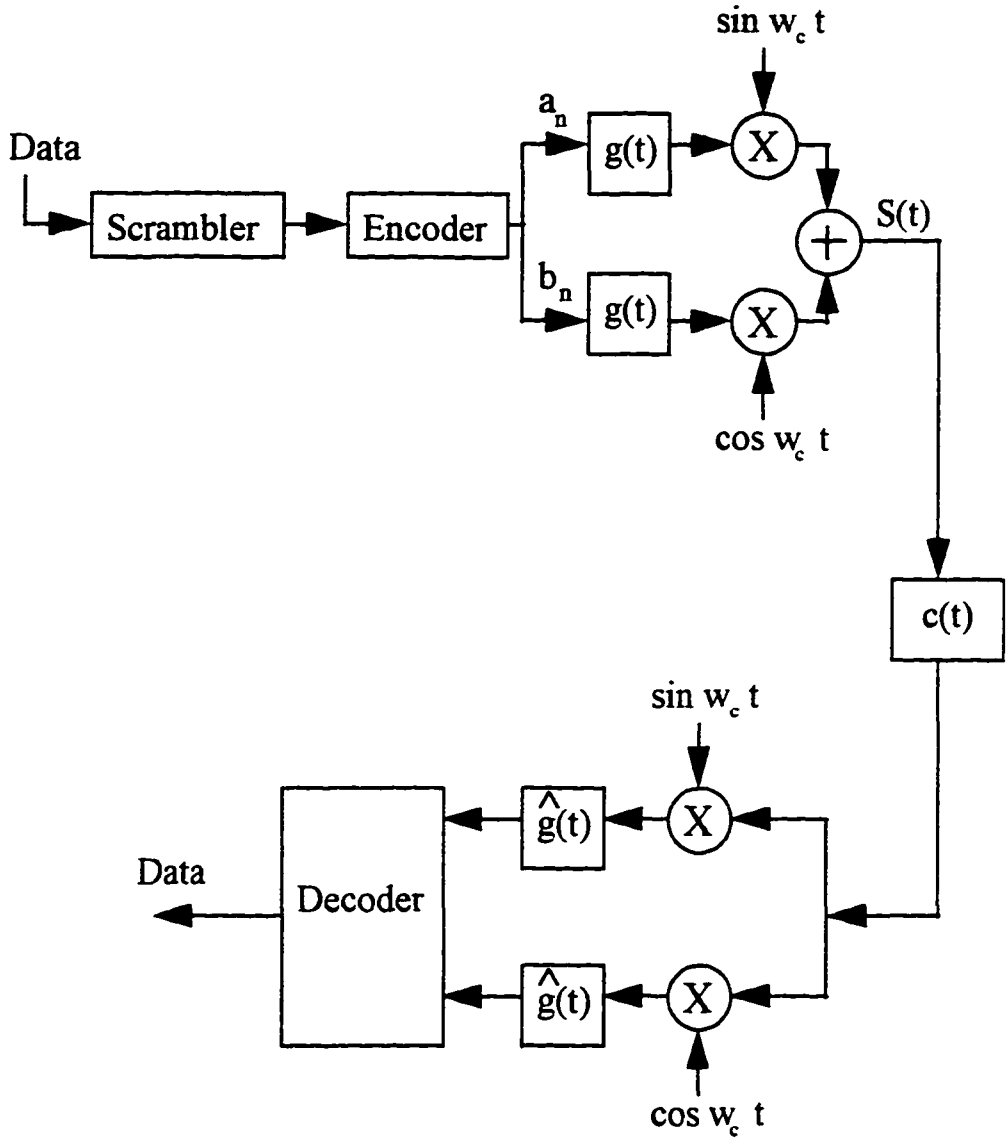

Figure 4.1 Quadrature amplitude modulation system.

Components of a canonical CAP modulator are shown in figure 4.2 . Scrambled data comes into the encoder, which maps blocks of n bits onto one of the 2^n complex symbols. The speed at which the transmitter transmits data here is:

$$(1/T) \cdot \log_2 p \qquad (4.2)$$

where p is the number of points used in the constellation and T is the symbol period.

The complex symbols ($a_n + j\, b_n$) from the encoder are fed to the in-phase and quadrature filters. The impulse responses of these two filters due to the orthogonality and 90 degrees phase difference between each other and consequently in their Fourier transform, form an Hilbert pair. The output of the filters then is added (or subtracted) and handed to a digital-to-analog (D/A) converter, which in turn pass the signal to a low pass filter to be transmitted over the medium.

The impulse responses of the in-phase and quadrature filters are:

$$s(t) = f(t) \cos (w_c t) \qquad (4.3)$$

$$\hat{s}(t) = f(t) \sin (w_c t) \qquad (4.4)$$

In equation 4.3 and 4.4, f(t) is a baseband pulse and $w_c = 2\pi f_c$. The center frequency (f_c) is the frequency above any frequency component in f(t). Now both impulse responses have passband type of characteristics since f(t), the baseband pulse, is multiplied with cosine and sine component. They basically shift the pulse from the origin to the center frequency location. More details of the transfer functions, impulse responses of the in-phase and quadrature filters are given in appendix C.

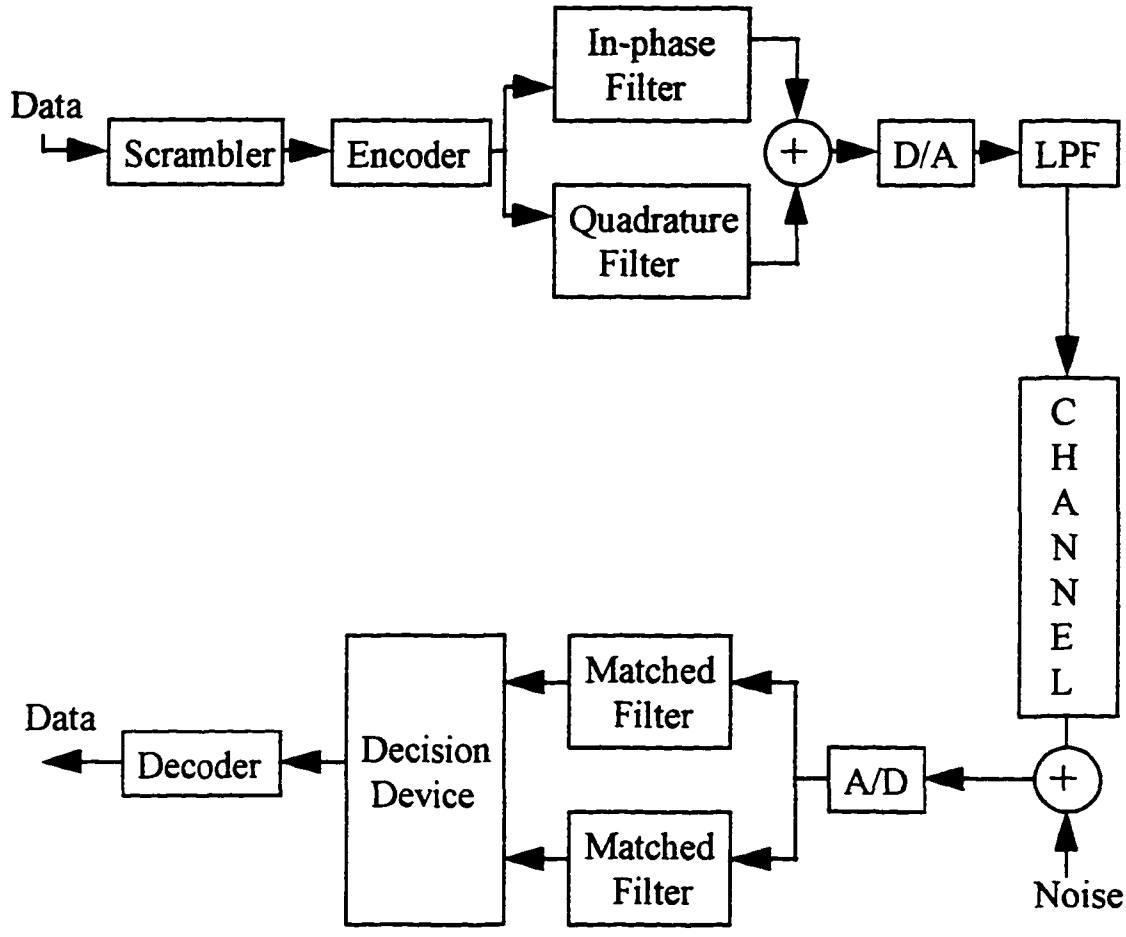

Figure 4.2 System with Carrierless amplitude and phase modulation.

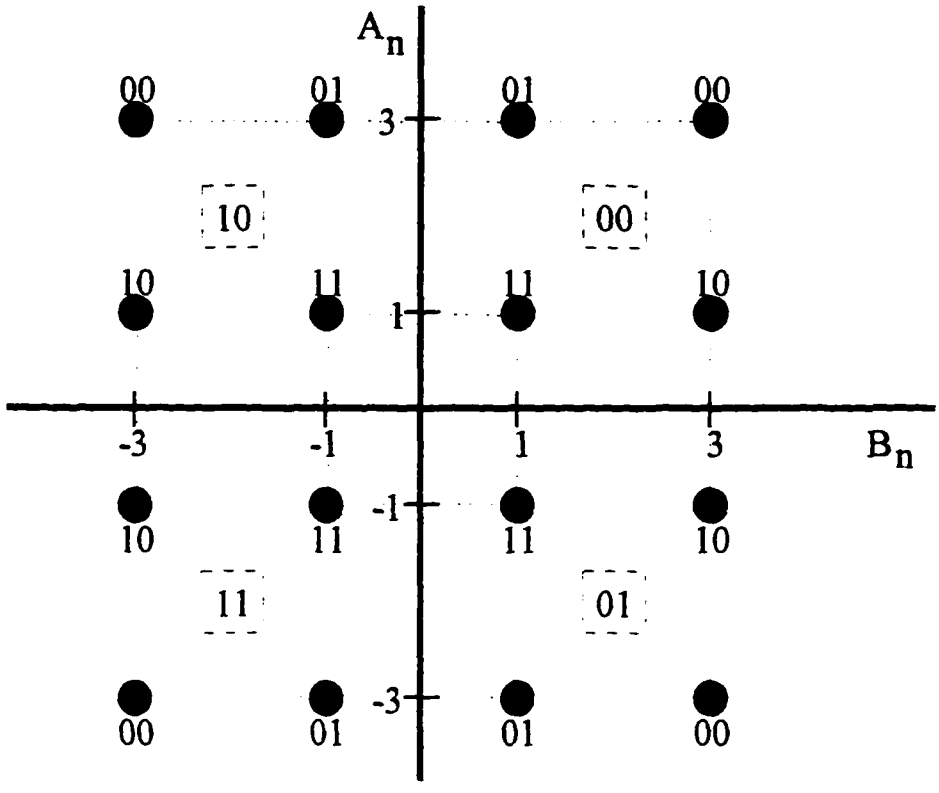

Figure 4. 3 16-CAP signal constellation.

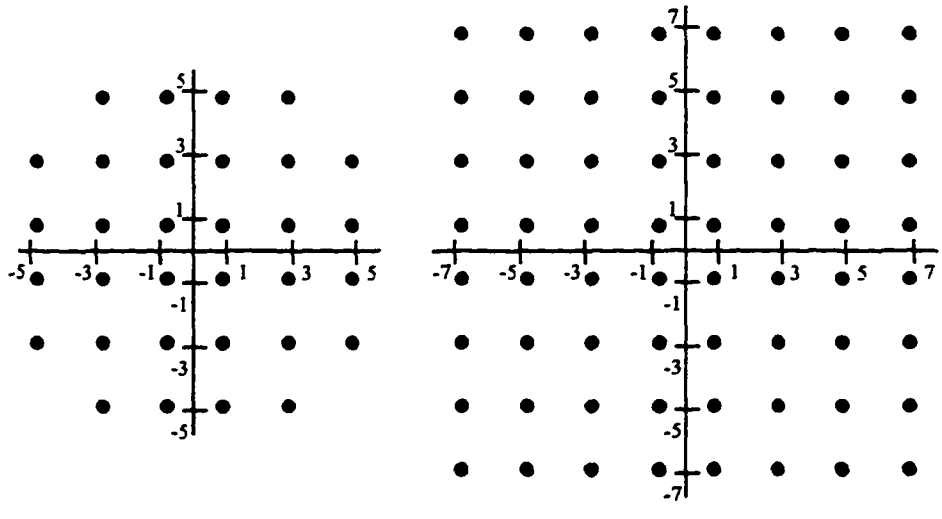

Figure 4.4 32 and 64-CAP signal constellation.

CHAPTER 5

5. Simulation setup for the system

The simulation techniques will verify the theoretical results using distribution system loop tests, where the basic system will consist of transmitter, channel and receiver. The computer aided design (CAD) environment consist typically of input, output, component databases, fixed databases and central processing facility (figure 5.1).

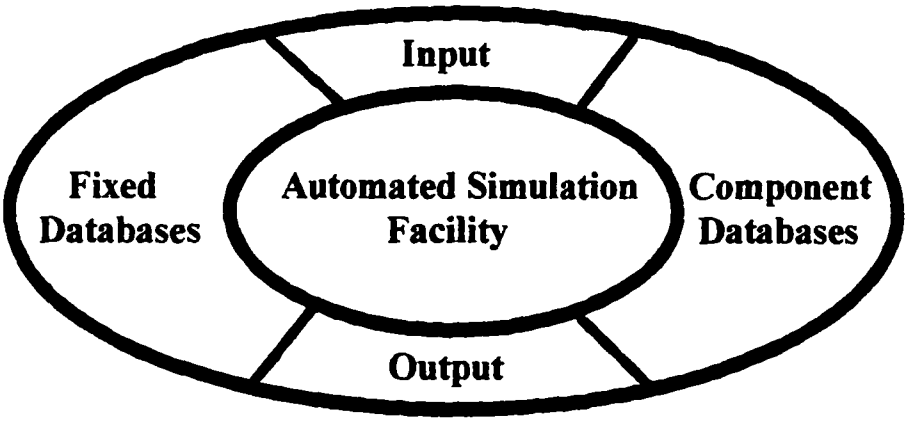

Figure 5.1 Simulation design environment

On the input side, three or four databases need to be accessed, and on the output side, three to six matrices of results are generated. In the databases to be accessed are the permanent or fixed databases and component databases. The first ones basically contain information on loop surveys, cable characteristics, impulse noise, and crosstalk impairment. The second set contains data on components devices that have filtering and regenerative type of capabilities.

5.1. Premises distribution system (PDS) loops

The simulation is basically tested on non-standard loops, since they are not specified by any standards organization. These loops describe characteristics of a passive bus type of architecture. There is a total of eight such types of loops, each with two cases (Figure 5.2, 5.3, 5.4 and 5.5). These loops can be defined for the upcoming very high bit rate digital subscriber loop (VDSL) standard.

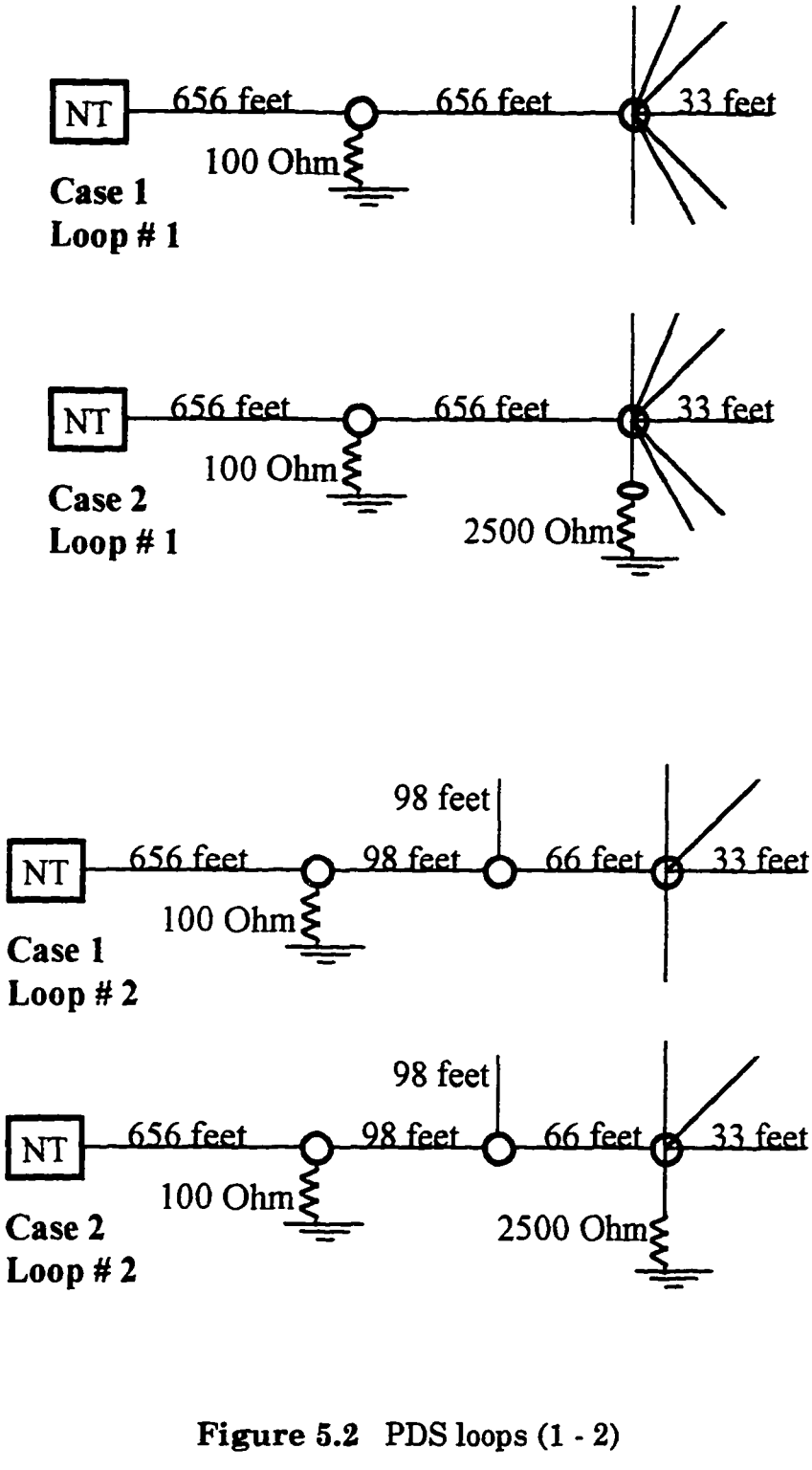

Figure 5.2 PDS loops (1 - 2)

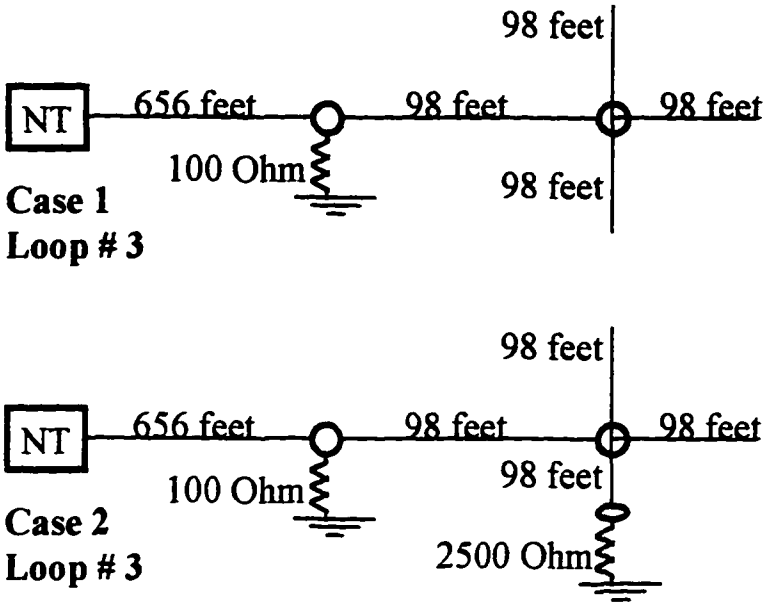

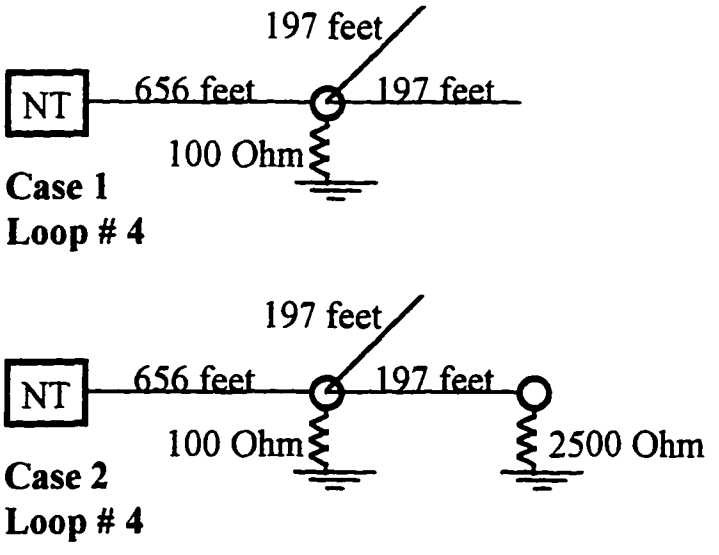

Figure 5.3 PDS loops (3 - 4)

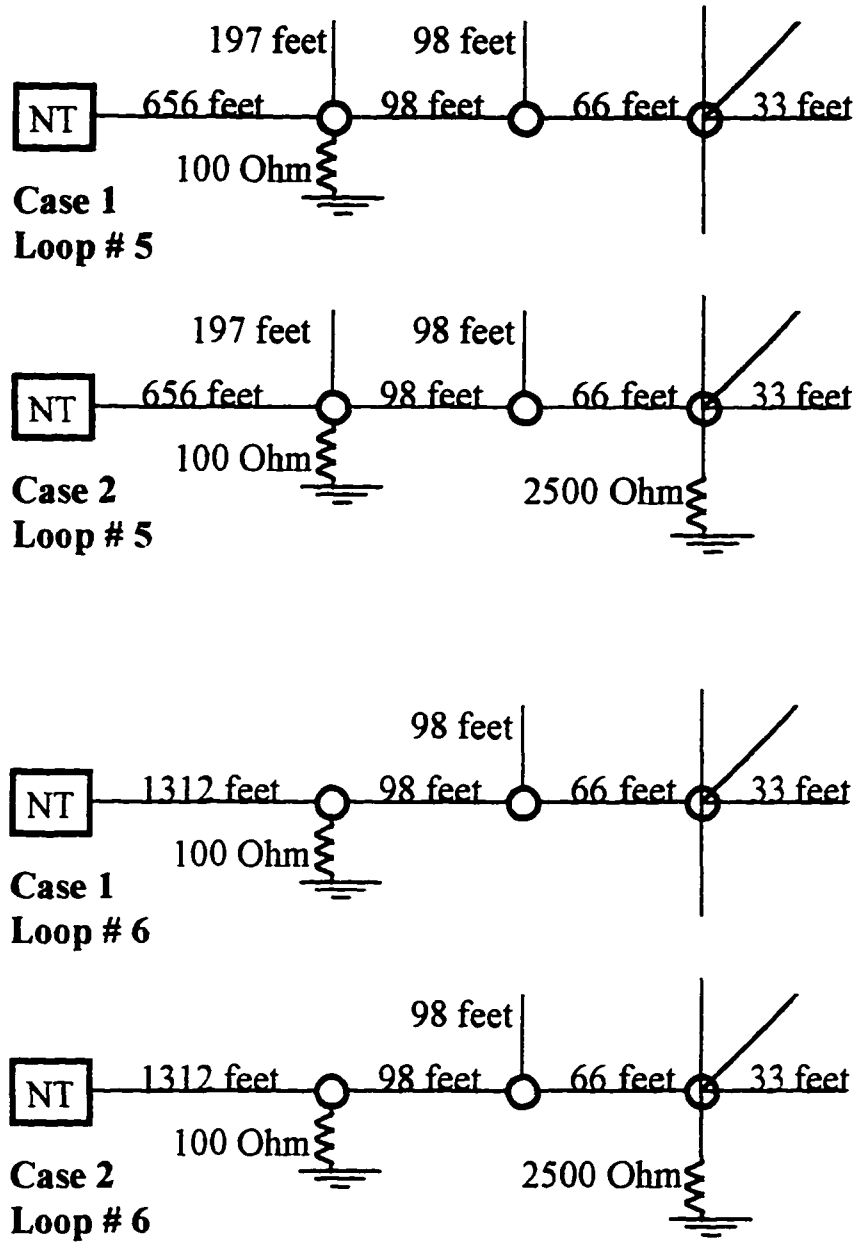

Figure 5.4 PDS loops (5 - 6)

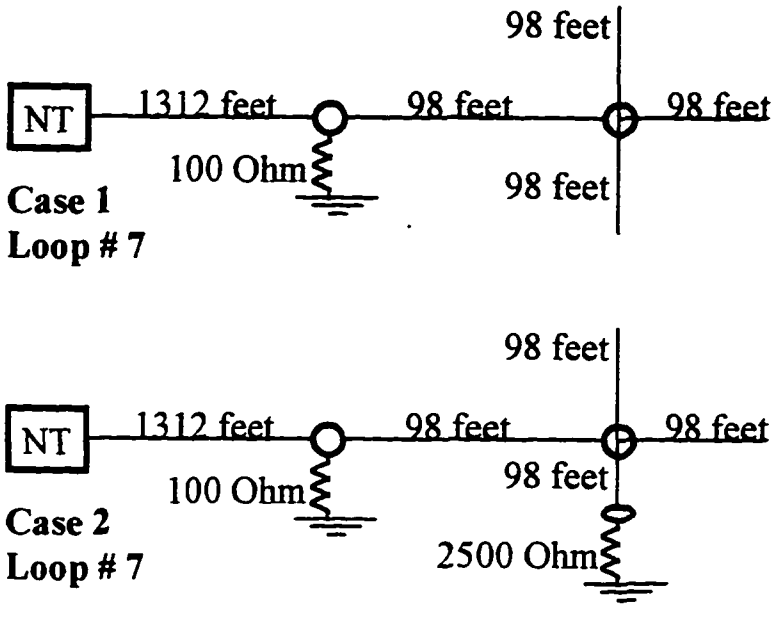

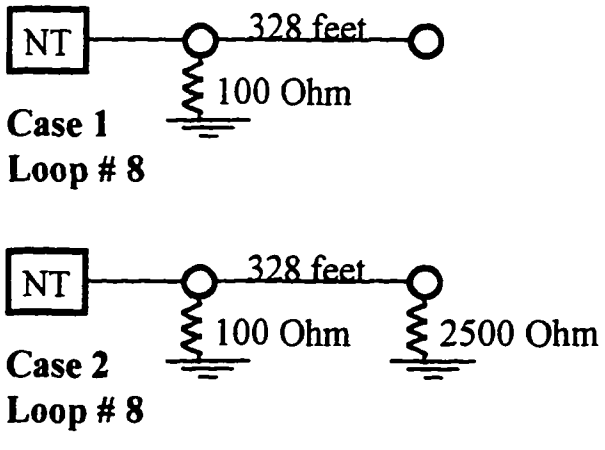

Figure 5.5 PDS loops (7 - 8)

5.2. Loop computations

Figure 5.6 presents an example of a simple loop with two different types of gauge. To obtain all system characteristics or the transfer function, a transmission system model must be constructed. The simplest such model is the two port network (figure 5.7).

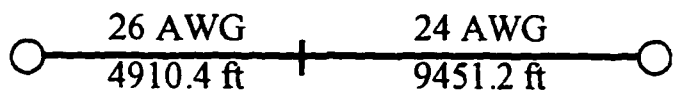

Figure 5.6 Sequence of two different gauge unshielded twisted wire pair (UTP), category type 3 cable.

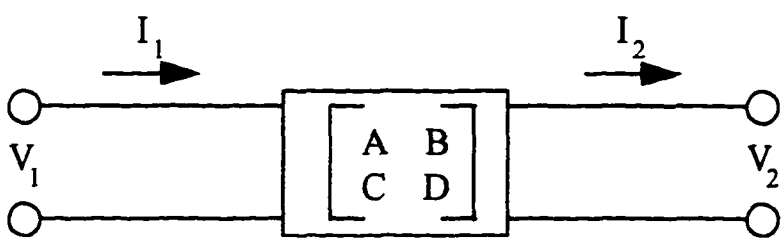

Figure 5.7 2-port network, with A, B, C and D matrix parameters.

From the transmission matrix the transfer function can be obtained. Therefore, the first step is to find the A, B, C and D parameters. These parameters are related to the input and output voltages and currents through a simple set of equations:

$$V_1 = AV_2 + BI_2 \tag{5.1}$$

$$I_1 = CV_2 + DI_2 \tag{5.2}$$

The coefficients A, B, C and D are complex functions of frequency and characterize the electrical properties of the two port network. For a cable of length x, the values for these coefficients can be calculated through equation A.38 in appendix A.

One of the important properties of the A, B, C and D matrix is how easily it can handle a sequence of two port networks. Figure 5.8 display a sequence, where the input output relationship can be found by using the following matrix arrangement:

$$\begin{bmatrix} V_1 \\ I_1 \end{bmatrix} = \begin{bmatrix} A_1 & B_1 \\ C_1 & D_1 \end{bmatrix} \begin{bmatrix} A_2 & B_2 \\ C_2 & D_2 \end{bmatrix} \begin{bmatrix} V_2 \\ I_2 \end{bmatrix} = \begin{bmatrix} A & B \\ C & D \end{bmatrix} \begin{bmatrix} V_2 \\ I_2 \end{bmatrix} \tag{5.3}$$

The matrix multiplication principle can be extended to as many elements as necessary; it is referred as the chain rule.

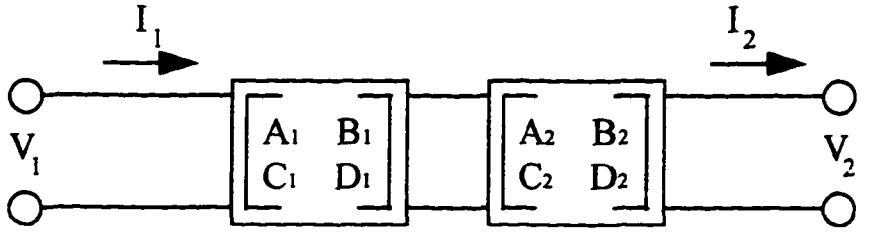

Figure 5.8 Chain of two 2-port networks.

Once the A, B, C and D matrix of an end-to-end circuit is obtained, it completely asseverate the desired electrical properties of the transmission channel considered. For instance the transfer function H(jω), given in equation 5.5, is a relatively simple function of the matrix elements and the source and termination impedances Z_s and Z_L (figure 5.9).

$$H(j\omega) = \frac{V_2}{V_1} = \frac{Z_L I_2}{Z_s I_1} \qquad (5.4)$$

and from (5.2) and (5.1),

$$H(j\omega) = \frac{Z_L}{Z_s (C Z_L + D)} \qquad (5.5)$$

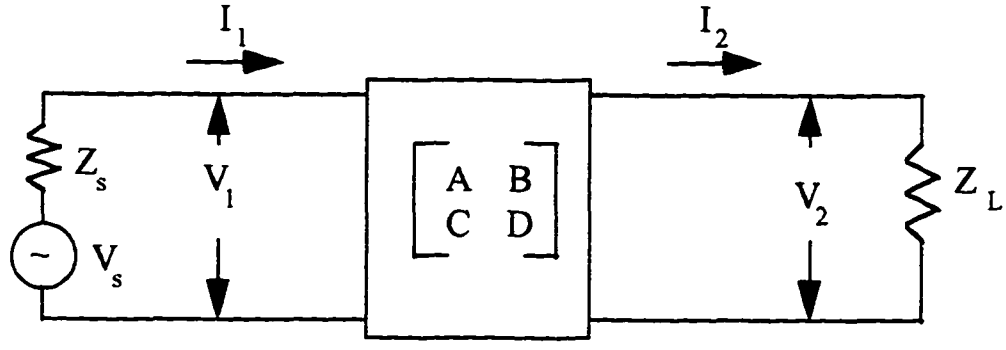

Figure 5.9 2-port network with source and termination impedances.

An example of A, B, C and D matrix calculation can be performed by using data available in figure 5.6, where two AWG (26 and 24) cables of length 4910.4 feet and 9451.2 feet are used. Now by making use of table 5.1 (secondary constants) and equation A.38 for a frequency of 1 kHz the matrices and their product can be found (equations 5.6, 5.7 and 5.8).

$$\begin{bmatrix} A_1 & B_1 \\ C_1 & D_1 \end{bmatrix} = \begin{bmatrix} 0.99 + j\,0.1 & 410.5 + j\,16.3 \\ -1.3 \times 10^{-5} + j\,4.87 \times 10^{-4} & 0.99 + j\,0.1 \end{bmatrix} \quad (5.6)$$

$$\begin{bmatrix} A_2 & B_2 \\ C_2 & D_2 \end{bmatrix} = \begin{bmatrix} 0.98 + j\,0.2 & 482.8 + j\,50.7 \\ -7.7 \times 10^{-5} + j\,9.21 \times 10^{-4} & 0.98 + j\,0.2 \end{bmatrix} \quad (5.7)$$

$$\begin{bmatrix} A & B \\ C & D \end{bmatrix} = \begin{bmatrix} 0.9 + j\,0.7 & 876.6 + j\,207.1 \\ -2.9 \times 10^{-4} + j\,1.39 \times 10^{-3} & 0.9 + j\,0.6 \end{bmatrix} \quad (5.8)$$

5.2.1 Impedance Mismatch

Whenever there is an impedance mismatch, some form of echo is produced in the transmission system. Part of the echoed signal is received by the receiver and another by the transmitter. The two port network in figure 5.9 has characteristic impedance Z_0 , propagation constant γ (both defined in appendix A), termination impedance Z_L and source impedance Z_s . If $Z_0 = Z_L = Z_s$, then there is no reflection (thus no echo) at either port, and the terminations are said to be matched. Hence, if $Z_0 = Z_s$, but $Z_0 \neq Z_L$ then there is a presence of reflection at port two; which will propagate back into port one. Therefore, it is necessary that all three impedances must be balanced. For this purpose it is required that the input impedance at port one be calculated, such that, reflection coefficient can be determined. Consequently this result in the computation of echo signal.

The advantage in calculating the input impedance comes from the fact that, the reflected signal at port one can be computed without doing any signal calculations at port two. If port two in figure 5.7 is terminated in impedance Z_2 , then $I_2 = V_2/Z_2$. Substituting this into equations 5.1 and 5.2, and solving it, can determine Z_{in} at port one (equation 5.9).

$$Z_{in} = \frac{V_1}{I_1} = \frac{AZ_2 + B}{CZ_2 + D} \qquad (5.9)$$

5.2.2 Bridge Taps

Most of the old premises distribution system (PDS) loops have bridge tap embedded into their topology. Figure 5.10 displays a bridge tap loop configuration and figure 5.11 shows a two port network A, B, C and D representation of the loop shown. And figure 5.12 is an equivalent configuration circuit for the same loop.

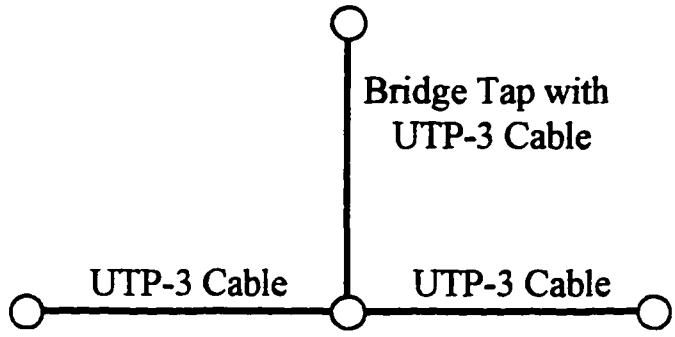

Figure 5.10 Cable loop with bridge tap.

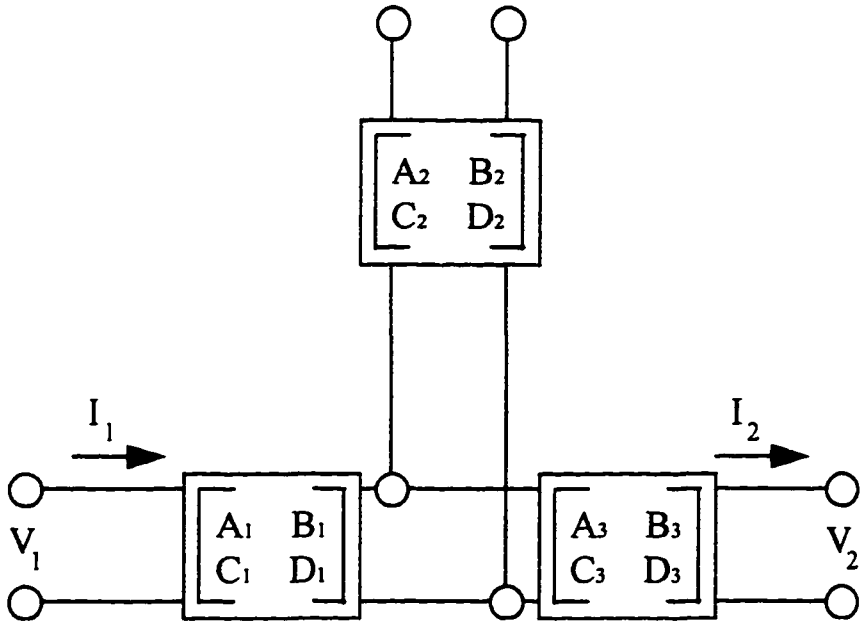

Figure 5.11 2-port representation of the loop in figure 5.10.

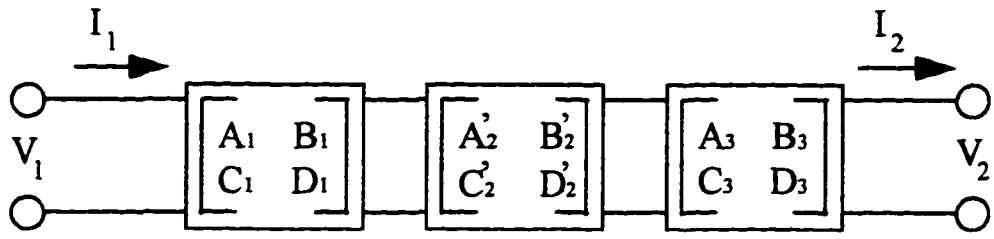

Figure 5.12 Equivalent circuit, 2-port representation of figure 5.11.

The bridge tap can be simulated as a shunt impedance across the loop. The A, B, C and D matrix for a shunt impedance, $Z_{bridge\ tap}$ is:

$$\begin{bmatrix} A'_2 & B'_2 \\ C'_2 & D'_2 \end{bmatrix} = \begin{bmatrix} 1 & 0 \\ \dfrac{1}{Z_{bridge\ tap}} & 1 \end{bmatrix} \qquad (5.10)$$

Assuming that it is not terminated, $Z_{bridge\ tap}$ can be calculated as,

$$Z_{bridge\ tap} = \frac{A_2}{C_2} \qquad (5.11)$$

Therefore, combining 5.10 and 5.11,

$$\begin{bmatrix} A_2' & B_2' \\ C_2' & D_2' \end{bmatrix} = \begin{bmatrix} 1 & 0 \\ \frac{C_2}{A_2} & 1 \end{bmatrix} \qquad (5.12)$$

The main effect introduced by a bridge tap is loss. Now since shunt capacitance does not absorb power, the loss introduced is primarily reflection loss.

Table 5.1 Secondary constants calculations for 24 and 26 gauge cables, with primary constants R, L, G and C obtained from digital audio-visual council standard (DAVIC).

Gauge	Frequency (kHz)	Characteristic Impedance (Ohms)	Propagation Constant (μNeper/ft) (μRadians/ft)
24	1	518 - j 507	49 + j 51
24	2	370 - j 355	70 + j 74
24	3	306 - j 286	85 + j 91
26	1	654 - j 645	64 + j 64
26	2	466 - j 453	89 + j 93
26	3	383 - j 367	108 + j 114

CHAPTER 6

6. Simulation Results in the Frequency Domain for PDS Loops

The first set of results are the loop responses for different frequencies, where the loss of each loop is calculated in dB. This loss is mainly due to the bridge taps involved and the R, L, G, C components of the loops. Two graphs are shown for each loop (figure 6.2 - 6.9), one is spectral analysis for frequencies of up to 5 MHz and the other is for frequencies of up to 30 MHz. The second graph shows how the loops behave in presence of bridge taps. The first graph is more detailed version of the second graph, and it determines frequency rates which are acceptable for use by the different codes. The conjunction of both graphs determines if the loop is acceptable or not for use. The graph at the bottom of each page is relevant for lower transmission rates while the upper shows characteristics of higher rates for the loops considered. The maximum frequency of 30 MHz is maintained in conformity to FCC regulations to avoid radiation problems.

6.1. Spectrum Allocation to Achieve Maximum Bit Rate

The maximum acceptable loss is 30 dB = -30 dB, which means frequencies that provide up to -30 dB loss can be further used by the codes being analyzed. This threshold is basically taken from a practical point of view. It gives a range of loss which is acceptable by the receiver without serious compromise to an error. Table 6.2 gives a detailed description of acceptable frequencies for which all the loops are viable, considering a maximum of 30 dB loss.

6.2. Impairments

The basic impairments seen here are due to bridge taps, propagation loss and loop termination. Impairments which would have resulted from impedance mismatch due to change in cable gauge are avoided by using uniform cabling in all the loops. Since at this point only the frequency response of the loops is analyzed, impairments due to NEXT are not considered in this section.

6.2.1. Bridge Taps

Previous to 1990, most loops on the premises distribution system (PDS) had bridge taps installed. Bridge taps are open circuit pairs, that is, extensions

fanning out of the distribution or main cable (also called working cable). They are connected in shunt with working twisted pairs. The main reason behind them is flexibility and future additions to the loop as for increase in service demand.

The new premises distribution system (loop # 8) has no bridge taps, which are replaced by pedestals at the network termination and these spawn cables that are connected to splitters inside the premises.

The main impairments introduced by bridge taps are: 1) Power loss of the transmitting signal, which is mainly due to the partial dissipation of the main signal into the bridge tap. This dissipated energy reflect back and adds a delayed signal to the main signal, which is received by the receiver. Also some of it echoes back to the transmitter. 2) Another impairment is the introduction of nulls in the transfer function of the loop. These dips are mainly a result of a subtraction in amplitude between two frequency components. The main signal at the bridge location is combined with the signal reflected from the bridge tap. The latter has a phase difference compared to the main signal, therefore resulting in a null at the particular frequency.

The location of a bridge tap can be determined by taking (A.36) and (A.37), that gives the input impedance,

$$Z_i = V(x)/I(x) = \frac{V_l \cosh(\gamma x) + I_l Z_0 \sinh(\gamma x)}{I_l \cosh(\gamma x) + (V_l / Z_0)\sinh(\gamma x)} \qquad (6.1)$$

Taking the input impedance for the bridge tap and multiplying the numerator and denominator by $(1/I_l)$,

$$Z_{Btap} = \frac{Z_l \cosh(\gamma x) + Z_0 \sinh(\gamma x)}{\cosh(\gamma x) + (Z_l / Z_0)\sinh(\gamma x)} \qquad (6.2)$$

Now since the bridge tap is an open circuit ($Z_l = \infty$), (6.2) can be written as:

$$Z_{Btap} = \frac{\cosh(\gamma x)}{(1 / Z_0)\sinh(\gamma x)} \qquad (6.3)$$

A null correspond to a minima in the transfer function and since the impedance of the bridge tap is directly proportional to the transfer function, the minima can be found through the bridge tap impedance.

Therefore the minima for Z_{Btap} is when the imaginary part of γ is equal to,

$$\beta x = (2n + 1)\,\pi/2 \quad \text{for} \quad n = 0,1,2... \qquad (6.4)$$

Combining (A.13) and (6.4),

$$\omega \sqrt{LC} \;.\; x \;=\; (2n + 1)\,\pi/2 \qquad (6.5)$$

and from (6.5):

$$f = \frac{(2n + 1)}{4 \;.\; x \;.\; \sqrt{LC}} \qquad (6.6)$$

For 24 AWG wire the typical values for L and C are 0.95 (mH/mile) and 83 (nF/mile) respectively. Taking the initial value n = 0, equation (6.6) becomes,

$$f = \frac{28.154}{x_{miles}} = \frac{148.653}{x_{kft}} \quad \text{kHz} \qquad (6.7)$$

Other nulls can be calculated at frequencies which are odd multiples of f in equation (6.7), that is, for n = 1, 2, 3 and so on.

In figure 6.2 (loop 5, case 1, 19 AWG) the bridge tap has a length of 197 feet, therefore applying equation (6.7) it is located at a approximation of f = 761 kHz.

Equation (6.7) basically can be applied to loops with single bridge tap and that contain no termination. Loops that are perfectly terminated (case 2 of each loop) introduce a lower loss in the transfer function. This is due to the balancing effect that take place between loop impedance and load impedance. Still a flat loss is introduced, since perfect balancing is impossible to achieve.

Loops that contain several bridge taps have their nulls determined through superpositioning of the methods seen before. The importance of locating nulls lies in that they are regions where the signal is at its minimal level and therefore spectrum placement should be avoided. Also, by locating where the nulls occur, equalizer taps can be adjusted and the signal can be properly equalized for the frequency region considered.

6.2.2. Propagation Loss

The transfer function for a perfectly terminated loop can be written as,

$$G(\omega,x) = e^{-x\gamma(\omega)} \qquad (6.8)$$

where $\gamma(\omega)$ is the cable's propagation constant. The loop loss can be calculated by the following expression:

$$Loop_{loss,\,dB} = -20 \log |G(\omega,x)| = -20 \log \left| e^{-x\alpha(\omega)} . e^{-jx\beta(\omega)} \right|$$

$$\cong 8.686 \,.\, x \,.\, \alpha(\omega) \qquad (6.9)$$

Figure 6.2 - 6.9 shows the frequency response of the PDS loops (fig. 5.1-5.8). As seen the responses drop rapidly at higher frequencies. Therefore, frequency is the primary component along with distance x (equation 6.9) and cable gauge (fig. 6.3, 6.5) in determining the loop loss.

From (A.13) and (A.9),

$$2 \cdot \alpha \cdot \omega \cdot \sqrt{LC} = \omega (LG + RC)$$

and

$$\alpha(\omega) = \frac{1}{2}\left(R \cdot \sqrt{\frac{C}{L}} + G \cdot \sqrt{\frac{L}{C}} \right) \qquad (6.10)$$

Therefore, from (6.10) and (6.9) the loop loss is:

$$4.343 \cdot x \cdot \left(R \cdot \sqrt{\frac{C}{L}} + G \cdot \sqrt{\frac{L}{C}} \right) \qquad (6.11)$$

At higher frequencies the loss increases proportional to resistance (eq. 6.11), and because of the skin effect, R(ω) increases as the square root of frequency. Since skin effect relates to the resistance of surface area, the loss is inversely proportional to the conductor diameter or as the gauge increases so does the loss. This can be checked over in figure 6.2 - 6.9 .

For a 24 AWG twisted pair, at 70° F, and frequency of 30 MHz the capacitance (C) is 55.18 nF/km = 16.82 nF/kft, the inductance (L) is 586.83 μH/km = 178.91 μH/kft, the resistance is 2384 Ω/km = 726.83 Ω/kft and the conductance (G) is 26.48 mS/Km = 8.07 mS/kft [48]. The propagation loss (or

insertion loss) per unit of loop length (x = 1 kft) is derived from equation 6.11 and is equal to 34.23 dB/kft. Table 6.1 gives the loss for other frequencies.

Table 6.1 and equation 6.11 attains the following findings:

$$R \cdot \sqrt{\frac{C}{L}} = K_1 \cdot \sqrt{f} \quad ; \quad f > 100 \text{ kHz} \qquad (6.12)$$

$$G \cdot \sqrt{\frac{L}{C}} = K_2 + K_3 \cdot f \quad ; \quad f > 50 \text{ kHz} \qquad (6.13)$$

Equation 6.13 has a coefficient of linear correlation equal to 0.99993, which indicates a strong linear relation between conductance (G) and high frequencies, which is normal since resistance increases at square root of f.

When taking the values into account, the constants can be found as $K_1 = 0.04$, $K_2 = -0.00277$ and $K_3 = 0.0000277$. Now combining equation 6.11, 6.12, 6.13 and the constant values it is obtained the loss versus frequency,

$$Loop_{loss.\,dB} = 0.00012\,f + 0.04\,\sqrt{f} - 0.01203 \qquad (6.14)$$

The upper and lower bound for equation 6.14 are 30 MHz and 100 kHz respectively. Figure 6.1 shows the loop loss for 1000 feet for the ranges given.

Table 6.1. Characteristics and Propagation Loss for 24 gauge wire at 70° F for a spectrum of 30 MHz.

f(kHz)	R(Ω/kft)	L(μH/kft)	C(μF/kft)	G(mS/kft)	Loss(dB/kft)
5	54.5732	211.8323	0.0169	0.0009	2.1174
10	54.5732	211.7561	0.0169	0.0021	2.1178
50	55.7927	210.9939	0.0169	0.0110	2.1721
100	58.8415	209.8994	0.0169	0.0223	2.3015
500	96.3415	201.7195	0.0169	0.1174	3.8799
1000	133.5366	195.1220	0.0168	0.2405	5.5009
5000	296.9512	182.6006	0.0168	1.2683	12.9558
10000	419.5122	180.3445	0.0168	2.5945	18.7666
20000	593.5976	179.2500	0.0168	5.3110	27.3580
30000	726.8293	178.9116	0.0168	8.0732	34.2253

Table 6.2. Maximum frequency, in MHz, attainable by the PDS loops considered, for a loss of 30 dB or better, for 70° F and Category-3 type TWP.

Loop # (case #)	AWG 19	AWG 22	AWG 24	AWG 26
Loop 1 (case 1)	4.81	4.64	4.49	3.37
Loop 1 (case 2)	4.81	4.64	4.49	3.37
Loop 2 (case 1)	4.93	4.83	4.63	4.21
Loop 2 (case 2)	4.94	4.84	4.67	4.24
Loop 3 (case 1)	1.75	1.70	1.67	1.63
Loop 3 (case 2)	1.75	1.71	1.67	1.65
Loop 4 (case 1)	30.00	30.00	30.00	30.00
Loop 4 (case 2)	30.00	30.00	30.00	30.00
Loop 5 (case 1)	4.91	4.20	4.12	3.96
Loop 5 (case 2)	4.91	4.20	4.12	3.97
Loop 6 (case 1)	4.86	4.08	3.68	3.15
Loop 6 (case 2)	4.87	4.10	3.70	3.20
Loop 7 (case 1)	1.82	1.59	1.47	1.45
Loop 7 (case 2)	1.82	1.59	1.47	1.46
Loop 8 (case 1)	30.00	30.00	30.00	30.00
Loop 8 (case 2)	30.00	30.00	30.00	30.00

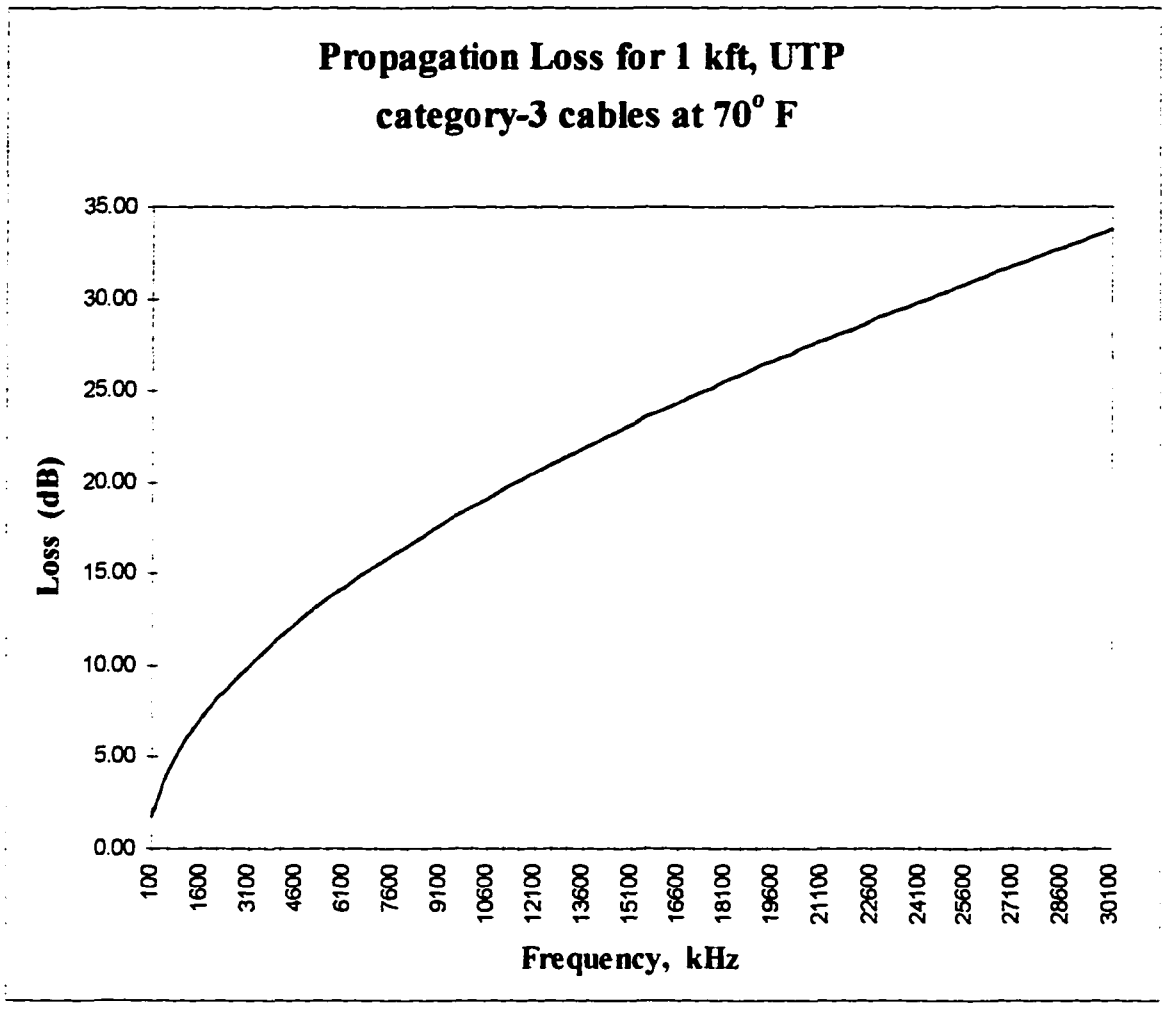

Figure 6.1 Propagation loss for category-3 unshielded twisted wire pair, at 70° F for a length of 1000 feet.

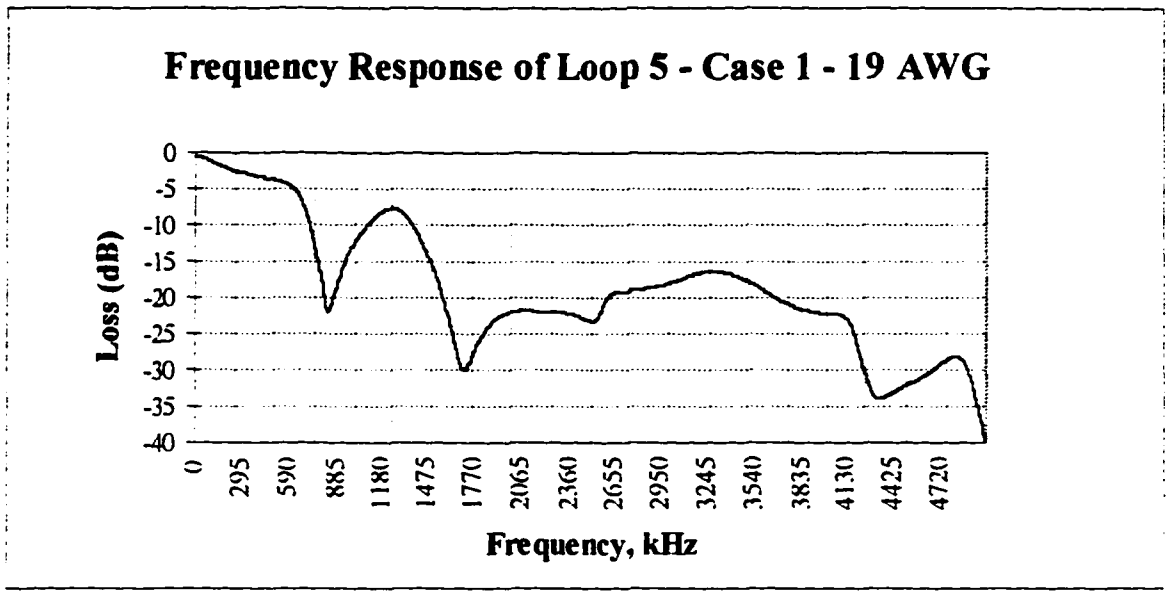

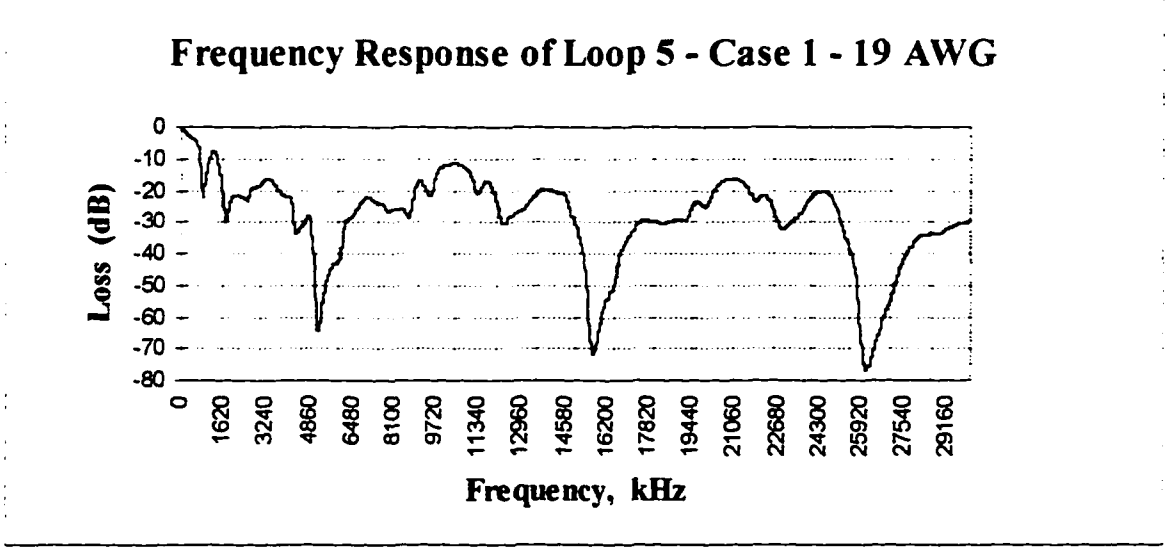

Figure 6.2 Frequency Response of Loop 5 (19 AWG), case with no termination and frequency range of 5MHz and 30 Mhz.

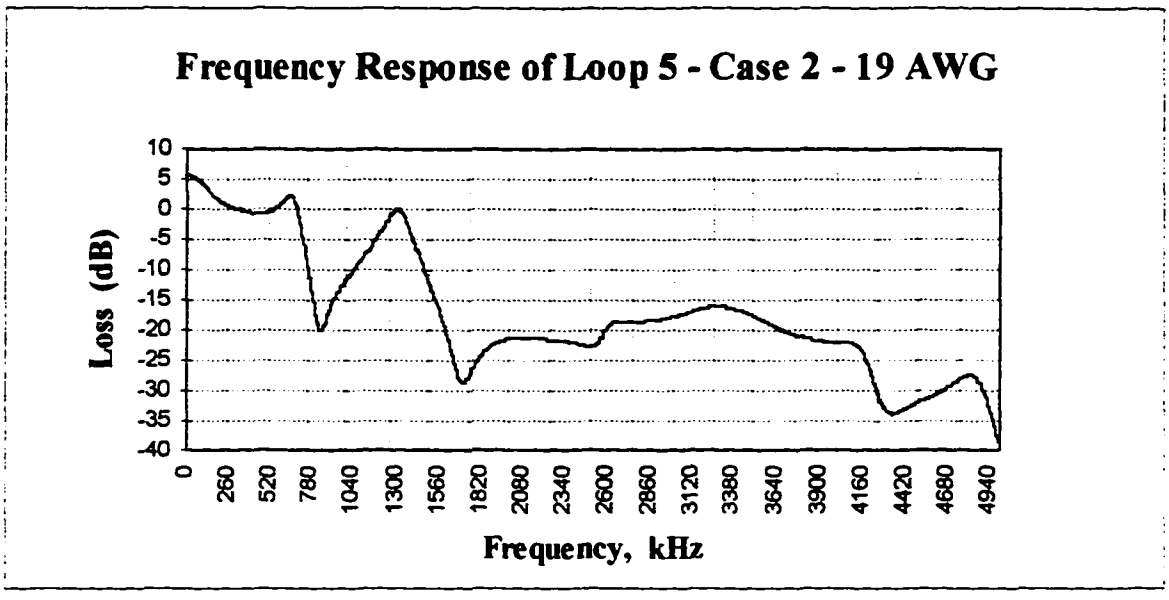

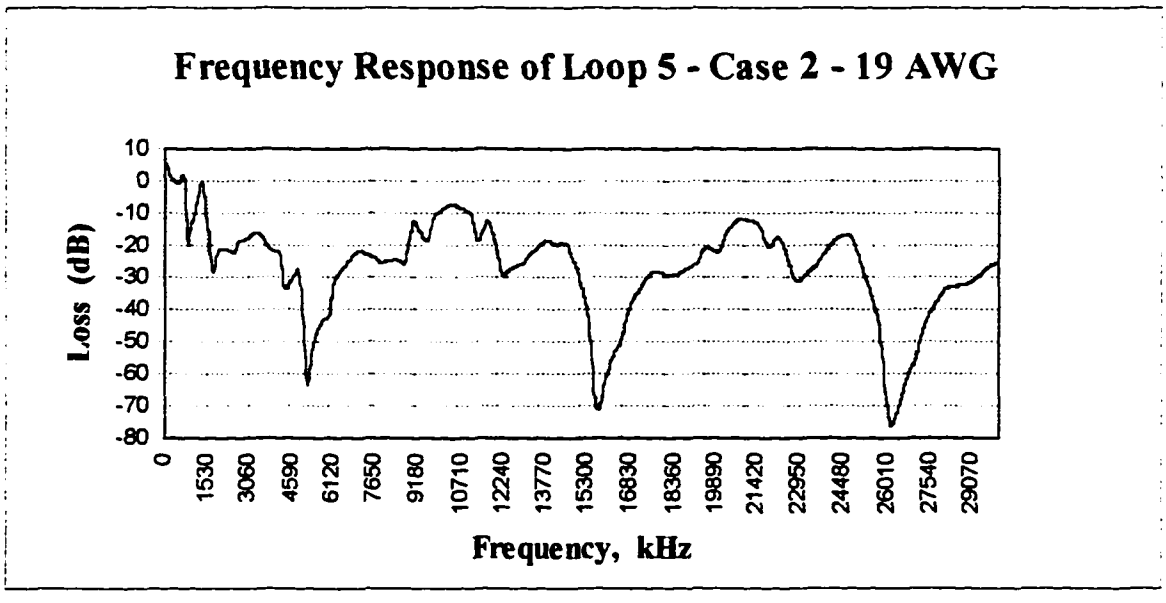

Figure 6.3 Frequency Response of Loop 5 (19 AWG), case with termination and frequency range of 5MHz and 30 MHz.

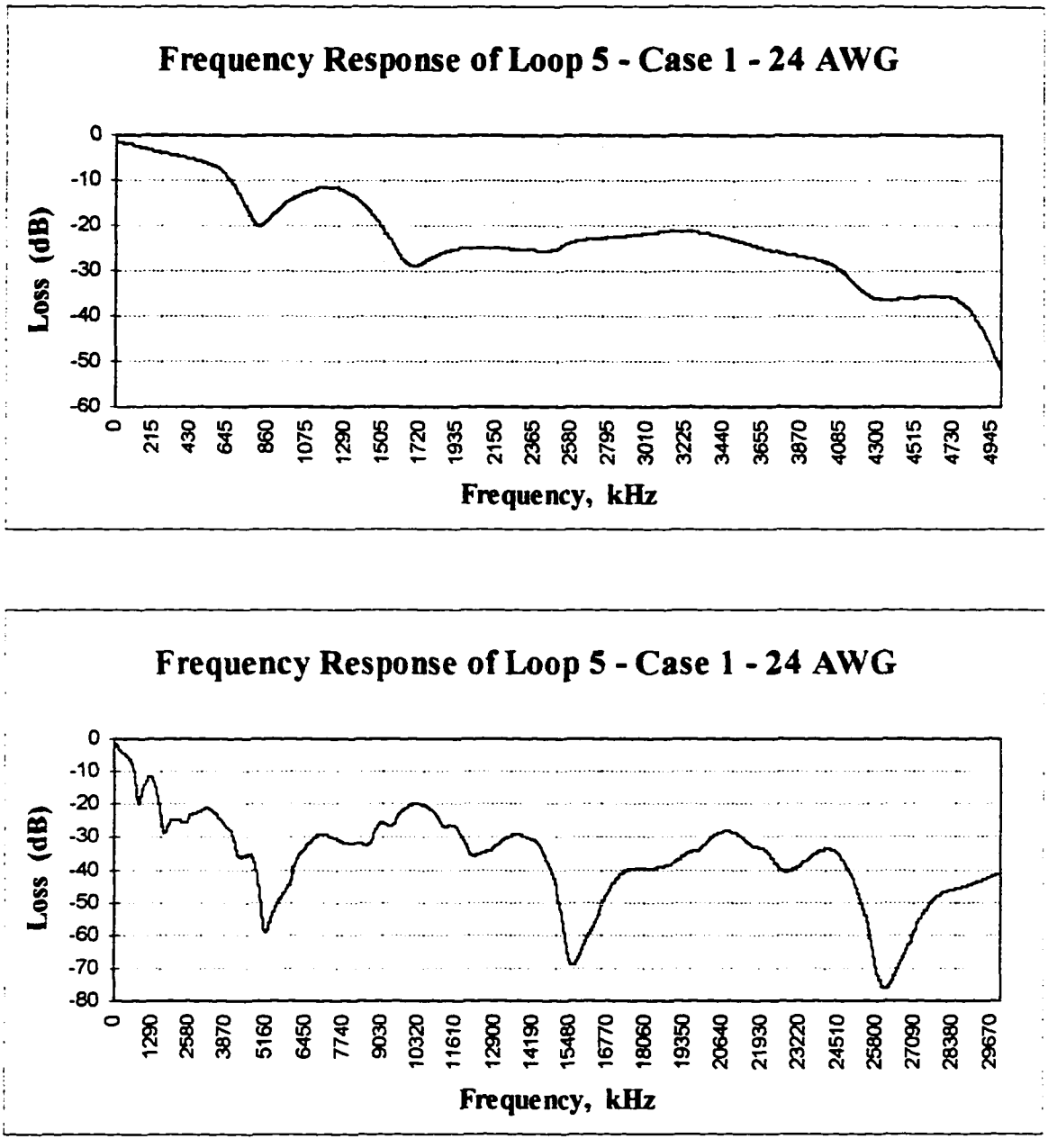

Figure 6.4 Frequency Response of Loop 5 (24 AWG), case with no termination and frequency range of 5MHz and 30 MHz.

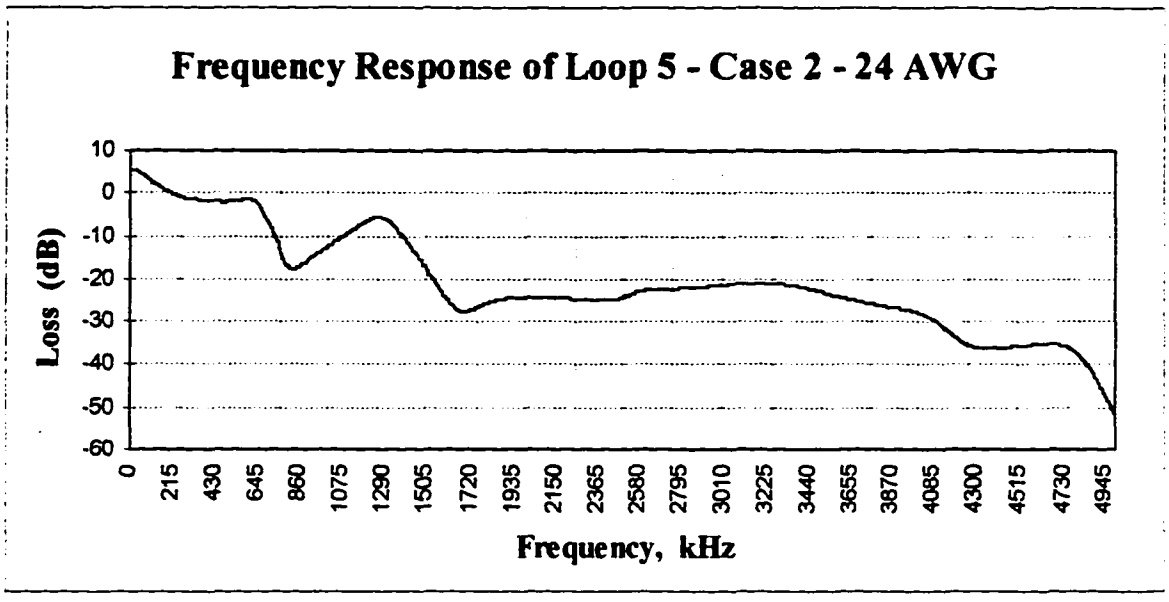

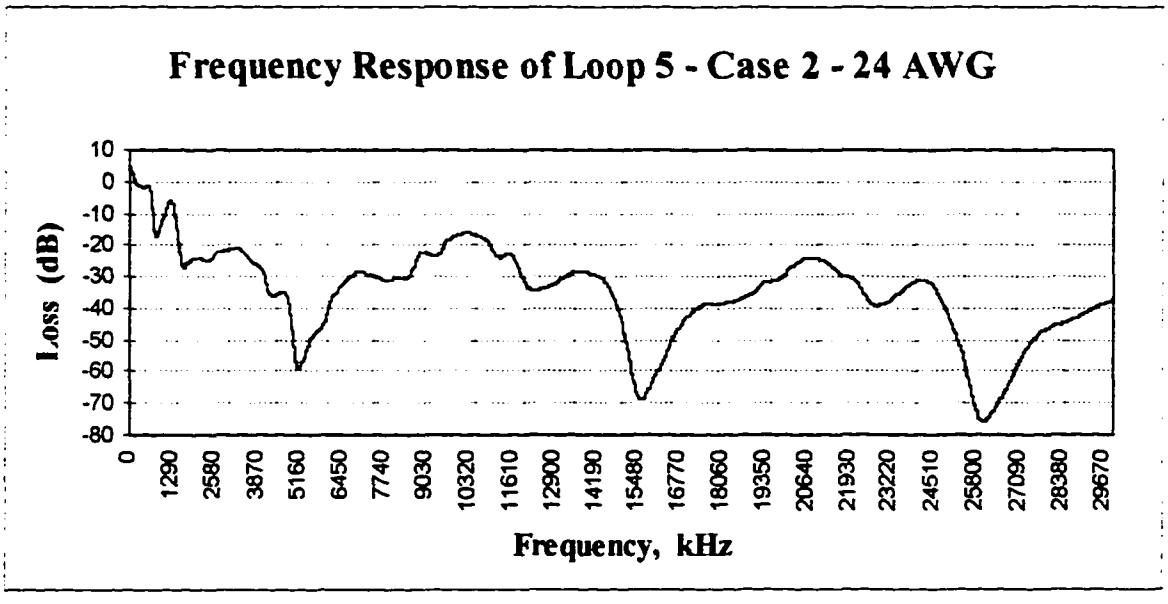

Figure 6.5 Frequency Response of Loop 5 (24 AWG), case with termination and frequency range of 5MHz and 30 MHz.

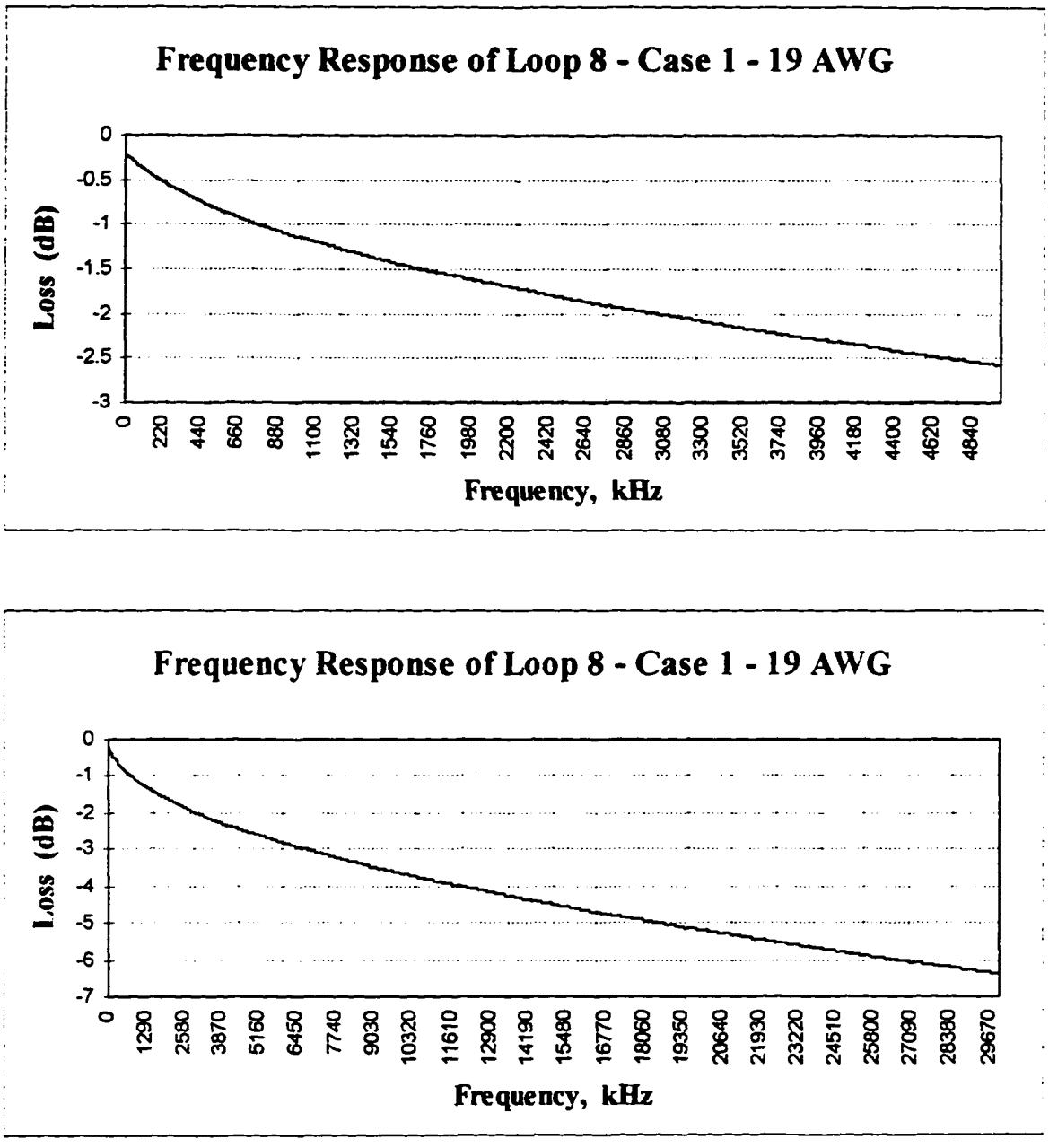

Figure 6.6 Frequency Response of Loop 8 (19 AWG), case with no termination and frequency range of 5MHz and 30 MHz.

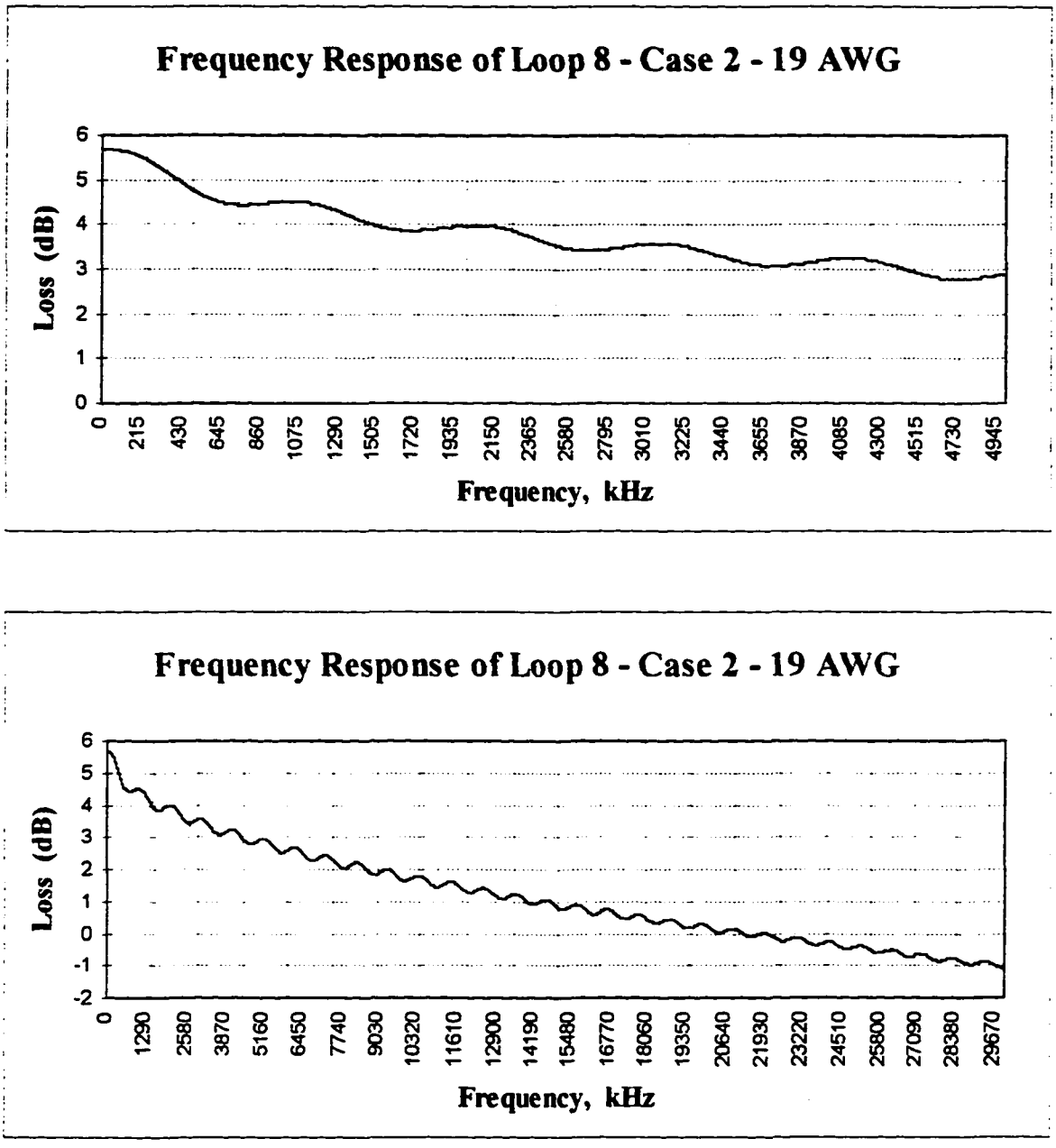

Figure 6.7 Frequency Response of Loop 8 (19 AWG), case with termination and frequency range of 5MHz and 30 MHz.

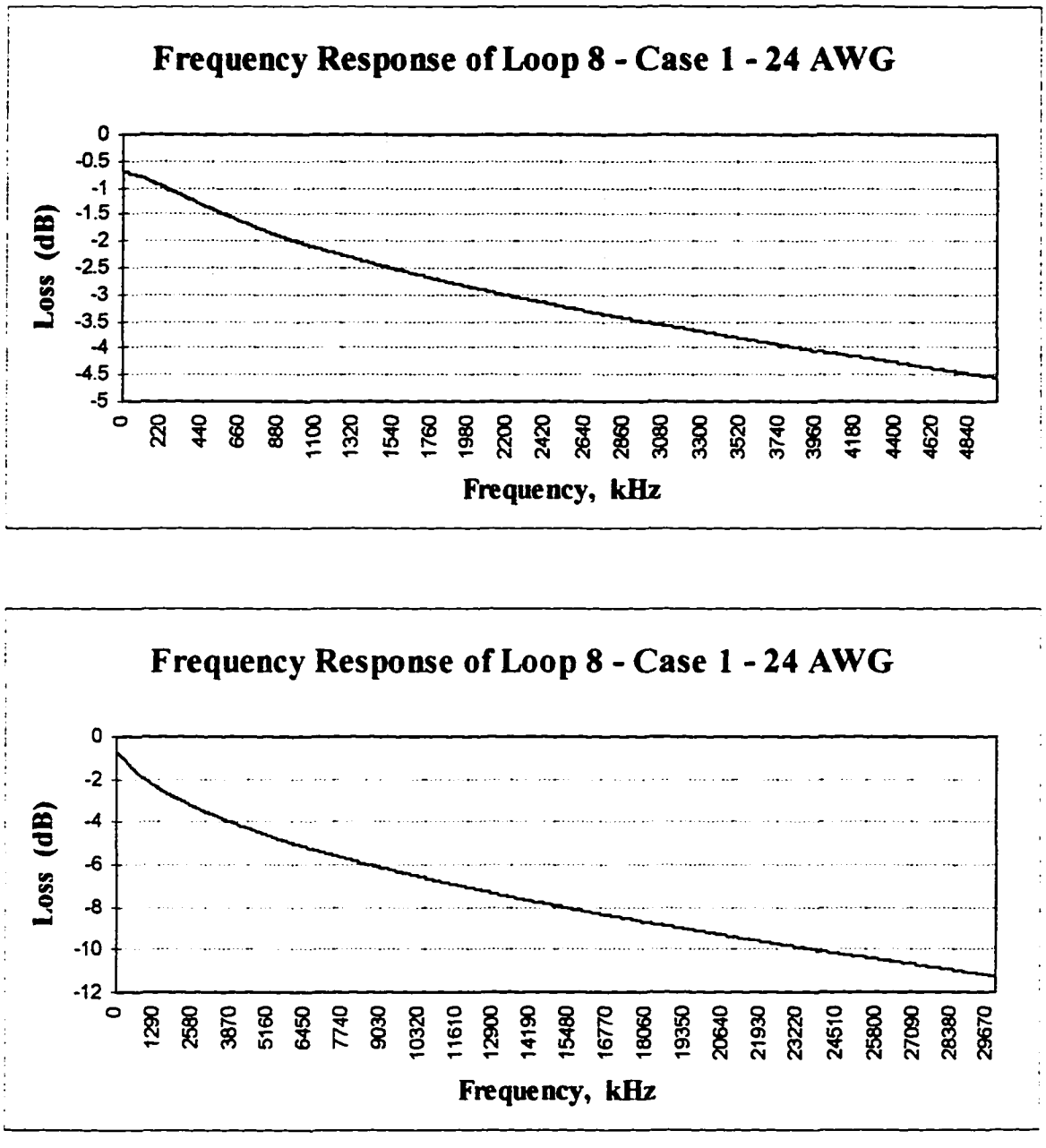

Figure 6.8 Frequency Response of Loop 8 (24 AWG), case with no termination and frequency range of 5MHz and 30 MHz.

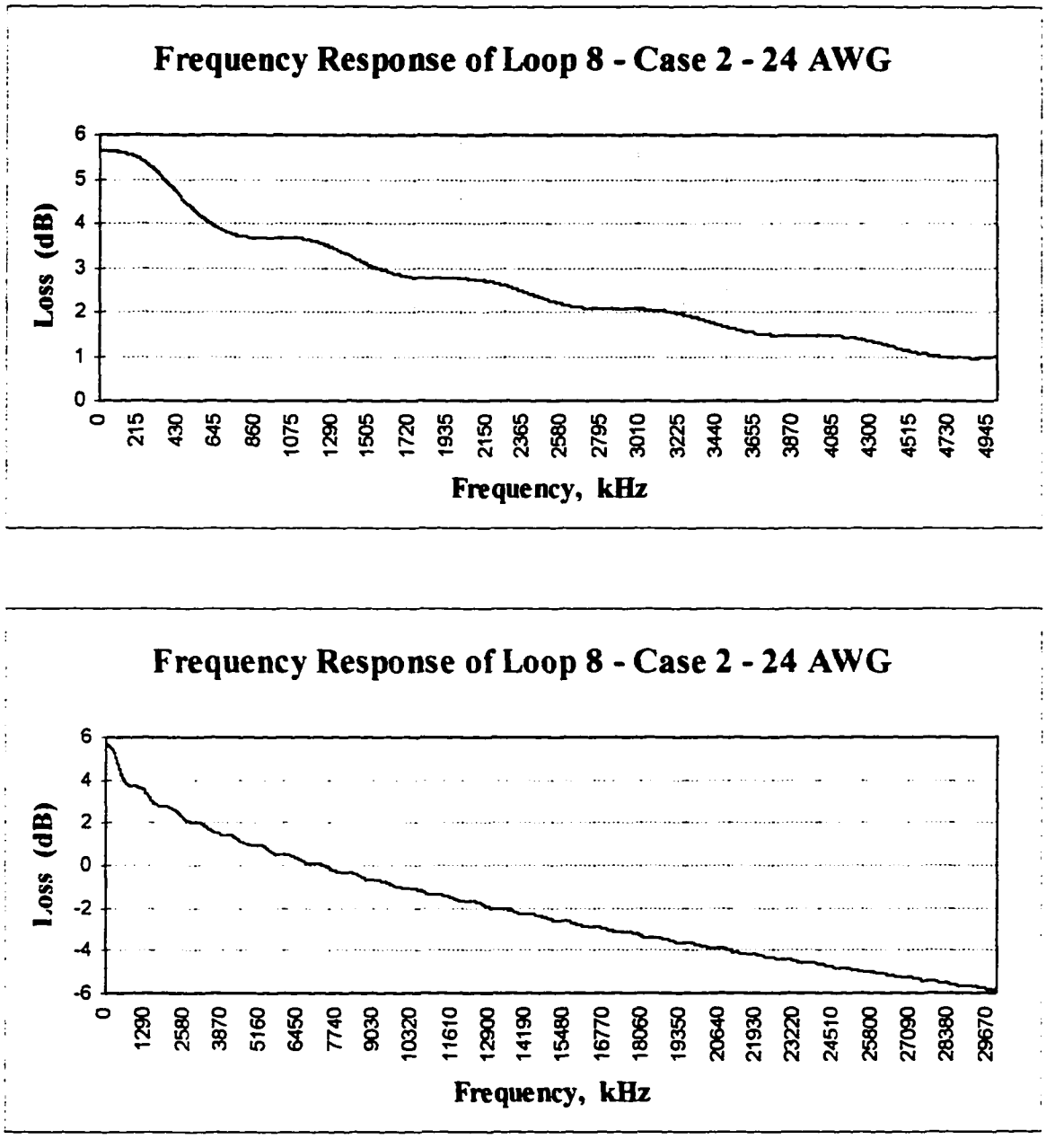

Figure 6.9 Frequency Response of Loop 8 (24 AWG), case with termination and frequency range of 5MHz and 30 MHz.

CHAPTER 7

7. Channel Modeling

A sequence of bits is mapped onto M level symbols. The data symbols are then transmitted as impulse stream through signal shaping filters (baseband or passband). The transmitter output is the convolution of the pulse shape and the symbol sequence. This signal can be interpreted as a sequence of superimposed pulses with the amplitude of each determined by a symbol value and occurring in a time interval T , i.e. equation 7.1.

$$\text{signal}(t) = \sum_{d=-\infty}^{\infty} \text{symbol} \times \text{impulse}(t - dT) \qquad (7.1)$$

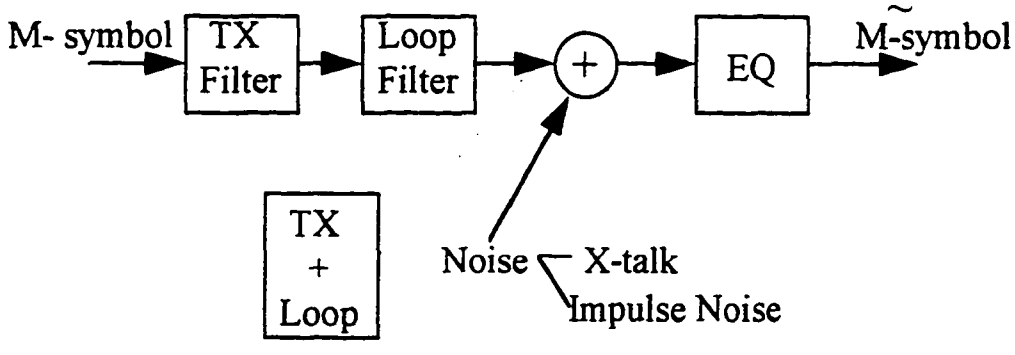

Figure 7.1 Simulated System.

The loop filter or the channel modifies the shape of the signal, where the loop loss is basically due to length of the cable, bridge taps and propagation loss. Another addition to the signal is the noise factor which can be in form of crosstalk (noise generated from other cables), impulse noise (generated from outside sources, i.e. electric devices) and additive white Gaussian noise (AWGN) which is uniform across the whole range of frequencies (flat spectrum). Proper equalization is needed at the receiver such that the signal recovery can be made possible.

7.1. Transmitter

Power spectral density (PSD) or frequency response of digital 2B1Q, 16-CAP, 8-PAM and 64-CAP transmitters is shown in figure 7.2 and 7.5 respectively. Scrambled bit sequence is fed to an encoder, which groups the bits into successive blocks. These are mapped onto multilevel symbols. For a bit rate of B_r and k bits per block, the symbols are generated at a rate of B_r/k and transmitted in a symbol period of T. Therefore, the symbol rate is $1/T$, which is equal to the symbol generation rate.

For one dimensional 2B1Q and 8-PAM code, the minimum bandwidth that a Nyquist filter can achieve theoretically is equal to half the symbol rate, therefore,

$$\text{Nyquist}_{\text{min. bandwidth, 1-D}} = \frac{1}{2T} \qquad (7.2)$$

The minimum bandwidth for two dimensional 16-CAP and 64-CAP for the same filter is twice that of the 1-D codes, i.e.,

$$\text{Nyquist}_{\text{min. bandwidth. 2-D}} = \frac{1}{T} \qquad (7.3)$$

For example, if symbol rate is 25.92 Mbauds/s , then with Nyquist shaping filters the bandwidth used will be 25.92/2 = 12.96 MHz for 1-D codes and 25.92 MHz for 2-D codes.

Nyquist minimum bandwidth is almost impossible to reach, therefore an extra bandwidth is added to it, which is called excess bandwidth or rolloff factor (α). Figure 7.8, 7.9, 7.10 and 7.11 shows 16-CAP, 2B1Q, 64-CAP and 8-PAM transmitters with rolloff factors of 15% and 50% and their respective spectrum utilization.

The Nyquist pulse offers reasonably good bandwidth efficiency, but it is not used for practical purposes, since it is very hard to maintain a long or large pulse and therefore requires an infinite duration to achieve the minimum spectrum of 1/2T. For that, square-root raised-cosine pulses are used by the transmitter filters used in this simulation study (more details about square-root raised-cosine pulses are given in appendix C).

For the 16-CAP passband transmitter in figure 7.2 the bit rate B_r is equal to 51.84 Mbits/s, and since it is 16-CAP blocks of 4 bits are assembled, therefore the symbol rate is 51.84/4 = 12.96 Mbauds/s. The rolloff factor is 15% , and the guard band is (ψ) 120 kHz. The transfer function's total bandwidth is 12960 x 1.15 = 14904 kHz, and the spectrum's center frequency can be calculated as,

$$120 + 14904/2 = 7572 \text{ kHz}$$

Through the center frequency the lowest and highest frequencies of the bandwidth that will be used can be determined.

In similar fashion for the 2B1Q baseband transmitter in figure 7.2 the bit rate B_r is equal to 51.84 Mbits/s, and since it has four levels, blocks of 2 bits are assembled, therefore the symbol rate is 51.84/2 = 25.92 Mbauds/s. The

rolloff factor is 15% , and the guard band (ψ) is 120 kHz. The transfer function's total bandwidth is 25920 x 1.15 = 29808 kHz, and the spectrum's upper band limit can be calculated as,

$$120 + 29808/2 = 15024 \text{ kHz}$$

Spectrum for 64-CAP and 8-PAM can be determined in the same way. Tables 7.2, 7.5, 7.8 and 7.11 gives the calculations for all other rates and tables 7.3, 7.6, 7.9 and 7.12 provide calculations when the rolloff factor (α) is 50% for B_r = 51.84 Mbits/s.

The guard band used has the purpose of separating the different bands, which can be divided into the transmitter band and receiver band, since transmission from the transmitter and receiver is done on the same cable. Therefore, avoiding inter-symbol interference (ISI) type of problems between them. Usually the values for ψ are taken as 5% to 15% of the symbol rate.

7.2. Transmitter and Loop Response Spectrum

When the transmitter and loop transfer functions are combined the total response can be seen in figures 7.3, 7.4, 7.6 and 7.7. The loss is calculated for each loop through the power loss equation 7.4 .

$$\text{Loop}_{\text{power loss, dB}} = 10 \log \left(\frac{P_{in}}{P_{out}} \right) \qquad (7.4)$$

where P_{in} is the average power of the symbols before transmission and P_{out} is the average power after they have gone through the channel. As seen in figures mentioned, when the signal passes through the transmitter and loop sequence it is decayed. Some of the worst loops (i.e., loop # 6, case 1) shows a steep decay and nulls, while simple loops (i.e., loop # 8, case 2) display very little degradation of the signal. The power loss is smaller for 64-CAP than 16-CAP and 8-PAM than 2B1Q, this is due to the fact that the spectrum has changed from one category to another, and since in 64-CAP and 8-PAM smaller frequencies are used, more power is retained. Tables 7.4, 7.7, 7.10 and 7.13 gives the power loss for 16-CAP, 2B1Q, 64-CAP and 8-PAM respectively in sequence of different rates for all PDS loops presented.

Figures 7.12, 7.13, 7.14 and 7.15 display the performance of the codes for all the rates considered (T1 to OC-1). From these figures a peak-power to average power (PAR) relationship with loss can be obtained. PAR is the ratio of squared magnitude of the maximum amplitude of a signal and its average power. It is a indicator of a line code's susceptibility to nonlinear channel impairments, and quantization noise (when A/D is performed on the receiver

side). Usually a bigger PAR is responsible in making a code more susceptible to these impairments. Also, a signal with larger PAR will generate more crosstalk for a fixed average transmit power. For one dimensional codes the PAR can be defined as,

$$PAR_{1\text{-}D} = \frac{(\text{Largest Symbol Power})^2}{\text{Average Power}} \qquad (7.5)$$

and for two dimensional, $PAR_{2\text{-}D}$ is equal to:

$$\frac{\left[(\text{Larg. Real Symb. Pwr})^2 + (\text{Lar. Imag. Symb. Pwr})^2\right]}{\text{Average Power}} \qquad (7.6)$$

Therefore, for 16-CAP the average power is:

$$\text{Avg. Pwr.} = 4.[\,(1)^2 + (1)^2 + (1)^2 + (3)^2 + (3)^2 + (1)^2 + (3)^2 + (3)^2\,]/16$$

$$= 10$$

And the peak-power to average power ratio (PAR) is:

$$PAR_{16\text{-}CAP} = \frac{[(+3)^2 + (+3)^2]}{10} = 1.80$$

Table 7.1. Peak-power to average power (PAR) values for CAP codes and their conceivable equivalent PAM codes.

PAR for CAP Codes	PAR for PAM Codes
$PAR_{16\text{-}CAP} = 1.80$	$PAR_{2B1Q} = 1.80$
$PAR_{32\text{-}CAP} = 1.70$	$PAR_{6\text{-}PAM} = 2.14$
$PAR_{64\text{-}CAP} = 2.33$	$PAR_{8\text{-}PAM} = 2.33$
$PAR_{128\text{-}CAP} = 2.07$	$PAR_{10\text{-}PAM} = 2.45$

In 2-D coding it is verified that as the constellation become denser, the PAR is augmented, with the exception of constellation with odd powers of two. Examples of this are 32 and 128 point constellations, which have 5 and 7 as powers of two. One of the better CAP codes are 32-CAP, since the bandwidth and PAR are both reduced for this code. This reduction is achieved by eliminating the four highest voltage pairs in the constellation, considering that only eight pairs are required per quadrant.

For 1-D codes when the number of levels is increased, even though a smaller bandwidth is achieved the PAR grows. Thus, the assertion "narrower the bandwidth more the inter-symbol interference (ISI)" becomes true. Even for 2-D codes, with the growth of constellation levels a smaller spectrum is achieved, but the unfavorable aspect of the ISI start taking its toll.

7.3. Efficiency Factor

Line codes effectiveness can be demonstrated through usage of smaller bandwidth for a fixed data rate or by providing higher data rate for a fixed bandwidth. Both cases lead to an improvement in efficiency.

Parameters that will measure sufficiency of line codes are: The symbol period (T), symbol transmission rate (1/T), bit rate (B_r), bandwidth utilized (W) and the efficiency factor ($E_{factor} = B_r / W$).

A point of reference for the efficiency factor is the polar code examined in chapter three, it transmits 1 bit per level, consequently the symbol rate is equal to the bit rate, i.e. $B_r = 1/T$. From the transfer function and figure 3.10 the effective bandwidth utilized by the polar code for a symbol period of T is 1/T.

Therefore the efficiency factor for the polar code can be summarized as,

$$E_{factor} = \frac{B_r}{W} = \frac{1/T}{1/T} = 1 \text{ bit per second/Hz}$$

As multilevel coding comes in, efficiency factor is improved dramatically, table 7.2 demonstrate some line codes and their properties. Examples of two dimensional multilevel encoding are: CAP-16, CAP-32 and CAP-64.

Another parameter that ameliorate efficiency is spectral shaping of a codes impulse response. The pulses used are special cases of a family of pulses called raised-cosine family, they offer certain advantages over the simple Nyquist pulse in that they have longer duration than Nyquist pulse.

From equation 7.2 a multilevel code using Nyquist type of filter utilize a bandwidth (W) larger than the minimum bandwidth achievable theoretically (1/2T for 1-D and 1/T for 2-D). The excess bandwidth or rolloff factor therefore can be determined as,

$$\alpha = W - \frac{1}{2T} \qquad \text{(1-D)} \qquad (7.7)$$

$$\alpha = W - \frac{1}{T} \qquad \text{(2-D)} \qquad (7.8)$$

The excess bandwidth can be expressed as a percentage of Nyquist minimum, therefore,

$$\alpha = \frac{\left[W - \frac{1}{2T}\right]}{\frac{1}{2T}} \qquad \text{(1-D)} \qquad (7.9)$$

$$\alpha = \frac{\left[W - \frac{1}{T}\right]}{\frac{1}{T}} \qquad \text{(2-D)} \qquad (7.10)$$

Hence, for all 1-D and 2-D line codes that employ Nyquist shaping filter or square-root raised-cosine (present study), equation 7.9 and 7.10 can give the bandwidth that will be used, given the excess bandwidth.

Assume the bit rate (B_r) under consideration is 51.84 Mbits/s, the excess bandwidth is 15% and 50% . The design parameters for spectral shaping and usage of the bandwidth for 2B1Q and 16-CAP codes are as follows:

2B1Q transmits 2 bits per symbol, hence the symbol rate is:

$$\frac{1}{T} = 25.92 \text{ Mbauds/s}$$

for 50% excess bandwidth the total bandwidth utilized can be found through equation 7.9 as:

$$W = \frac{1}{2T} \cdot \alpha + \frac{1}{2T} = 19.44 \text{ MHz}$$

And for 15% excess bandwidth the total bandwidth utilized is 14.9 MHz. Efficiency due to spectral shaping for $\alpha = 0.5$ is 1.33 and for $\alpha = 0.15$ is 1.74.

16-CAP transmits 4 bits per symbol, hence the symbol rate is:

$$\frac{1}{T} = 12.96 \text{ Mbauds/s}$$

for 50% excess bandwidth the total bandwidth utilized can be found through equation 7.10 as:

$$W = \frac{1}{T} \cdot \alpha + \frac{1}{T} = 19.44 \text{ MHz}$$

And for 15% excess bandwidth the total bandwidth utilized is 14.9 MHz. Efficiency due to spectral shaping for $\alpha = 0.5$ is 1.33 and for $\alpha = 0.15$ is 1.74.

As seen in table 7.3 and 7.4 both 2B1Q and 16-CAP codes offer same performance theoretically (uniform total bandwidth and spectral shaping efficiency). The effective bandwidth as displayed in figure 7.8 and 7.9 is less than the total bandwidth, since filter cutoff points are considered in the graphs. Even though both codes have same performance, 16-CAP outperform 2B1Q due to the passband characteristics versus baseband nature of the latter.

An important aspect of passband filtering is the shift in the spectrum, such that for transmission from transmitter is able to use a different spectrum as compared to the one used by transmission from receiver. This would avoid interference between both signals transmitted on same cable pair.

Table 7.2. Properties of line codes, when efficiency is investigated through number of levels and bits per symbol relationship.

Code	Number of Levels	Transmission Rate per Symbol (Bits/Symbol)	Efficiency (bps/Hz)
AMI	3	1	1
HDB3	3	1	1
B6ZS	3	1	1
Diphase	2	0.5	0.5
4B3T	3	1.33	1.33
PR-4	4	2	2
2B1Q	4	2	2
16-CAP	16	4	2
32-CAP	32	5	2.5
8-PAM	8	3	3
64-CAP	64	6	3

Table 7.3. Properties of line codes, when efficiency is investigated through spectral shaping with excess bandwidth equal to 50% and bit rate of 51.84 Mbits/s.

Code	Number of Levels	Transmission Rate per Symbol (Bits/Symbol)	Total Bandwidth Utilization when $\alpha = 0.5$	Efficiency (bps/Hz)
AMI	3	1	38.88	1.33
HDB3	3	1	38.88	1.33
B6ZS	3	1	38.88	1.33
Diphase	2	0.5	77.76	1.33
4B3T	3	1.33	29.23	1.33
PR-4	4	2	19.44	1.33
2B1Q	4	2	19.44	1.33
16-CAP	16	4	19.44	1.33
32-CAP	32	5	15.55	1.33
8-PAM	8	3	12.96	1.33
64-CAP	64	6	12.96	1.33

Table 7.4. Properties of line codes, when efficiency is investigated through spectral shaping with excess bandwidth equal to 15% and bit rate of 51.84 Mbits/s.

Code	Number of Levels	Transmission Rate per Symbol (Bits/Symbol)	Total Bandwidth Utilization when $\alpha = 0.15$	Efficiency (bps/Hz)
AMI	3	1	29.81	1.74
HDB3	3	1	29.81	1.74
B6ZS	3	1	29.81	1.74
Diphase	2	0.5	59.62	1.74
4B3T	3	1.33	22.41	1.74
PR-4	4	2	14.90	1.74
2B1Q	4	2	14.90	1.74
16-CAP	16	4	14.90	1.74
32-CAP	32	5	11.92	1.74
8-PAM	8	3	9.94	1.74
64-CAP	64	6	9.94	1.74

Table 7.5. Transmitter rates and filter coefficients for a 16-point constellation, rolling factor (α) = 0.15, guard band (ψ) = 120 kHz, oversampling ratio (ξ) = T/3, Number of taps = 128.

	Bit Rate (Mb/s)	Baud Rate (Mbaud/s)	Sampling freq. (kHz)	Center freq. (kHz)
T1	1.544	0.386	1158.0	341.95
E1	2.048	0.512	1536.0	414.40
T2	6.312	1.578	4734.0	1027.35
E2	8.448	2.112	6336.0	1334.40
E3	34.368	8.592	25776.0	5060.40
T3	44.736	11.184	33552.0	6550.80
OC-1	51.840	12.960	38880.0	7572.00

Table 7.6. Transmitter rates and filter coefficients for a 16-point constellation, rolling factor (α) = 0.5, guard band (ψ) = 120 kHz, oversampling ratio (ξ) = T/3, Number of taps = 128.

	Bit Rate (Mb/s)	Baud Rate (Mbaud/s)	Sampling freq. (kHz)	Center freq. (kHz)
OC-1	51.840	12.960	38880.0	9840.00

Table 7.7. Attenuation when 16-CAP Transmitter and PDS-loops are combined for T1, E1, T2, E2, E3, T3 and OC-1 rates.

Loop # (case #)	$L_{loss, dB}$ (T1)	$L_{loss, dB}$ (E1)	$L_{loss, dB}$ (T2)	$L_{loss, dB}$ (E2)	$L_{loss, dB}$ (E3)	$L_{loss, dB}$ (T3)	$L_{loss, dB}$ (OC-1)
Loop 1 (case 1)	10.44	11.07	15.23	16.72	26.20	28.24	29.43
Loop 1 (case 2)	6.13	7.00	12.14	13.84	24.44	26.50	27.80
Loop 2 (case 1)	8.66	9.11	12.44	13.95	22.64	24.09	25.23
Loop 2 (case 2)	4.52	5.23	8.80	10.43	19.33	20.67	21.91
Loop 3 (case 1)	8.98	9.64	14.49	16.00	20.36	21.56	22.18
Loop 3 (case 2)	5.22	6.18	11.84	13.56	17.59	18.76	19.37
Loop 4 (case 1)	9.89	11.01	13.42	14.03	18.00	18.93	19.59
Loop 4 (case 2)	6.84	8.17	10.28	10.93	14.87	15.80	16.49
Loop 5 (case 1)	9.49	10.21	15.26	17.00	26.78	27.90	28.86
Loop 5 (case 2)	6.06	6.35	11.16	12.91	22.71	24.05	24.87
Loop 6 (case 1)	10.92	11.53	15.63	17.24	26.99	29.51	30.97
Loop 6 (case 2)	6.69	7.52	11.97	13.70	23.57	25.95	27.45
Loop 7 (case 1)	11.21	12.00	17.34	19.04	27.08	28.93	29.91
Loop 7 (case 2)	7.35	8.39	14.48	16.38	24.53	26.31	27.21
Loop 8 (case 1)	6.21	6.31	7.02	7.28	9.31	9.87	10.21
Loop 8 (case 2)	0.03	0.28	1.30	1.61	3.79	4.36	4.71

Table 7.8. Transmitter rates and filter coefficients for a 64-point constellation, rolling factor (α) = 0.15, guard band (ψ) = 120 kHz, oversampling ratio (ξ) = T/3, Number of taps = 128.

	Bit Rate (Mb/s)	Baud Rate (Mbaud/s)	Sampling freq. (kHz)	Center freq. (kHz)
T1	1.544	0.257	771.9	268.0
E1	2.048	0.341	1023.9	316.3
T2	6.312	1.052	3156.0	724.9
E2	8.448	1.408	4224.0	929.6
E3	34.368	5.728	17184.0	3413.6
T3	44.736	7.456	22368.0	4407.2
OC-1	51.840	8.640	25920.0	5088.0

Table 7.9. Transmitter rates and filter coefficients for a 64-point constellation, rolling factor (α) = 0.5, guard band (ψ) = 120 kHz, oversampling ratio (ξ) = T/3, Number of taps = 128.

	Bit Rate (Mb/s)	Baud Rate (Mbaud/s)	Sampling freq. (kHz)	Center freq. (kHz)
OC-1	51.840	8.640	25920.0	6600.0

Table 7.10. Attenuation when 64-CAP Transmitter and PDS-loops are combined for T1, E1, T2, E2, E3, T3 and OC-1 rates.

Loop # (case #)	$L_{loss, dB}$ (T1)	$L_{loss, dB}$ (E1)	$L_{loss, dB}$ (T2)	$L_{loss, dB}$ (E2)	$L_{loss, dB}$ (E3)	$L_{loss, dB}$ (T3)	$L_{loss, dB}$ (OC-1)
Loop 1 (case 1)	10.02	10.47	13.64	14.89	23.21	25.24	26.41
Loop 1 (case 2)	5.41	6.07	10.19	11.68	21.11	23.36	24.65
Loop 2 (case 1)	8.45	8.75	10.82	12.05	19.95	21.88	22.86
Loop 2 (case 2)	3.99	4.51	7.24	8.40	16.62	18.63	19.54
Loop 3 (case 1)	8.60	9.01	12.52	14.02	19.12	19.94	20.76
Loop 3 (case 2)	4.45	5.14	9.66	11.30	16.50	17.22	18.05
Loop 4 (case 1)	9.10	9.77	**14.19**	**13.82**	16.98	17.75	18.27
Loop 4 (case 2)	5.64	6.62	**11.80**	**10.93**	13.84	14.60	15.14
Loop 5 (case 1)	9.18	9.55	13.48	14.81	23.97	26.14	27.06
Loop 5 (case 2)	5.78	6.18	9.59	10.78	19.87	22.37	22.97
Loop 6 (case 1)	10.50	10.95	13.83	15.20	23.84	26.00	27.22
Loop 6 (case 2)	5.96	6.62	10.14	11.52	20.45	22.63	23.76
Loop 7 (case 1)	10.62	11.18	15.24	16.84	24.65	26.36	27.41
Loop 7 (case 2)	6.41	7.21	12.14	13.90	22.22	23.89	24.92
Loop 8 (case 1)	6.36	6.43	6.96	7.17	8.82	9.27	9.56
Loop 8 (case 2)	0.03	0.19	1.14	1.42	3.26	3.74	4.03

Table 7.11. Transmitter rates and filter coefficients for 2B1Q code, rolling factor (α) = 0.15, guard band (ψ) = 120 kHz, oversampling ratio (ξ) = T/3, Number of taps = 128.

	Bit Rate (Mb/s)	Baud Rate (Mbaud/s)	Sampling freq. (kHz)	Upper Band Limit (kHz)
T1	1.544	0.772	2316.0	563.90
E1	2.048	1.024	3072.0	708.80
T2	6.312	3.156	9468.0	1934.70
E2	8.448	4.224	12672.0	2548.80
E3	34.368	17.184	51552.0	10000.80
T3	44.736	22.368	67104.0	12981.60
OC-1	51.840	25.920	77760.0	15024.00

Table 7.12. Transmitter rates and filter coefficients for 2B1Q code, rolling factor (α) = 0.5, guard band (ψ) = 120 kHz, oversampling ratio (ξ) = T/3, Number of taps = 128.

	Bit Rate (Mb/s)	Baud Rate (Mbaud/s)	Sampling freq. (kHz)	Upper Band Limit (kHz)
OC-1	51.840	25.920	77760.0	19560.00

Table 7.13. Attenuation when 2B1Q Transmitter and PDS-loops are combined for T1, E1, T2, E2, E3, T3 and OC-1 rates.

Loop # (case #)	$L_{loss, dB}$ (T1)	$L_{loss, dB}$ (E1)	$L_{loss, dB}$ (T2)	$L_{loss, dB}$ (E2)	$L_{loss, dB}$ (E3)	$L_{loss, dB}$ (T3)	$L_{loss, dB}$ (OC-1)
Loop 1 (case 1)	10.10	10.80	14.11	15.05	19.75	20.52	20.84
Loop 1 (case 2)	4.32	5.16	8.87	9.79	13.43	13.80	13.93
Loop 2 (case 1)	8.52	9.35	12.22	13.10	17.72	18.59	18.97
Loop 2 (case 2)	3.03	3.97	7.29	8.17	12.20	12.95	13.04
Loop 3 (case 1)	8.91	9.64	12.88	13.76	17.60	18.40	18.83
Loop 3 (case 2)	3.50	4.38	8.12	9.02	12.47	13.02	13.29
Loop 4 (case 1)	9.11	9.43	12.81	13.45	16.89	17.56	18.01
Loop 4 (case 2)	3.97	4.45	8.21	8.91	12.02	12.44	12.78
Loop 5 (case 1)	9.24	10.04	13.62	14.55	19.11	19.71	20.07
Loop 5 (case 2)	4.06	4.87	8.54	9.43	13.11	13.38	13.21
Loop 6 (case 1)	10.45	11.27	14.49	15.44	20.14	20.86	21.15
Loop 6 (case 2)	4.62	5.55	9.08	9.97	13.42	13.78	13.86
Loop 7 (case 1)	10.68	11.45	15.03	15.99	20.44	21.12	21.40
Loop 7 (case 2)	4.93	5.83	9.68	10.57	13.73	14.01	14.10
Loop 8 (case 1)	6.22	6.39	7.43	7.76	9.99	10.52	10.91
Loop 8 (case 2)	0.03	0.31	1.60	1.97	4.34	4.90	5.30

Table 7.14. Transmitter rates and filter coefficients for 8-PAM code, rolling factor (α) = 0.15, guard band (ψ) = 120 kHz, oversampling ratio (ξ) = T/3, Number of taps = 128.

	Bit Rate (Mb/s)	Baud Rate (Mbaud/s)	Sampling freq. (kHz)	Upper Band Limit (kHz)
T1	1.544	0.515	1544.0	415.93
E1	2.048	0.683	2048.0	512.53
T2	6.312	2.104	6312.0	1329.80
E2	8.448	2.816	8448.0	1739.20
E3	34.368	11.456	34368.0	6707.20
T3	44.736	14.912	44736.0	8694.40
OC-1	51.840	17.280	51840.0	10056.00

Table 7.15. Transmitter rates and filter coefficients for 8-PAM code, rolling factor (α) = 0.5, guard band (ψ) = 120 kHz, oversampling ratio (ξ) = T/3, Number of taps = 128.

	Bit Rate (Mb/s)	Baud Rate (Mbaud/s)	Sampling freq. (kHz)	Upper Band Limit (kHz)
OC-1	51.840	17.280	51840.0	13080.00

Table 7.16. Attenuation when 8-PAM Transmitter and PDS-loops are combined for T1, E1, T2, E2, E3, T3 and OC-1 rates.

Loop # (case #)	L_{loss}, dB (T1)	L_{loss}, dB (E1)	L_{loss}, dB (T2)	L_{loss}, dB (E2)	L_{loss}, dB (E3)	L_{loss}, dB (T3)	L_{loss}, dB (OC-1)
Loop 1 (case 1)	9.44	10.07	13.09	13.99	18.66	19.50	19.99
Loop 1 (case 2)	3.38	4.21	7.77	8.73	12.70	13.33	13.64
Loop 2 (case 1)	8.08	8.53	11.18	12.09	16.83	17.55	17.95
Loop 2 (case 2)	2.32	3.00	6.22	7.15	11.71	12.23	12.41
Loop 3 (case 1)	8.22	8.87	11.49	12.49	16.84	17.47	17.85
Loop 3 (case 2)	2.55	3.38	6.72	7.80	12.00	12.43	12.69
Loop 4 (case 1)	8.49	9.13	11.97	12.71	16.15	16.84	17.11
Loop 4 (case 2)	2.97	3.85	7.30	8.13	11.53	12.06	12.23
Loop 5 (case 1)	8.74	9.29	12.47	13.46	18.34	19.03	19.32
Loop 5 (case 2)	3.29	4.04	7.42	8.40	12.66	13.18	13.29
Loop 6 (case 1)	9.78	10.38	13.42	14.35	19.04	19.92	20.40
Loop 6 (case 2)	3.71	4.50	8.02	8.94	12.79	13.41	13.65
Loop 7 (case 1)	9.87	10.59	13.79	14.81	19.42	20.24	20.69
Loop 7 (case 2)	3.89	4.78	8.48	9.49	13.17	13.72	13.95
Loop 8 (case 1)	6.28	6.39	7.22	7.50	9.44	9.97	10.25
Loop 8 (case 2)	0.03	0.18	1.31	1.64	3.77	4.31	4.60

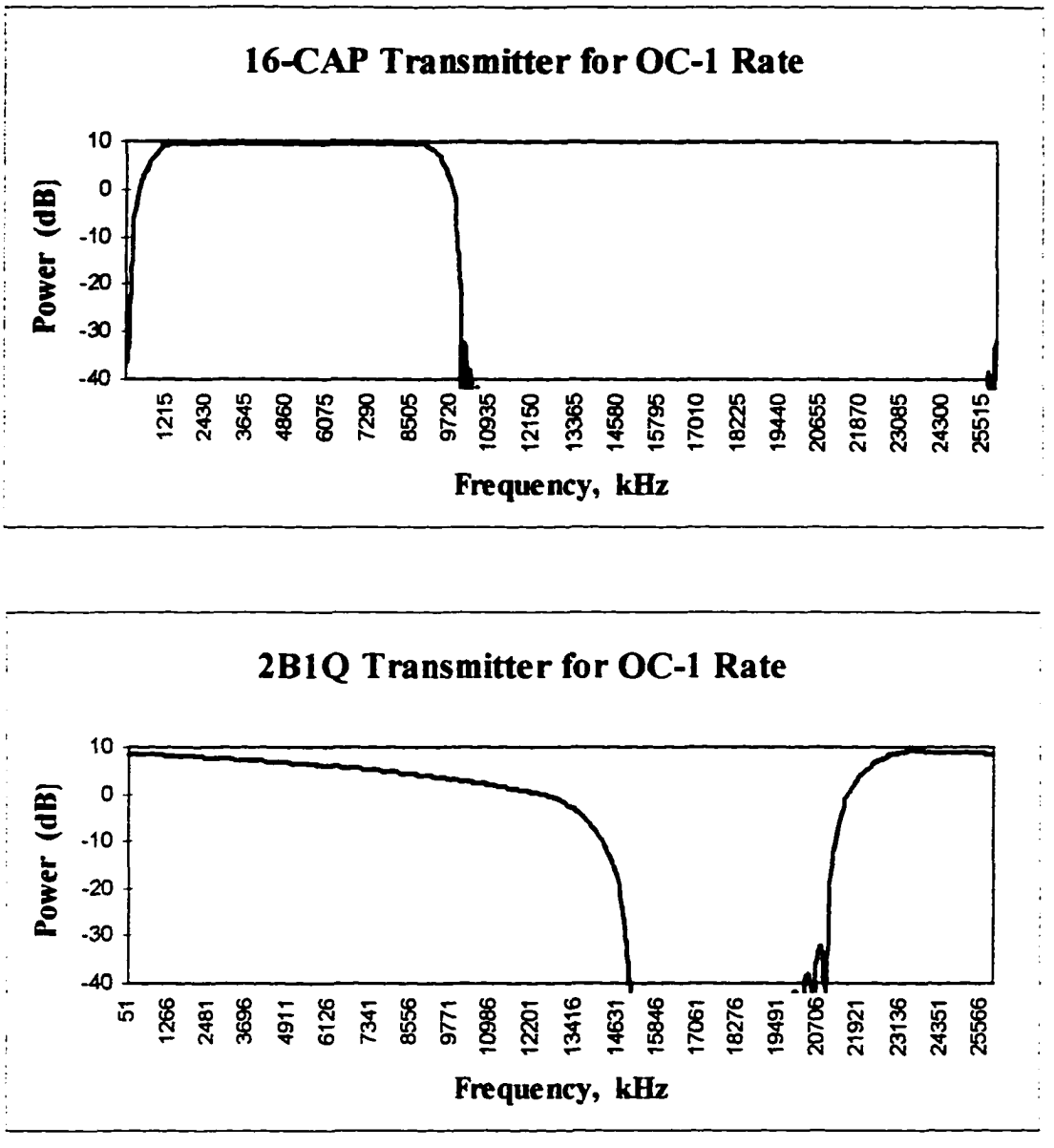

Figure 7.2 16-CAP and 2B1Q transmitter for OC-1 rate, rolling factor of 15%, guard band of 120 kHz, oversampling ratio of 3 and raised cosine shaping filter with 128 taps.

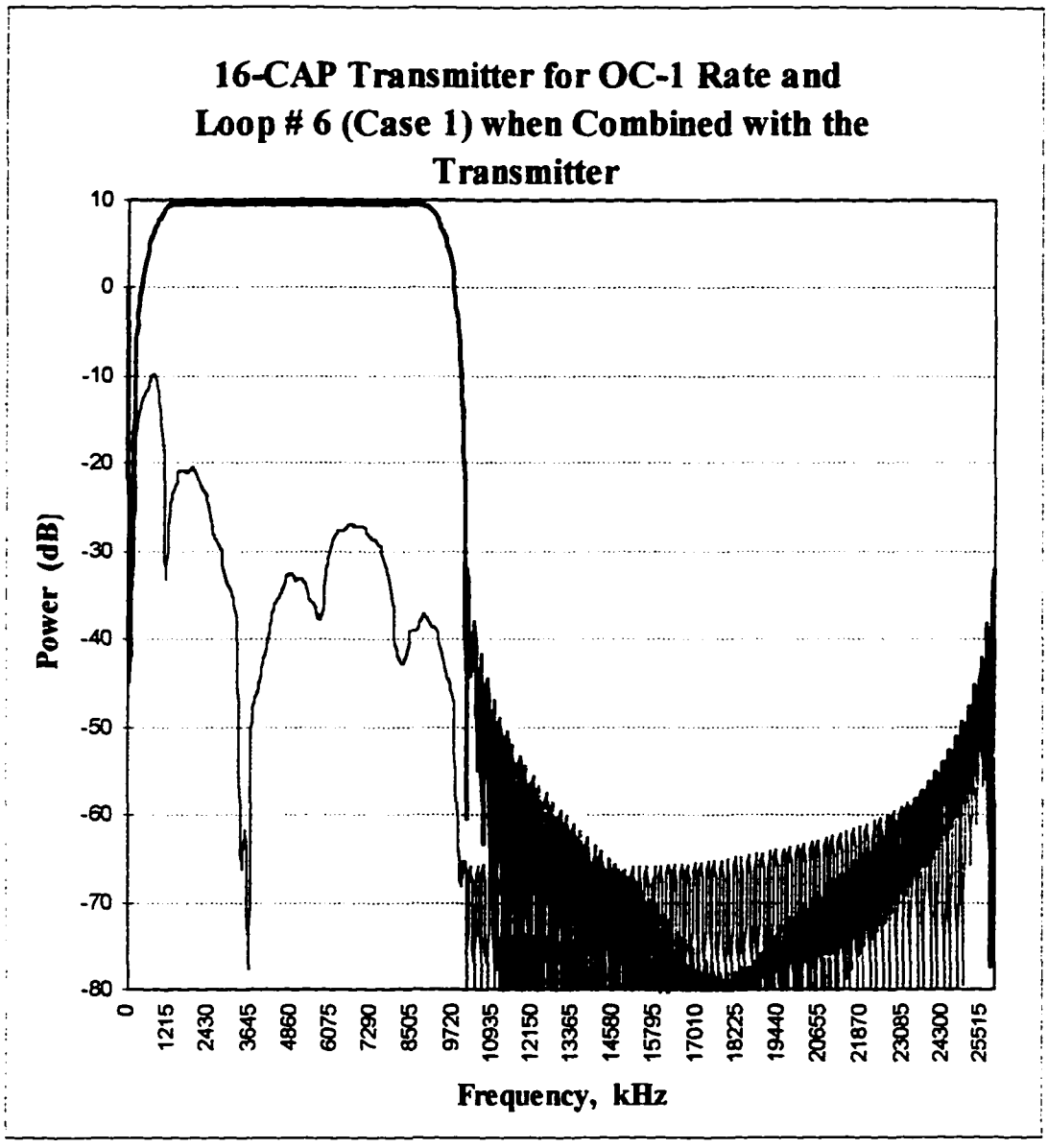

Figure 7.3 16-CAP transmitter for OC-1 rate and case 1 of loop 6 when combined with the transmitter filter.

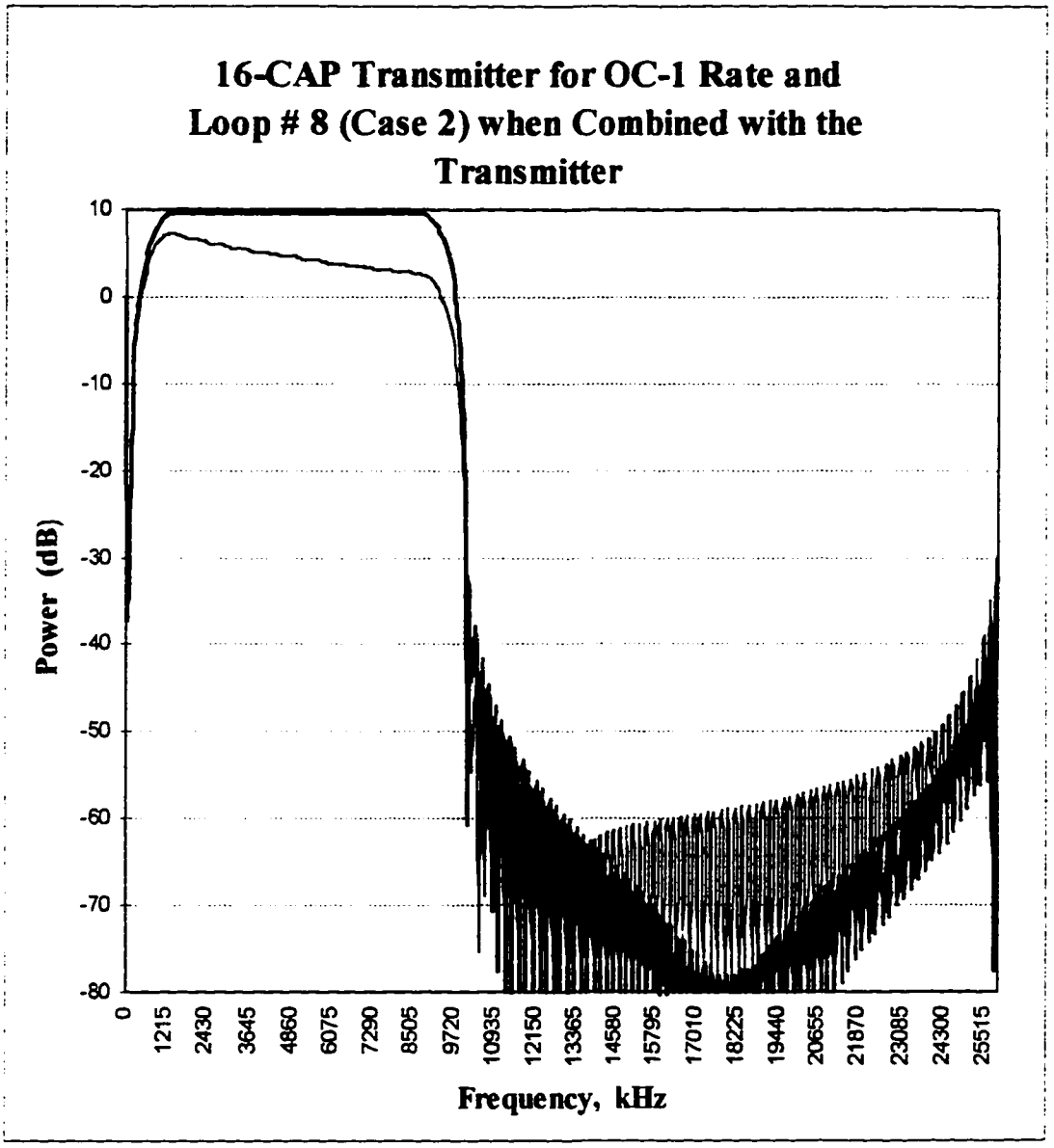

Figure 7.4 16-CAP transmitter for OC-1 rate and case 2 of loop 8 when combined with the transmitter filter.

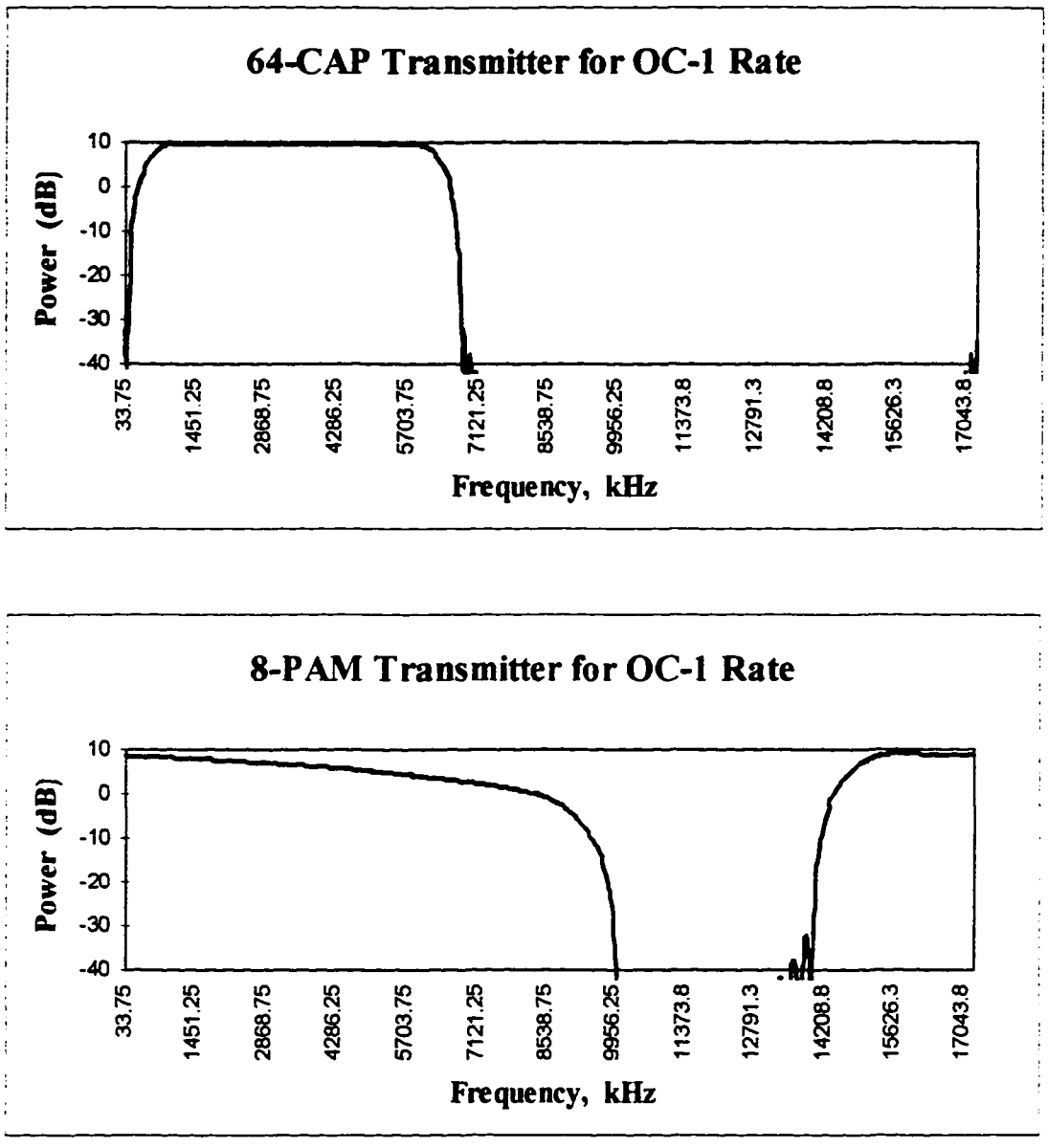

Figure 7.5 64-CAP and 8-PAM transmitter for OC-1 rate, rolling factor of 15%, guard band of 120 kHz, oversampling ratio of 3 and raised cosine shaping filter with 128 taps.

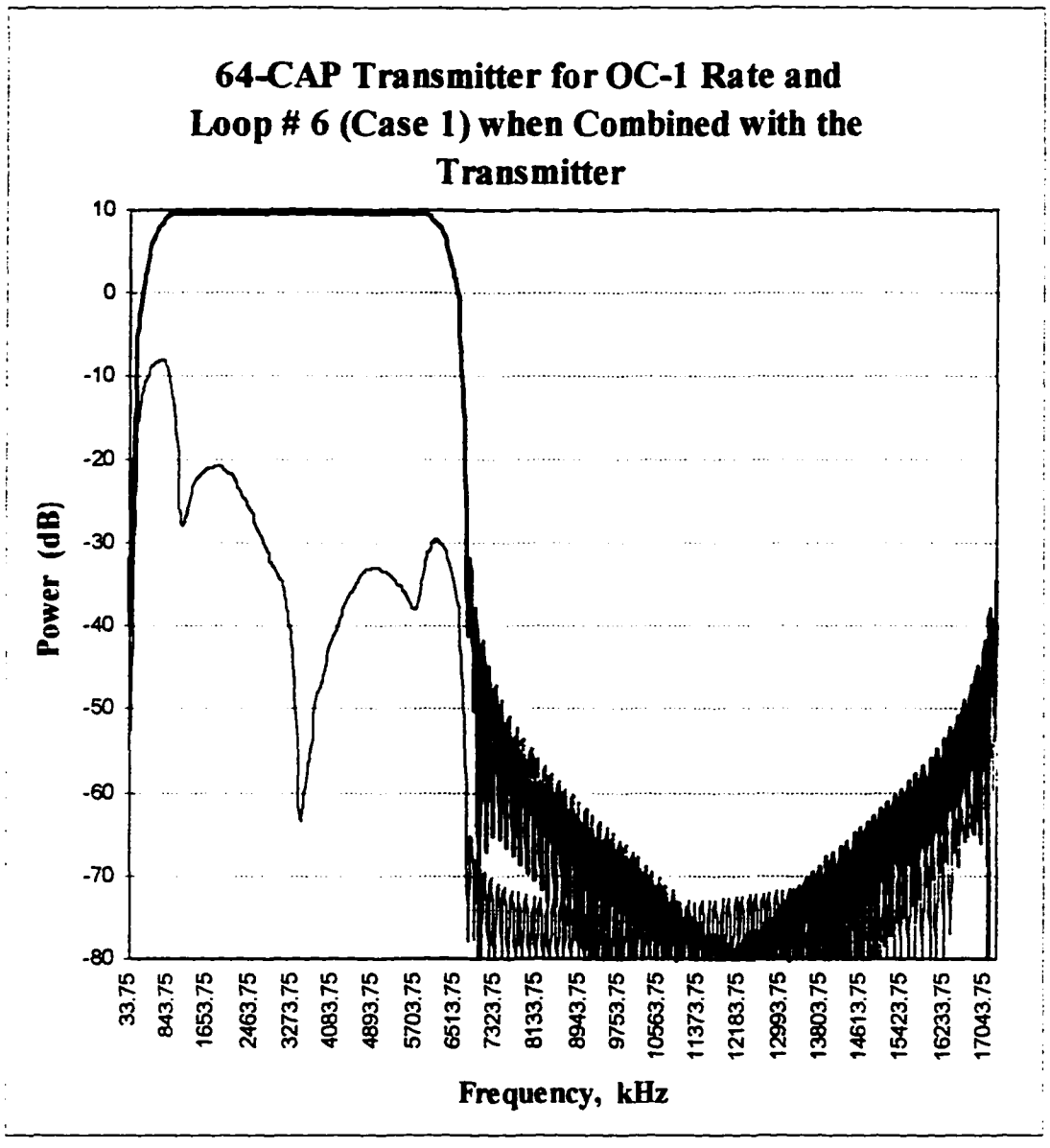

Figure 7.6 64-CAP transmitter for OC-1 rate and case 1 of loop 6 when combined with the transmitter filter.

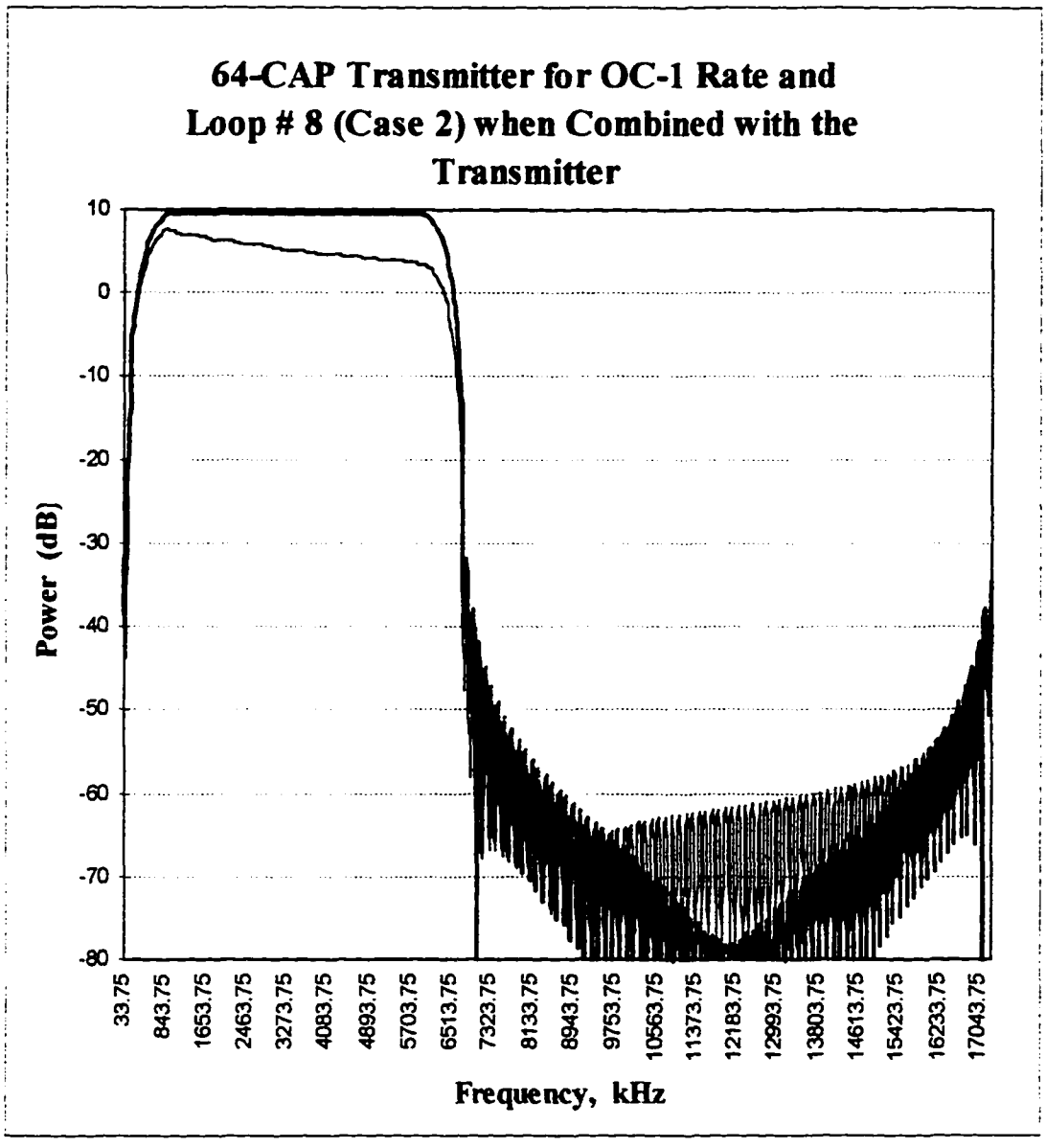

Figure 7.7 64-CAP transmitter for OC-1 rate and case 2 of loop 8 when combined with the transmitter filter.

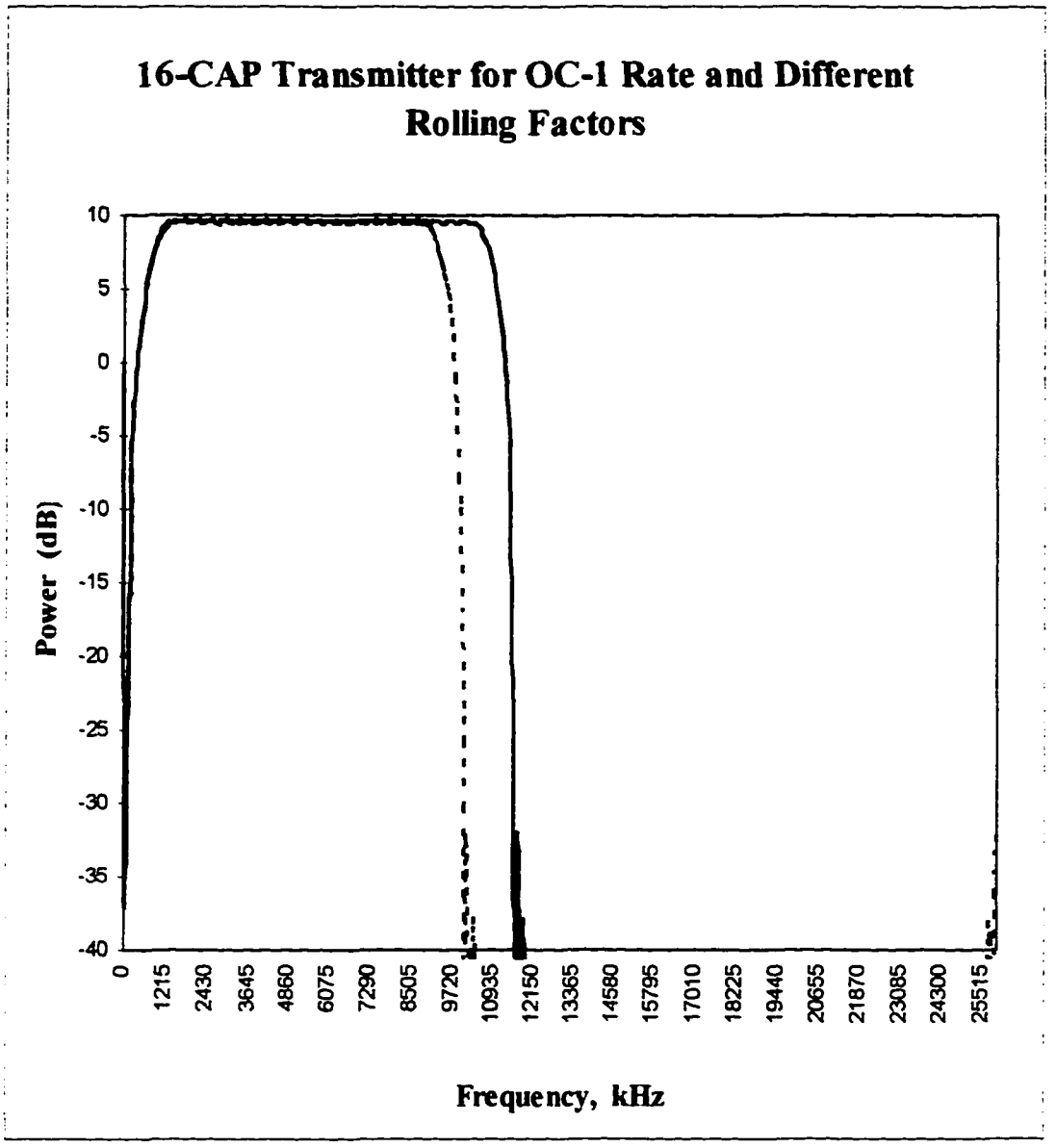

Figure 7.8 Effective bandwidth for 16-CAP transmitter with rolling factors of 15% and 50% and rate of 51.84 Mb/s.

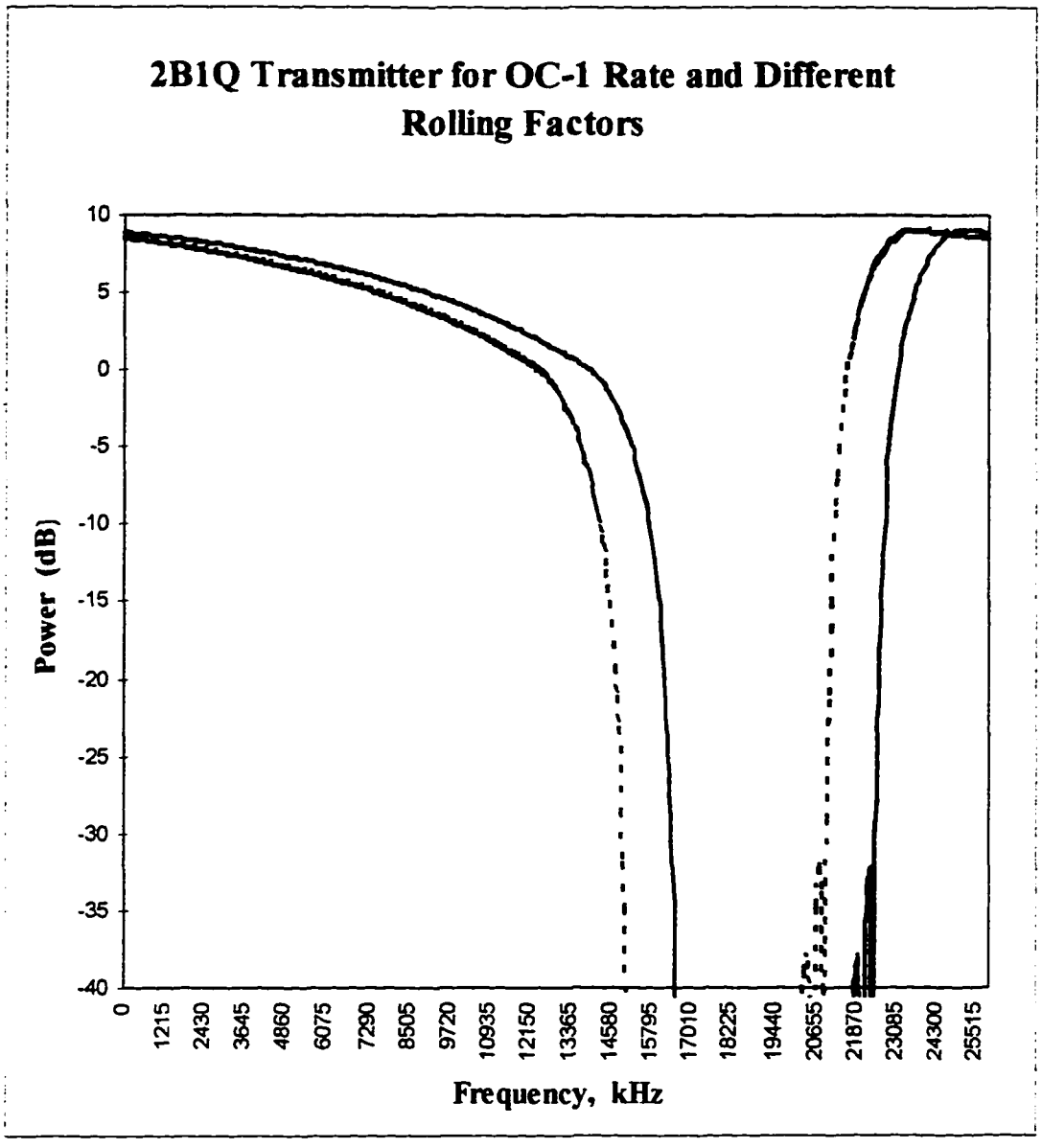

Figure 7.9 Effective bandwidth for 2B1Q transmitter with rolling factors of 15% and 50% and rate of 51.84 Mb/s.

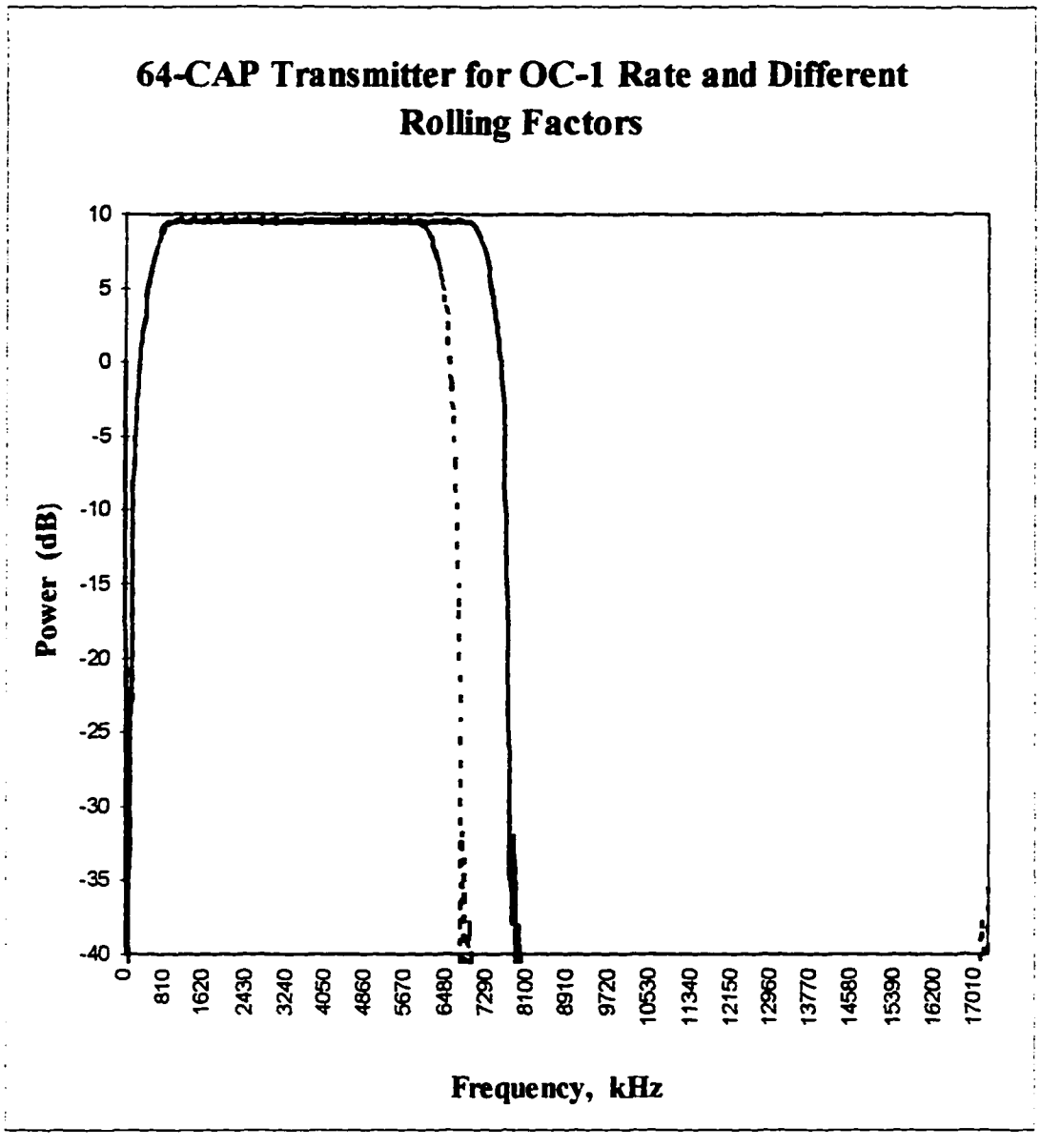

Figure 7.10 Effective bandwidth for 64-CAP transmitter with rolling factors of 15% and 50% and rate of 51.84 Mb/s.

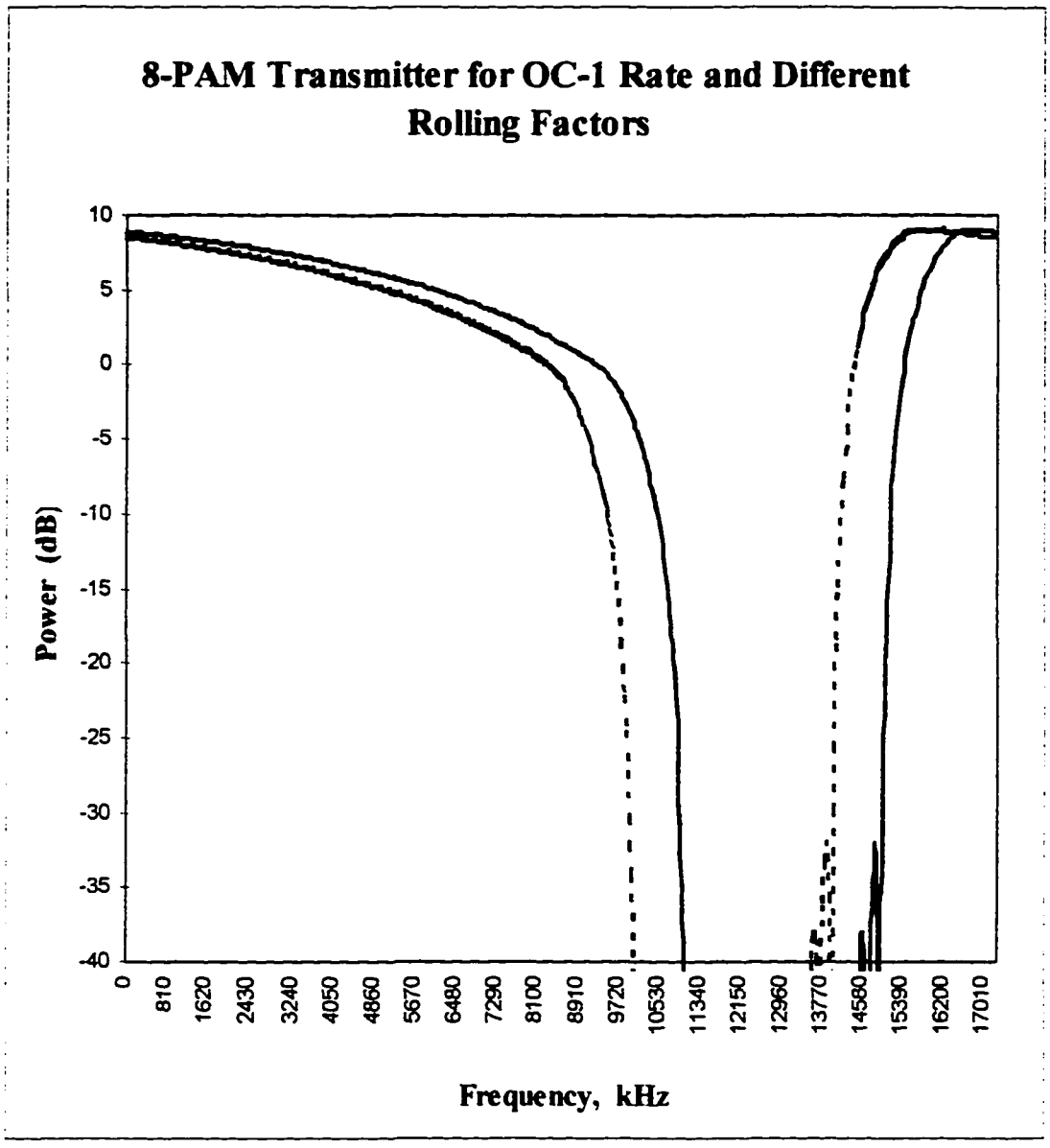

Figure 7.11 Effective bandwidth for 8-PAM transmitter with rolling factors of 15% and 50% and rate of 51.84 Mb/s.

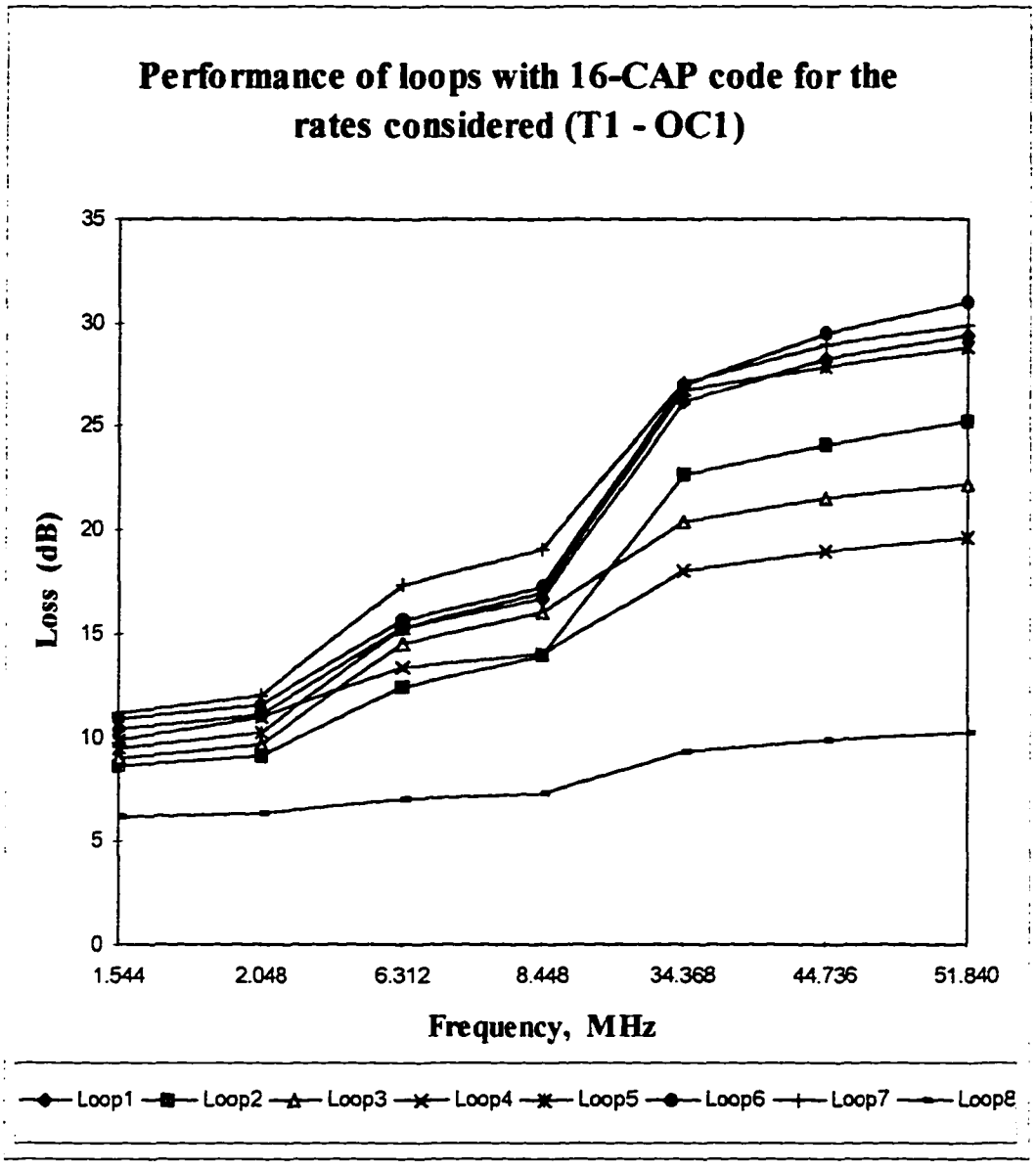

Figure 7.12 Performance consideration with 16-CAP code for loops without termination.

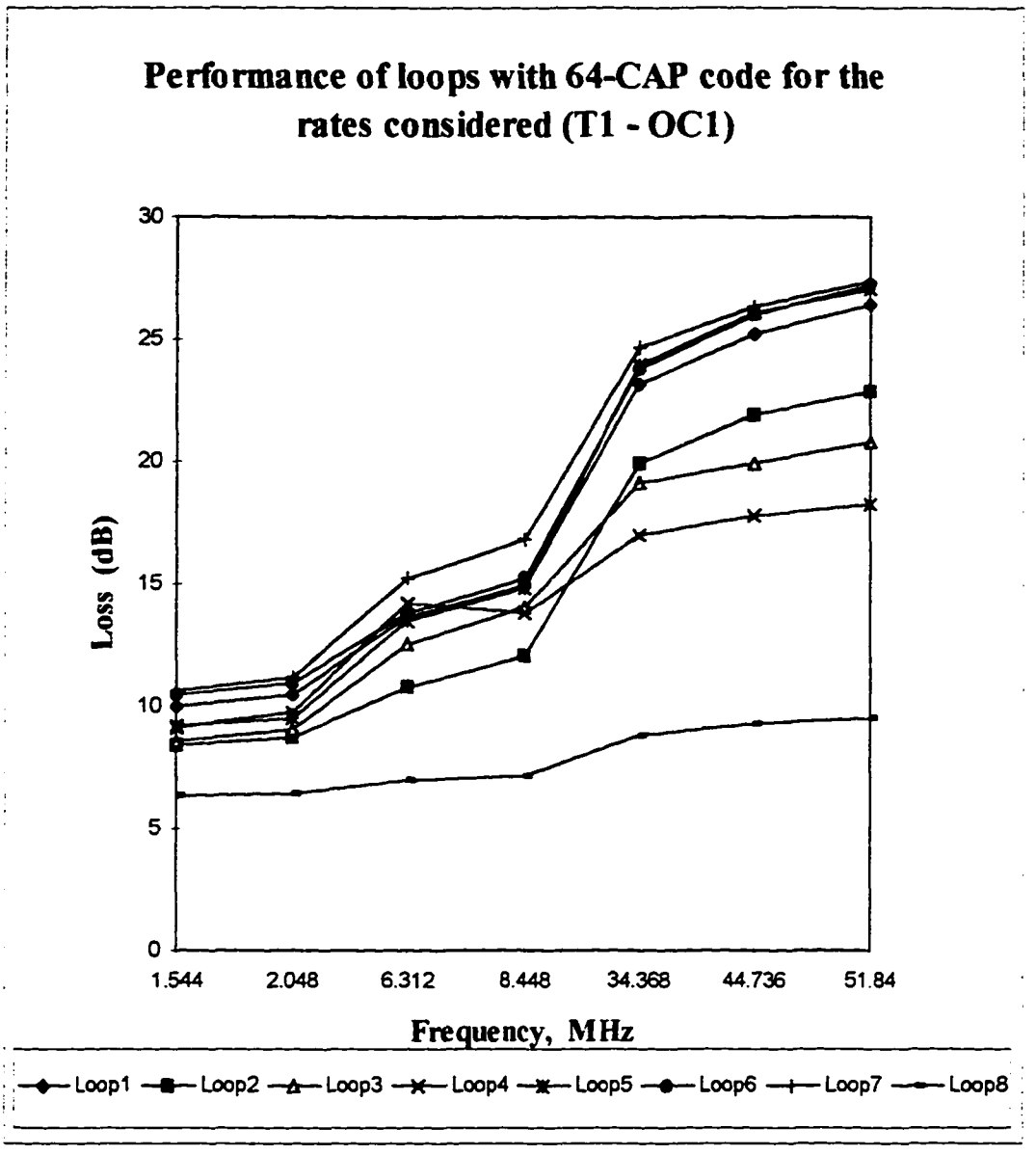

Figure 7.13 Performance consideration with 64-CAP code for loops without termination.

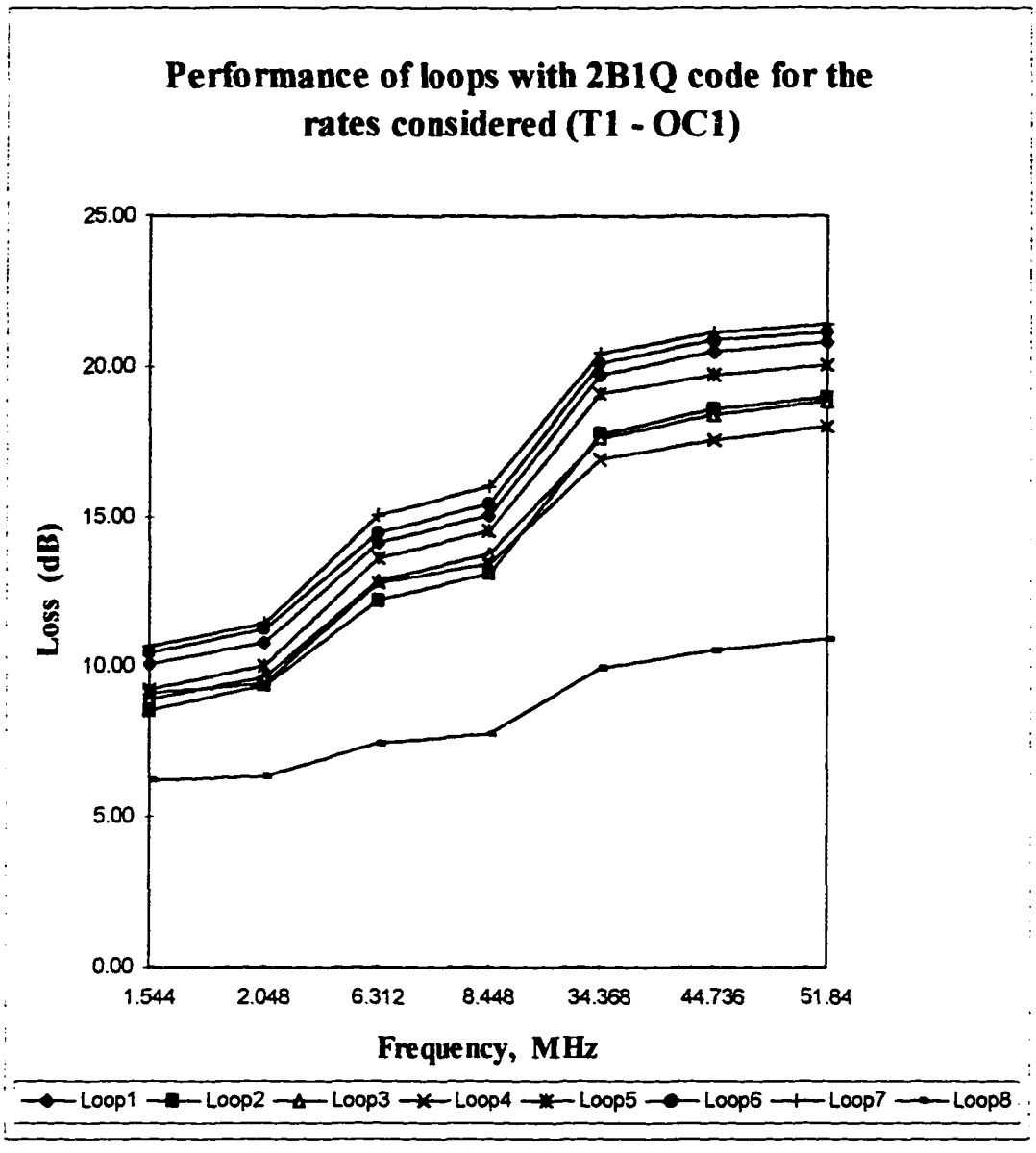

Figure 7.14 Performance consideration with 2B1Q code for loops without termination.

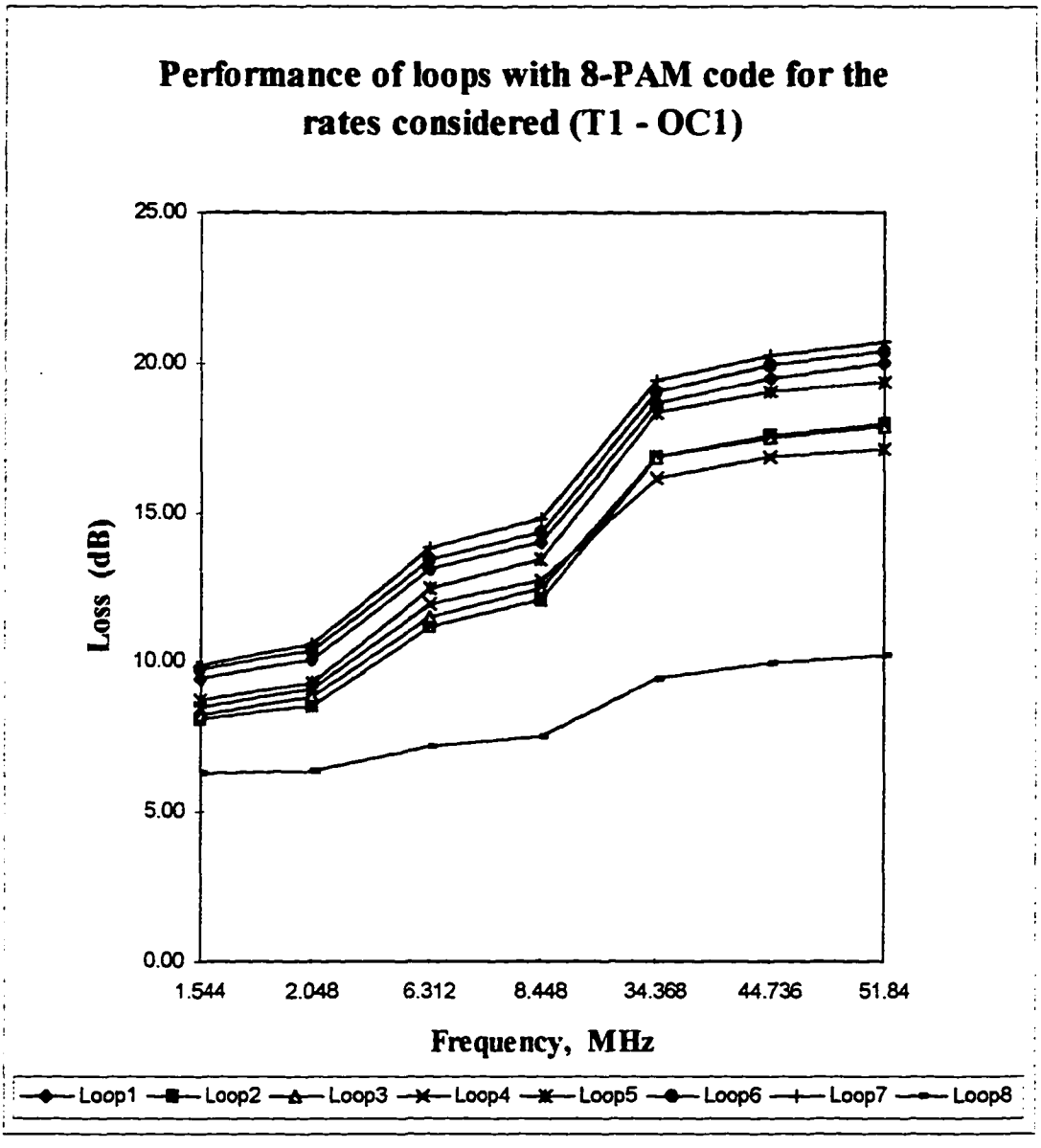

Figure 7.15 Performance consideration with 8-PAM code for loops without termination.

CHAPTER 8

7. Channel and Crosstalk Modeling

A transmitted signal creates electromagnetic field around the cable used. These fields induce voltages and currents on neighboring cables using the same sheath. To reduce these coupling of fields, pairs of cables are twisted, hence reducing the effect. The resulting coupling is now minimized, but still can cause serious damage to the immediate neighbor pairs.

This coupling is dependent on length of cable which is exposed, termination of the loop and frequency components, where as the frequencies rise higher so does the coupling effect.

Figure 8.1 show two cases of coupling, which are called near-end crosstalk (NEXT) and far-end crosstalk (FEXT). Pair k is considered as disturbed circuit while pair j is the disturbing circuit. As more than two active pairs are present in a bundled sheath there exist several of interfering circuits for every disturbed circuit.

Near-end crosstalk (NEXT) as seen in figure 8.1 is the transfer of energy (voltage) from j1 into the cable pair of transceiver k1, while far-end crosstalk (FEXT) displayed at the bottom of the figure is the transfer of energy from j1 into the cable pair of the k2 transceiver. Usually NEXT is more damaging then FEXT, since it does not propagate through the loop and therefore it will not undergo propagation loss, which almost eliminates FEXT when the loop has a considerable length.

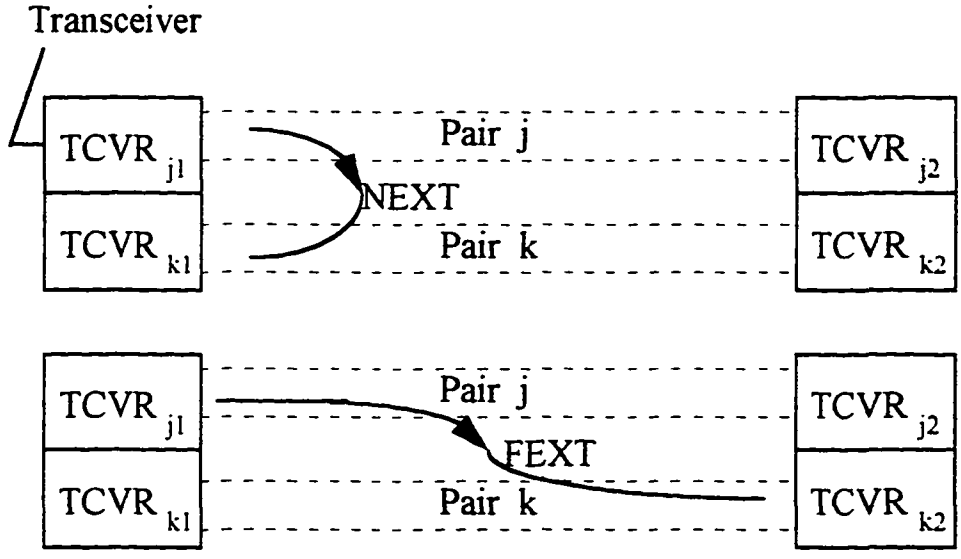

Figure 8.1 NEXT and FEXT coupling.

Interference due to NEXT as mentioned before is a function of loop length, cable characteristics (termination and electric properties), and spectral attributes of the system. Also the receiver filter should be able to differentiate maximum signal from noise. After maintaining loop length and cable properties as constant, and using line code bandwidth and transmitter waveform, NEXT can be controlled up to a certain level.

Attenuation of NEXT can be modeled through its transfer function given as,

$$|H_{NEXT}(f)|^2 = \tau f^{1.5} \qquad (8.1)$$

where $H_{NEXT}(f)$ is the NEXT signal transfer function, and τ is the coupling coefficient between pairs. Now the NEXT power sum loss can be determined by,

$$L_{NEXT.\,dB} = -10 \log|H_{NEXT}(f)|^2 = -10 \log \tau f^{1.5} \qquad (8.2)$$

Taking $-10 \log(\tau)$ as a constant equation 8.2 evolves into,

$$L_{NEXT.\,dB} = T - 15 \log(f) \qquad (8.3)$$

In equation 8.3, NEXT coupling for copper transmission media (UTP-3) increases as a function of frequency at about 15 dB per decade at frequencies above 20 kHz. Also in the same context, at 1 MHz the effect of one disturber on a single wire pair is computed as 41 dB. This value has been experimentally verified [51] for transmitter side self-NEXT[1] for most gauges. Hence, the loss due to one interferer is given as (figure 8.2),

$$L_{NEXT,\,dB,\,1\ Interferer} = 86 - 15\log(f) \qquad (8.4)$$

Now from equation 8.4 and 8.2 the coupling coefficient for one interferer and frequencies above 20 kHz is:

$$\tau = 0.794 \times 10^{-9}$$

At 80 kHz, the effect of 49 interferers on a single wire pair is computed and experimentally verified as to be 57 dB (figure 8.2). Hence,

$$L_{NEXT,\,dB,\,49\ Interferers} = 85.55 - 15\log(f) \qquad (8.5)$$

[1] Self-NEXT is NEXT when disturbed and disturbing signals have both same PSD, meaning that, it is caused by analogous transmitters in the same cable sheath while transmitting the same line code. It has been found to be the worst case of NEXT.

Henceforth, from equation 8.5 and 8.2 the coupling coefficient for 49 interferers and frequencies above 20 kHz is:

$$\tau = 2.8 \times 10^{-9}$$

The transfer function of the coupling channel elaborates into the following:

$$|H(f)| = \begin{cases} \sqrt{0.794 \times 10^{-9}}\ f^{\frac{3}{4}} & ;\ 1 \text{ Disturber} \\ \sqrt{2.8 \times 10^{-9}}\ f^{\frac{3}{4}} & ;\ 49 \text{ Disturbers} \end{cases} \qquad (8.6)$$

For equation 8.5 to be effective certain provisions have to be fulfilled and there contents can be summarized as:

1) Disturbing and disturbed transmitters utilizes the same binder group of transmitting and receiving cables.

2) Termination impedances and characteristic impedances are balanced at each frequency considered.

3) Loop length must appear to be infinite from a crosstalk perspective (i.e., loop length longer than 305 feet should be used).

7.1. Signal-to-Noise Ratio (SNR)

When a sinusoidal voltage with frequency f and amplitude ρ is applied to the disturbed and disturbing cables of individual transmitters, the loop with transfer function G(f,x) and NEXT coupling transfer function $H_{NEXT}(f)$ has a SNR of:

$$SNR(f) = \frac{\rho^2 |G(f,x)|^2}{\rho^2 |H_{NEXT}(f)|^2} \qquad (8.7)$$

From equation 6.8,

$$G(f,x) = e^{-x\,\alpha(f)} \cdot e^{-x\,j\,\beta(f)} \Rightarrow |G(f,x)| = e^{-x\,\alpha(f)}$$

Hence, equation 8.7 can be written as,

$$SNR(f) = \frac{e^{-2x\,\alpha(f)}}{\tau f^{1.5}} \qquad (8.8)$$

Combining equation 6.14 and 8.7, the SNR can be represented in term of loss as,

$$SNR_{dB}(f) = - Loop_{Loss.\,dB} + L_{NEXT.\,dB}$$

$$= 0.01203 - 0.00012 f - 0.04 \sqrt{f} + T - 15 \log f \qquad (8.9)$$

Equation 8.9 can be seen more explicitly in figure 8.3, where SNR for UTP-3 cable with length of 1 kft and 49 interferers is shown. The SNR becomes negative (noise has dominance over signal) for frequencies higher than about 15 MHz, which will result in a constraint of spectrum allocation of up to 15 MHz for the codes considered.

Figure 8.2 displays the loss for one and forty-nine interferers. When both losses are compared the difference for a spectrum of 30 MHz is about 4 to 5 dB, therefore the loss for one interferer is negligible and NEXT loss will be referenced only for 49 interferers (figure 8.4 - 8.7).

8.2. Simulated Signal-to-Noise Ratio (SNR)

When symbols are received at the input of the receiver, the SNR is defined as: SNR(f) = (Avg. Signal PWR)/(Avg. Noise PWR)

which is expressed in dB as,

$$SNR_{dB}(f) = 10 \log SNR(f) \qquad (8.10)$$

Figure 8.9 - 8.20 displays the SNR for all PDS loops at data rates of T-2, T-3 and OC-1 for all different codes being considered. The constellation and eye diagrams for loop 6 and 8 at data rates of T-2 and OC-1 are presented in figure 8.21 - 8.32.

7.2.1. Performance of Codes through Probability of Symbol Error

For a random variable N the Gaussian or normal probability density function is given as,

$$f_N(x) = \frac{1}{\sigma\sqrt{2\pi}} e^{\frac{-(x-\mu)^2}{2\sigma^2}} \quad ; \quad -\infty < x < \infty \text{ and } \sigma > 0 \qquad (8.11)$$

In equation 8.11 μ is the mean of N and the parameter σ^2 is the variance of N (hence σ is the standard deviation). The variance is a measure of spread around the mean μ. Therefore the probability of occurrence of certain variable is more likely to occur near the mean when σ^2 is small.

The distribution function F(x) for the density function is given as,

$$f_N(x) = P(N \leq x) = \frac{1}{\sigma\sqrt{2\pi}} \int_{-\infty}^{x} e^{-\frac{1}{2}\left(\frac{v-\mu}{\sigma}\right)^2} dv \qquad (8.12)$$

The crosstalk (NEXT) for the simulation is generated through a passband noise signal generator. It has a PSD that represents characteristics of a practical crosstalk signal. Since the noise source is representing a large number of transmitters (49), it is Gaussian with PSD equal to average transmitter PSD output.

For the simulation purpose, the noise PSD is produced by passing white Gaussian noise through a filter (outcome of filtered Gaussian is also Gaussian) that has same attenuation characteristics as the transmitter shaping filter. After that the signal is introduced into another filter that follows the 15 dB per decade model proposed by Bellcore [57].

As an example, the 2B1Q receiver can receive the following set of symbols {-3s, -1s, +1s, +3s}, and based on the Gaussian bell-shaped distribution curve a symbol is received correctly if it falls in a location intermediate to adjacent symbols. Hence the symbol +1s is received correctly, if it falls in the interval $0 < s + v < 2s$, otherwise an error has occurred.

The probability of an error when symbol +1s is received can be determined through,

$$f_N(s) = P(N > s) = \frac{1}{\sigma\sqrt{2\pi}} \int_s^{\infty} e^{-\frac{1}{2}\left(\frac{v-\mu}{\sigma}\right)^2} dv \qquad (8.13)$$

Now by doing the substitution $x = (v - \mu)/\sigma$ and $dx = dv/\sigma$,

$$P(N > s) = \frac{1}{\sqrt{2\pi}} \int_{\frac{s-\mu}{\sigma}}^{\infty} e^{-\frac{1}{2}(x)^2} dx \qquad (8.14)$$

when random variables with $\mu = 0$ are considered, equation (8.14) becomes,

$$P(N > s) = \frac{1}{\sqrt{2\pi}} \int_{\frac{s}{\sigma}}^{\infty} e^{-\frac{1}{2}(x)^2} dx = F_N(s/\sigma) \qquad (8.15)$$

Now let $s/\sigma = z$, then $F_N(s/\sigma)$ can be approximated by the following expressions[2]:

$$F_N(z) = P(N > s) = \frac{1}{\sqrt{2\pi}} \int_z^{\infty} e^{-\frac{1}{2}(x)^2} dx \approx \frac{1}{2\,z\,\sqrt{2\pi}}\, e^{-\frac{z^2}{2}} \qquad (8.16)$$

The probability of an error when symbol +1s is received is $2F_N(z)$ for the bell shaped curve, therefore,

$$F_N(z) = \frac{1}{z\,\sqrt{2\pi}} e^{-\frac{z^2}{2}} \qquad (8.17)$$

---

[2] In equation 8.16 the following set of relationships were used:

A. $\frac{1}{\sqrt{2\pi}} \int_{-\infty}^{\infty} e^{-\frac{1}{2}x^2} dx = 1$ B. $e^{-x^2} = \sum_{n=0}^{\infty} \frac{(-1)^n\, x^{2n}}{n!}$

C. substitution of x for z - u , hence: $\frac{1}{\sqrt{2\pi}}\, e^{-z^2} \int e^{2zu} \cdot e^{-u^2} du$

D. $\int_0^{\infty} x^n\, e^{-x} dx = n!$

With the same token the probability of an error when symbol +3s is received is $F_N(3s/\sigma) = F_N(3z)$, hence,

$$F_N(3z) = \frac{1}{3z\sqrt{2\pi}} e^{-\frac{9z^2}{2}} \approx [F_N(z)]^9 \qquad (8.18)$$

Symbol variances (assuming received symbols in their respective symbol periods are uncorrelated) for 1-D and 2-D codes can be written as:

$$\sigma^2_{1\text{-}D} = \frac{1}{M} \sum_{m=1}^{M} t_m^2 \qquad (8.19)$$

$$2\sigma^2_{2\text{-}D} = \frac{1}{M} \sum_{m=1}^{M} [a_m^2 + b_m^2] \qquad (8.20)$$

where M is the total number of symbols in a specific set and t_m, a_m (real), b_m (imaginary) are symbol values for one dimensional PAM and two dimensional CAP codes. Hence, the set of all symbol values for 1-D (e.g., 2B1Q and 8-PAM) codes to be used by equation 8.19 can be put as,

t_m = {-(M-1)s, -(M-3)s....., -3s, -1s, 1s, 3s, ..., (M-3)s, (M-1)s}

or $t_m = \pm(2m - 1)s$, $m = 1, 2, \ldots, M/2$ (8.21)

Therefore the symbol variance is:

$$\sigma_{1\text{-}D}^2 = \frac{1}{M} \sum_{m=-\frac{M}{2}}^{\frac{M}{2}} t_m^2 = \frac{2}{M} \sum_{m=1}^{\frac{M}{2}} [(2m-1)s]^2 = \frac{(M^2-1)s^2}{3} \qquad (8.22)$$

From equation 8.22, the signal-to-noise ratio (SNR) for 1-D codes can be written as,

$$SNR_{1\text{-}D} = \frac{\sigma_{1\text{-}D}^2}{\sigma_n^2} = \frac{(M^2-1)s^2}{3\,\sigma_n^2} \qquad (8.23)$$

The probability of an error when any symbol is received for 1-D codes can be found by averaging error probabilities for different symbols, that is,

$$P(\varepsilon) = 2\,(1 - 1/M)\,F_N(s/\sigma_n) \qquad (8.24)$$

Combining equation 8.24 with 8.23,

$$P(\varepsilon) = 2\left(1 - \frac{1}{M}\right) F_N\left(\sqrt{\frac{3\,SNR_{1\text{-}D}}{M^2-1}}\right) \qquad (8.25)$$

and solving F_N through equation 8.17,

$$P(\varepsilon) = 2\left(1 - \frac{1}{M}\right)\sqrt{\frac{M^2 - 1}{6\,\pi\,SNR_{1\text{-}D}}}\; e^{-\frac{3\,SNR_{1\text{-}D}}{2\,(M^2 - 1)}} \qquad (8.26)$$

and for SNR in dB,

$$P(\varepsilon) = 2\left(1 - \frac{1}{M}\right)\sqrt{\frac{M^2 - 1}{6\,\pi\,10^{0.1\,\times\,SNR_{1\text{-}D,\,dB}}}}\; e^{-\frac{3\,\times\,10^{0.1\,\times\,SNR_{1\text{-}D,\,dB}}}{2\,(M^2 - 1)}} \qquad (8.27)$$

The error probability of 2-D (16-CAP and 64-CAP) codes is,

$$P(\varepsilon) = 4\left(1 - \frac{1}{M}\right)\sqrt{\frac{M^2 - 1}{6\,\pi\,10^{0.1\,\times\,SNR_{2\text{-}D,\,dB}}}}\; e^{-\frac{3\,\times\,10^{0.1\,\times\,SNR_{2\text{-}D,\,dB}}}{2\,(M^2 - 1)}} \qquad (8.28)$$

since a squared CAP constellation can be considered as a superposition of two PAM codes. Figure 8.8 and table 8.1 gives numerical examples for equation 8.27 and 8.28.

Table 8.1. Signal-to-noise ratio (SNR) and respective probability of symbol error for 2B1Q, 16-CAP, 8-PAM and 64-CAP codes.

SNR (dB)	P(ε) for 2B1Q & 16-CAP	P(ε) for 8-PAM and 64-CAP
20	6.80999E-06	0.032361867
20.5	1.8977E-06	0.022848741
21	4.55667E-07	0.015570256
21.5	9.25803E-08	0.010196603
22	1.55951E-08	0.006386072
22.5	2.12874E-09	0.003804222
23	2.29497E-10	0.002142387
23.5	1.89867E-11	0.0011328
24	1.1671E-12	0.000558073
24.5	5.14055E-14	0.000253959
25	1.55774E-15	0.000105722
25.5	3.10271E-17	3.98268E-05
26	3.85937E-19	1.34123E-05
26.5	2.83054E-21	3.98296E-06
27	1.14764E-23	1.02712E-06
27.5	2.39286E-26	2.26081E-07
28	2.36571E-29	4.16631E-08

The range for accepting a loop as viable or non-viable is dependent on the values of probability error given in table 8.1. For the general case a loop is viable if it presents a SNR that can match the value of 10^{-7} or better as its probability error. For 2B1Q and 16-CAP the value is 21 dB or a higher value and for 8-PAM and 64-CAP it is 27.5 dB or higher. Tables 8.2 and 8.3 displays if loops are viable or not when using the codes considered for T-2, T-3 and OC-1 rates.

From table 8.2 and 8.3 it can be seen that for data rates of 6.312 Mbits/s (T2) all loops have 100% viability for three codes (16-CAP, 2B1Q and 64-CAP) and 56% of loops have viability when 8-PAM code is used. This signifies that when NEXT and Gaussian noise dominated constraints are applied, a signal consisting of any of the three codes (16-CAP, 2B1Q and 64-CAP) other than 8-PAM can be satisfactorily recovered at the receiver.

For data rates of 44.736 Mbits/s (T3) loop 8, case 2 is viable for 16-CAP and 64-CAP but fails for 2B1Q and 8-PAM. And for rates of 51.84 Mbits/s loop 8, case 2 is viable for 16-CAP, but fails for all other codes.

Table 8.2. Viability of loops using 16-CAP and 2B1Q codes, with probability of symbol error of 10^{-7} as the margin constraint. The rates used are T-2, T-3 and OC-1.

	16-CAP			2B1Q		
Loops	**T-2**	**T-3**	**OC-1**	**T-2**	**T-3**	**OC-1**
L11	Viable	Fail	Fail	Viable	Fail	Fail
L12	Viable	Fail	Fail	Viable	Fail	Fail
L21	Viable	Fail	Fail	Viable	Fail	Fail
L22	Viable	Fail	Fail	Viable	Fail	Fail
L31	Viable	Fail	Fail	Viable	Fail	Fail
L32	Viable	Fail	Fail	Viable	Fail	Fail
L41	Viable	Fail	Fail	Viable	Fail	Fail
L42	Viable	Fail	Fail	Viable	Fail	Fail
L51	Viable	Fail	Fail	Viable	Fail	Fail
L52	Viable	Fail	Fail	Viable	Fail	Fail
L61	Viable	Fail	Fail	Viable	Fail	Fail
L62	Viable	Fail	Fail	Viable	Fail	Fail
L71	Viable	Fail	Fail	Viable	Fail	Fail
L72	Viable	Fail	Fail	Viable	Fail	Fail
L81	Viable	Fail	Fail	Viable	Fail	Fail
L82	Viable	Viable	Viable	Viable	Fail	Fail

Table 8.3. Viability of loops using 64-CAP and 8-PAM codes, with probability of symbol error of 10^{-7} as the margin constraint. The rates used are T-2, T-3 and OC-1.

	64-CAP			8-PAM		
Loops	**T-2**	**T-3**	**OC-1**	**T-2**	**T-3**	**OC-1**
L11	Viable	Fail	Fail	Fail	Fail	Fail
L12	Viable	Fail	Fail	Viable	Fail	Fail
L21	Viable	Fail	Fail	Fail	Fail	Fail
L22	Viable	Fail	Fail	Viable	Fail	Fail
L31	Viable	Fail	Fail	Fail	Fail	Fail
L32	Viable	Fail	Fail	Viable	Fail	Fail
L41	Viable	Fail	Fail	Fail	Fail	Fail
L42	Viable	Fail	Fail	Viable	Fail	Fail
L51	Viable	Fail	Fail	Fail	Fail	Fail
L52	Viable	Fail	Fail	Viable	Fail	Fail
L61	Viable	Fail	Fail	Fail	Fail	Fail
L62	Viable	Fail	Fail	Viable	Fail	Fail
L71	Viable	Fail	Fail	Fail	Fail	Fail
L72	Viable	Fail	Fail	Viable	Fail	Fail
L81	Viable	Fail	Fail	Viable	Fail	Fail
L82	Viable	Viable	Fail	Viable	Fail	Fail

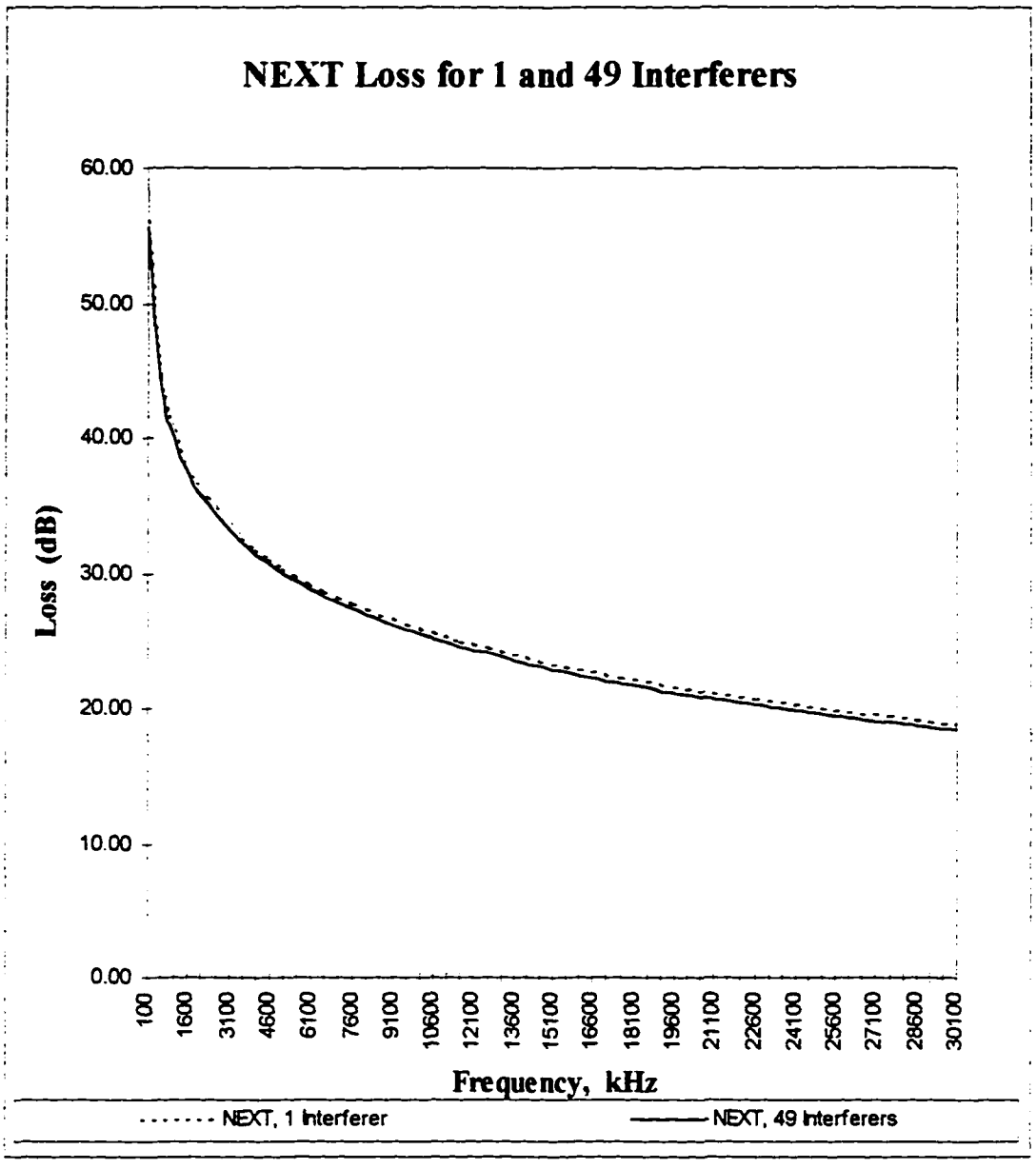

Figure 8.2 Measured NEXT loss for category-3 unshielded twisted wire pair, for one (1) and forty-nine (49) interferers.

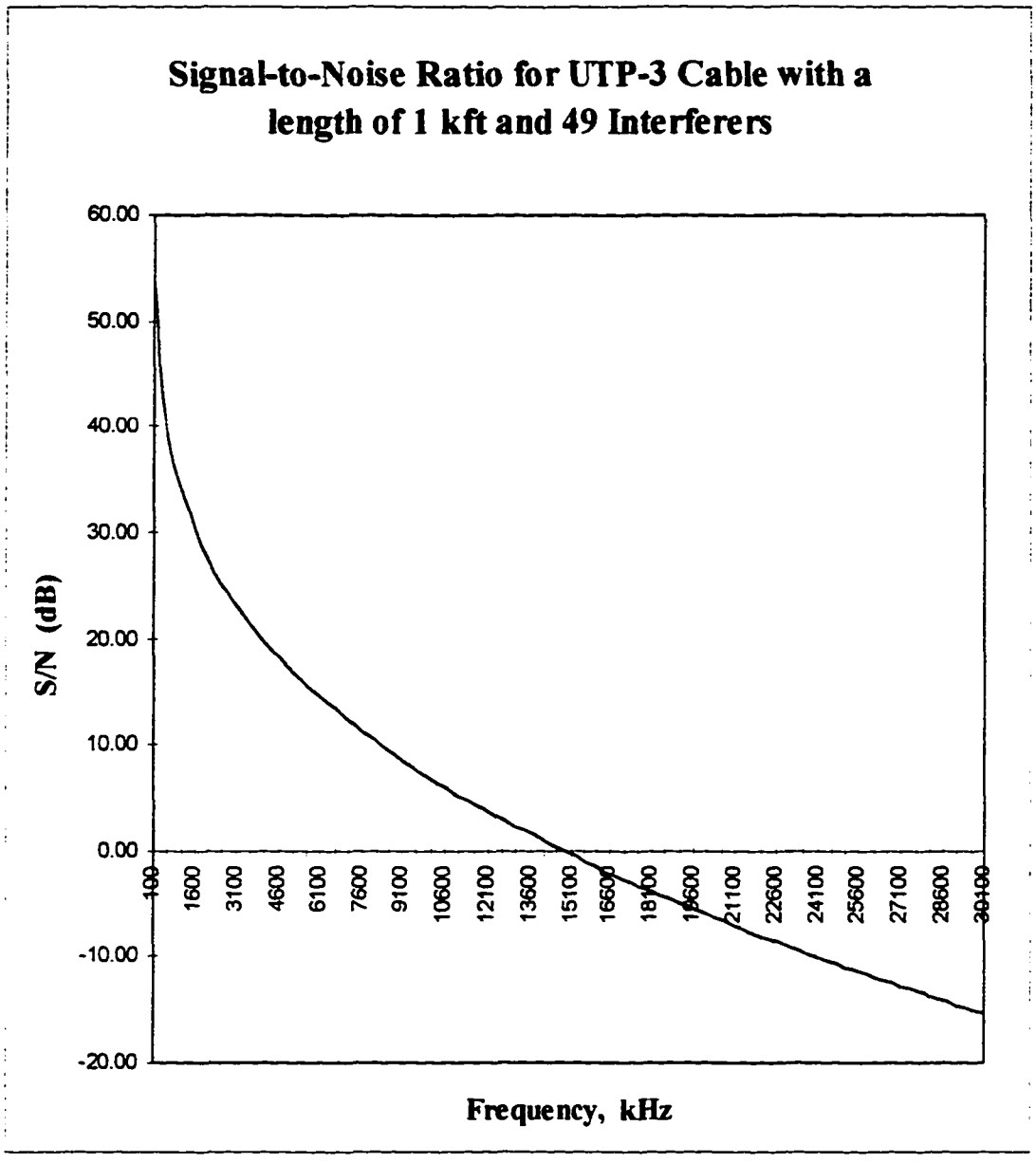

Figure 8.3 Signal-to-noise ratio (SNR) for category-3 unshielded twisted wire pair, at 70^0 F , length of 1000 feet and forty-nine (49) interferers.

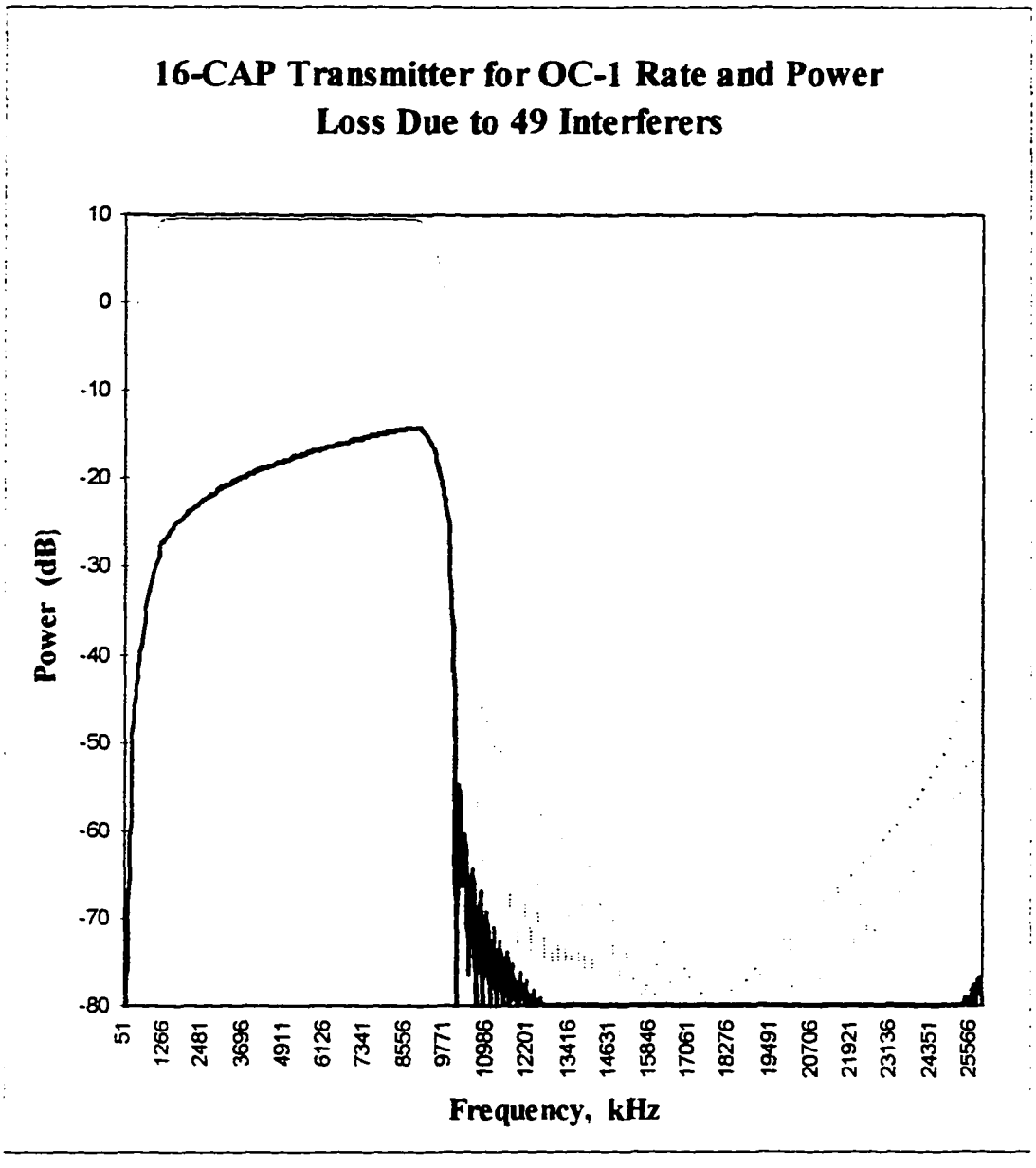

Figure 8.4 Transmitter (16-CAP) with NEXT loss for UTP-3 cable with 49 Interferers.

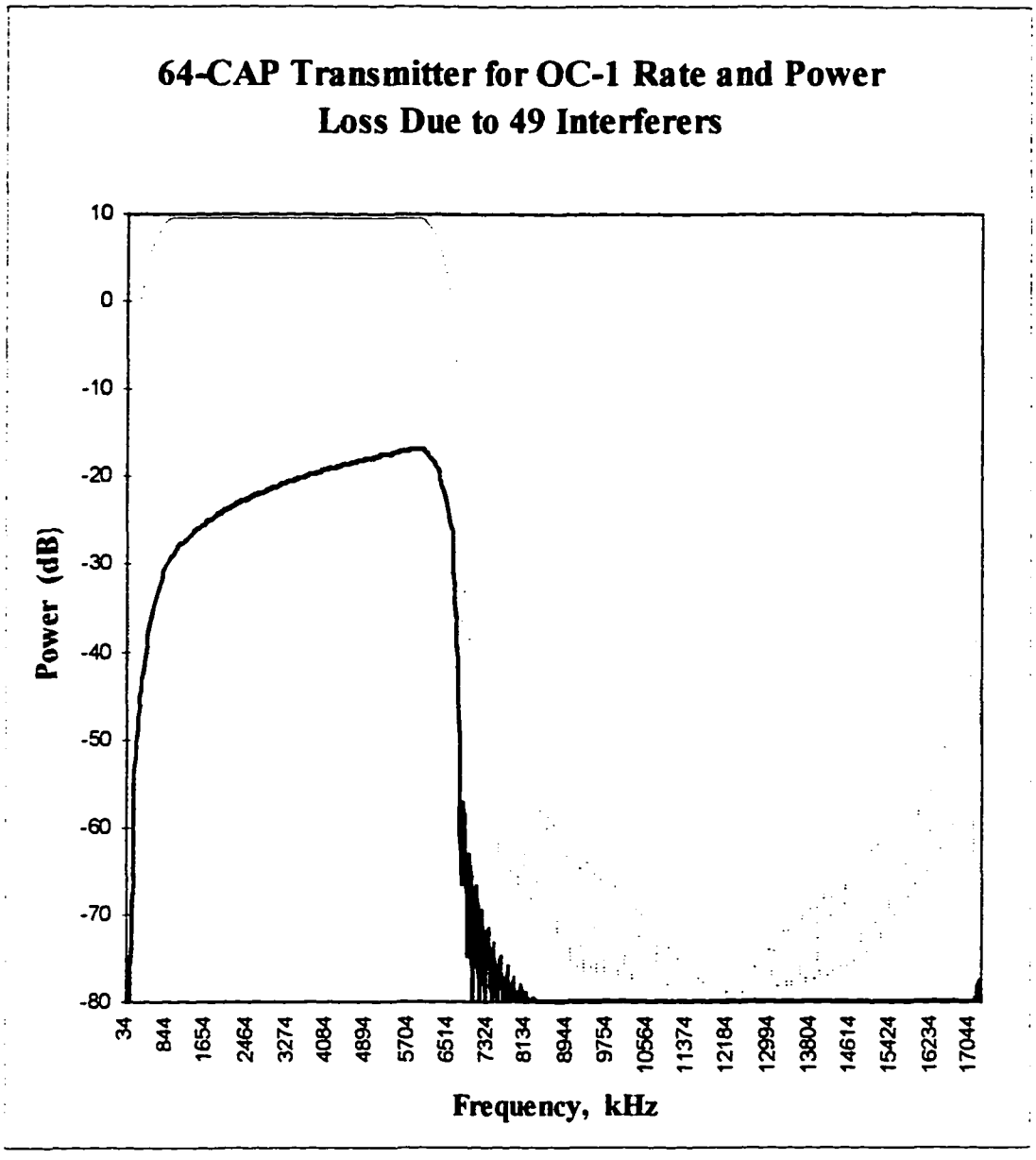

Figure 8.5 Transmitter (64-CAP) with NEXT loss for UTP-3 cable with 49 Interferers.

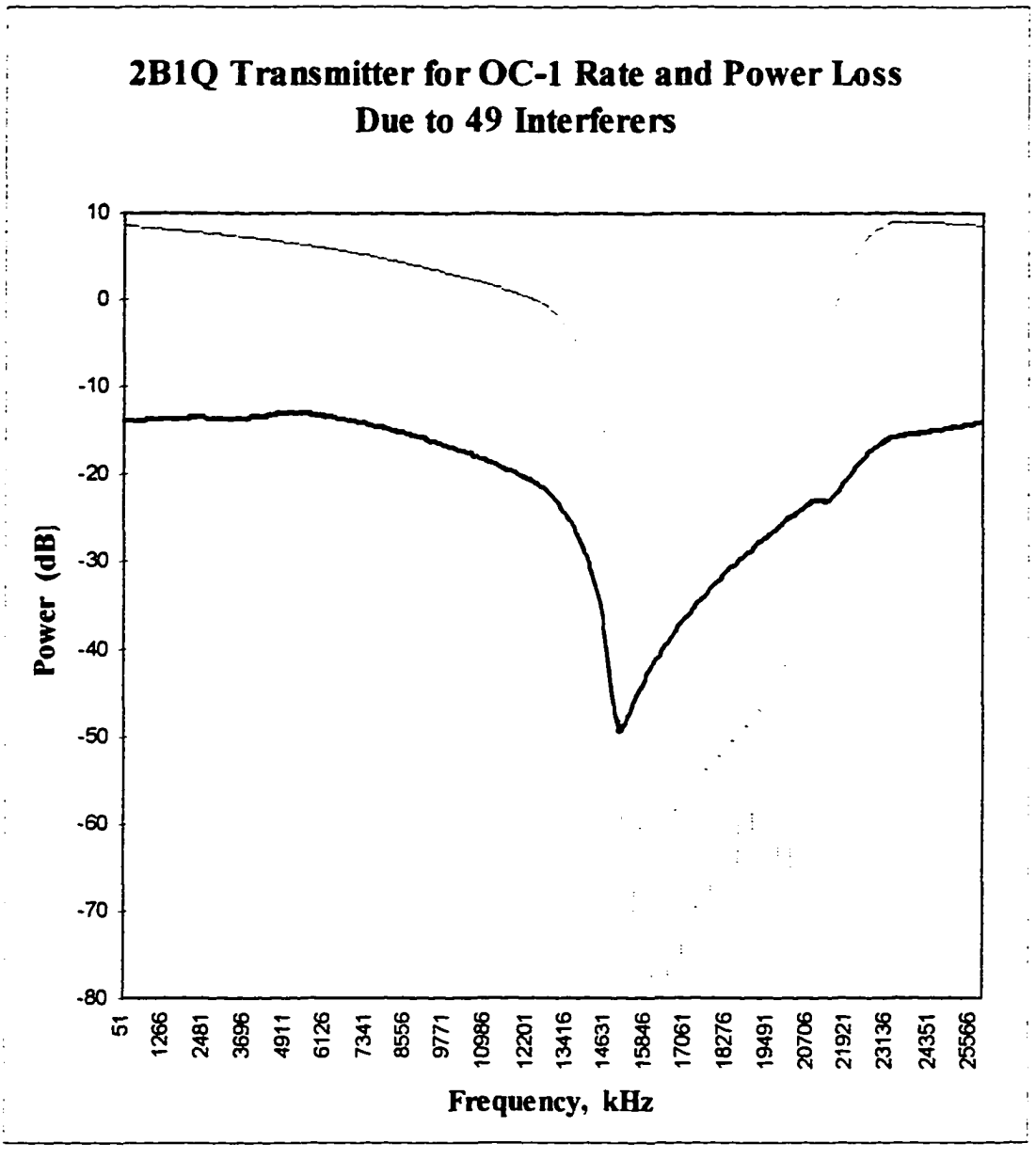

Figure 8.6 Transmitter (2B1Q) with NEXT loss for UTP-3 cable with 49 Interferers.

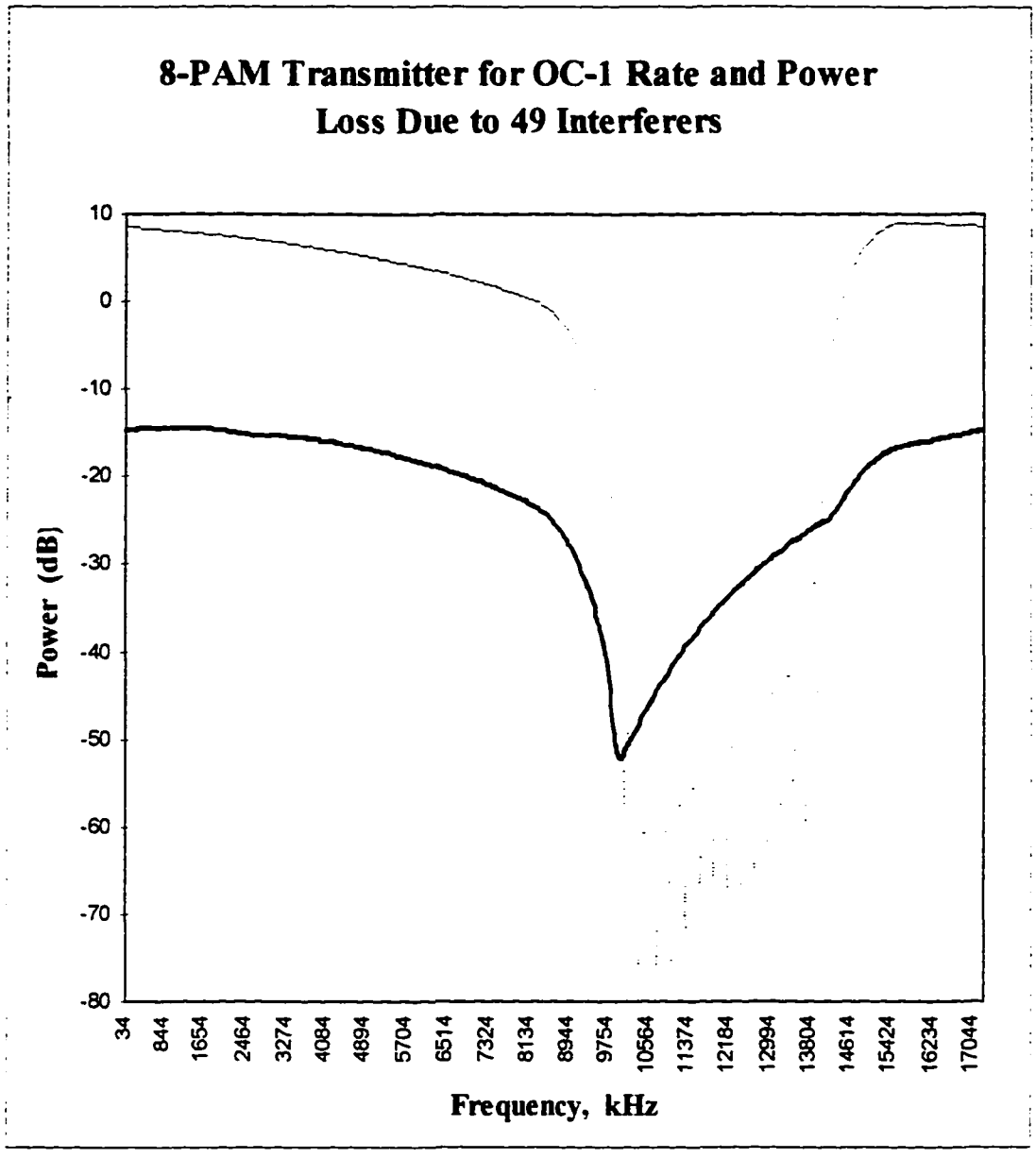

Figure 8.7 Transmitter (8-PAM) with NEXT loss for UTP-3 cable with 49 Interferers.

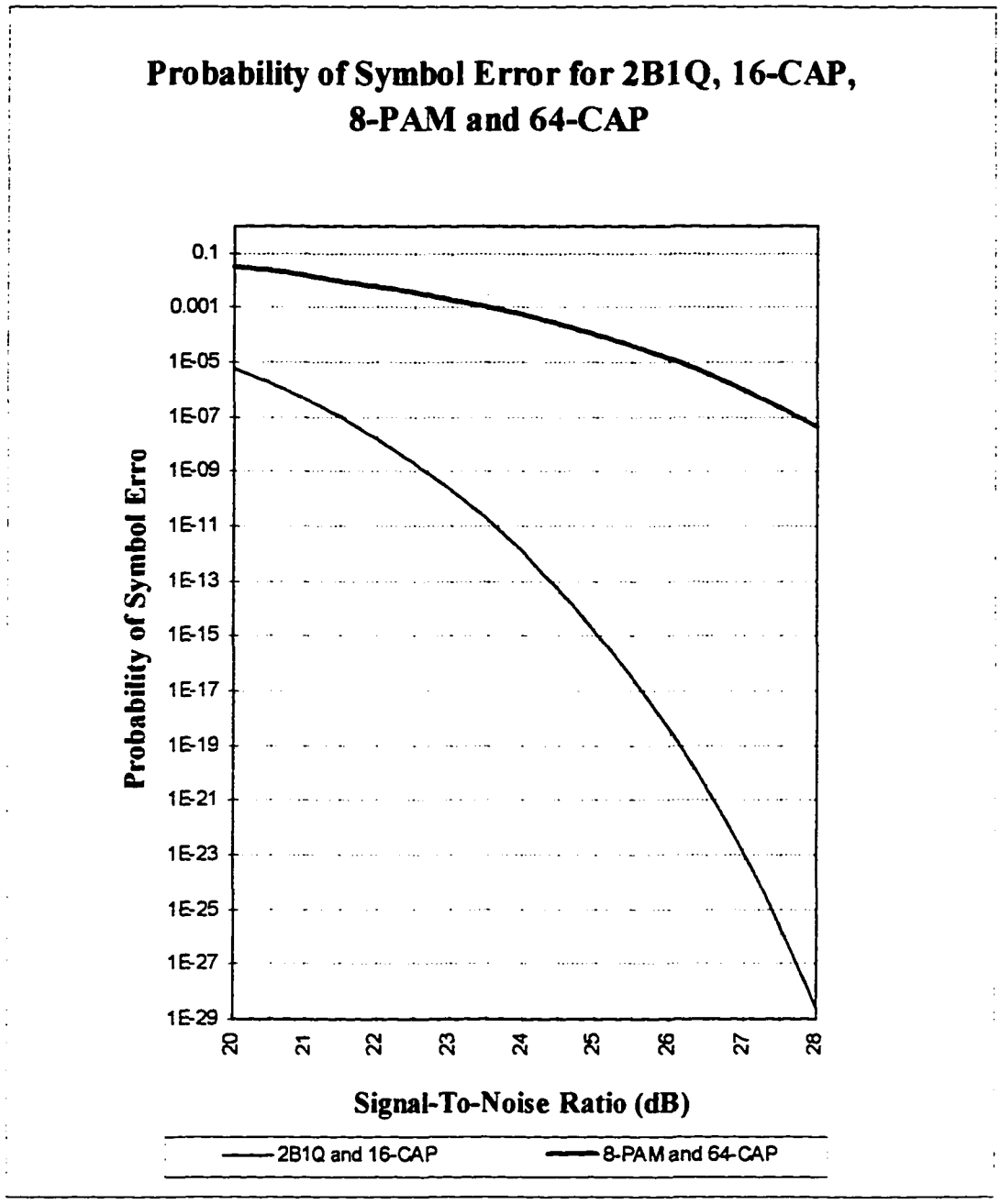

Figure 8.8 Probability of symbol error for 2B1Q, 16-CAP, 8-PAM and 64-CAP.

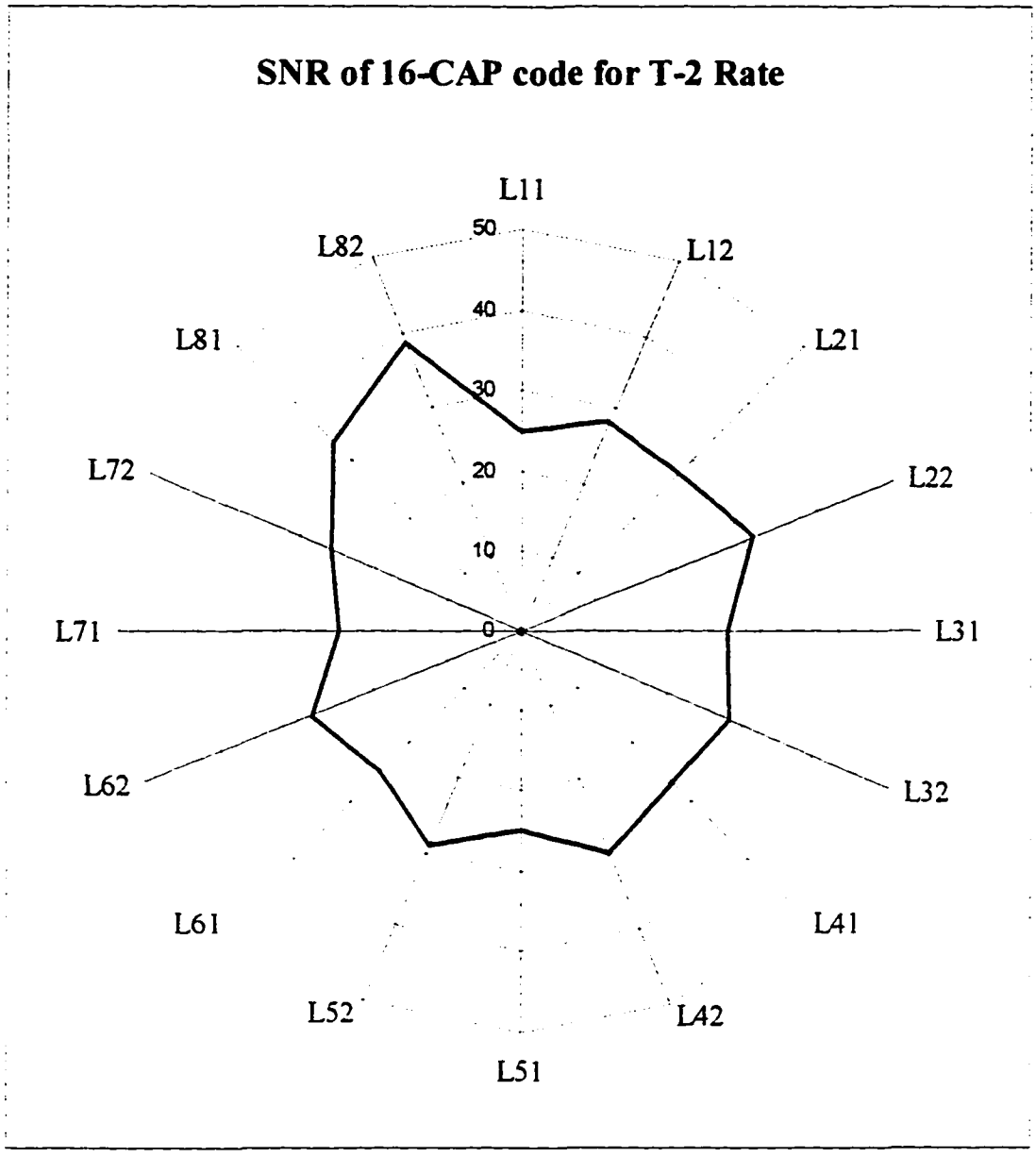

Figure 8.9 Signal-to-noise ratio (SNR, dB) of 16-CAP code for T-2 rate. Loop 1, case 1, is represented by L11 and loop 1, case 2, is represented by L12. Likewise, other loops are displayed.

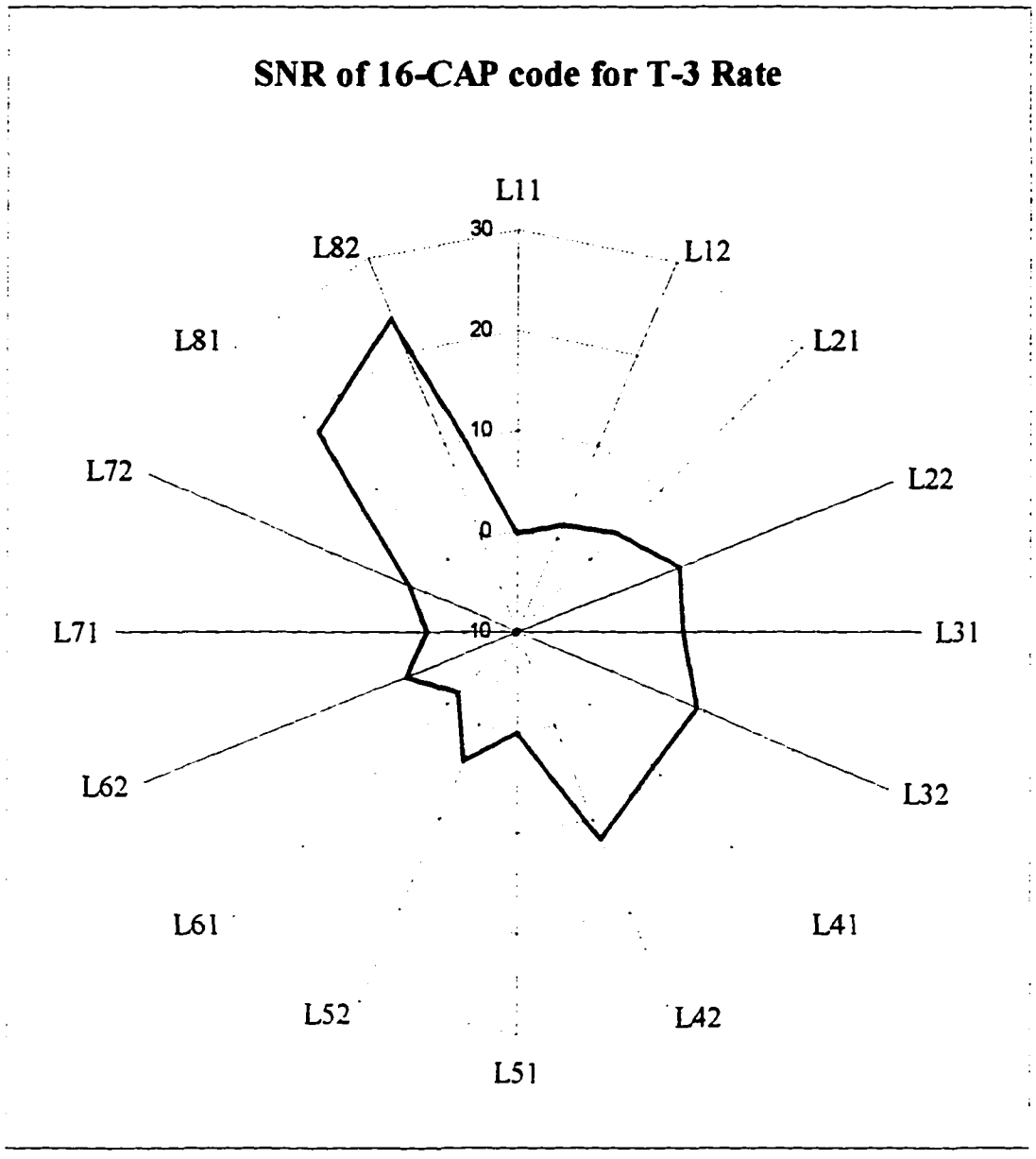

Figure 8.10 Signal-to-noise ratio (SNR, dB) of 16-CAP code for T-3 rate.

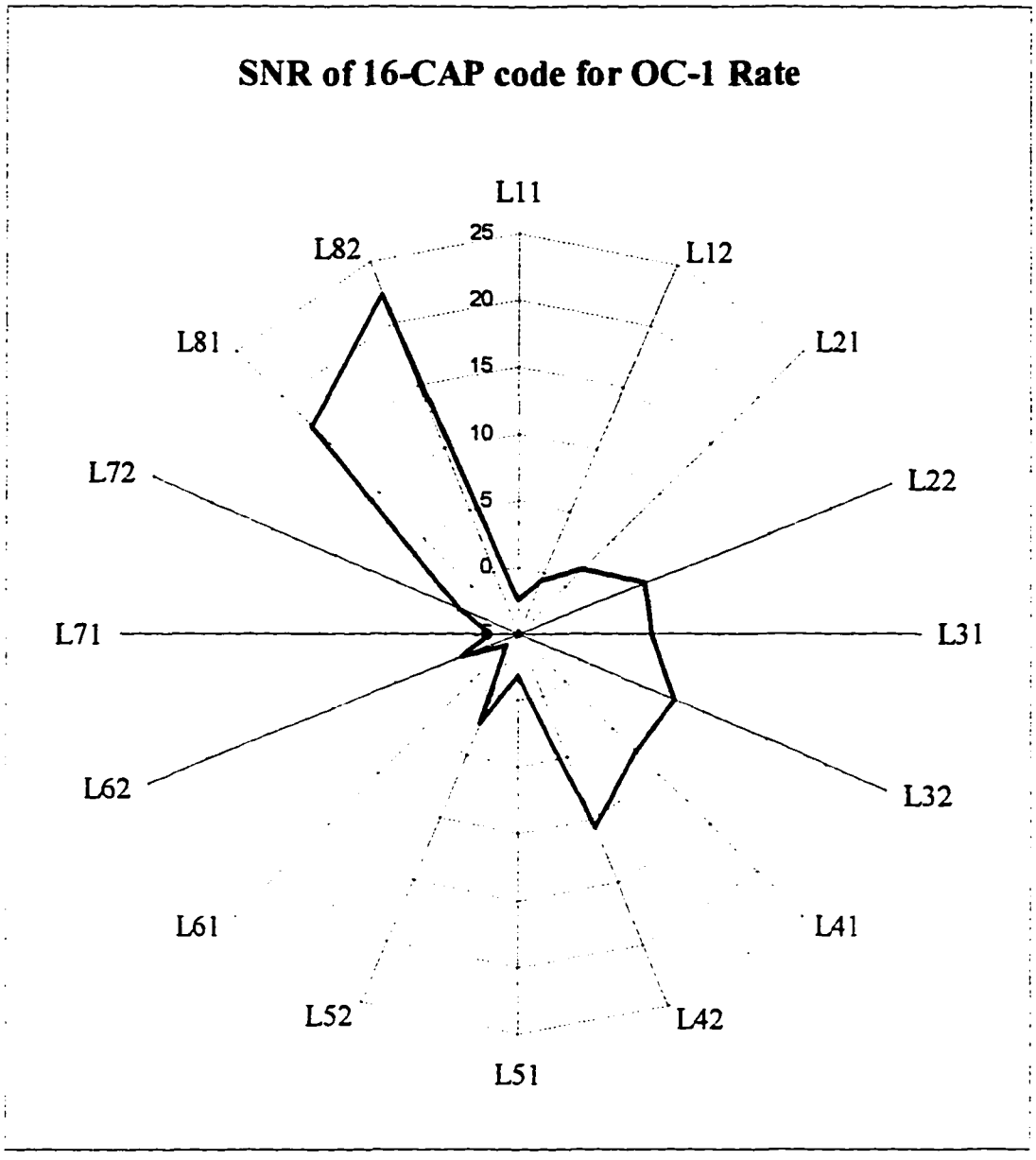

Figure 8.11 Signal-to-noise ratio (SNR, dB) of 16-CAP code for OC-1 rate.

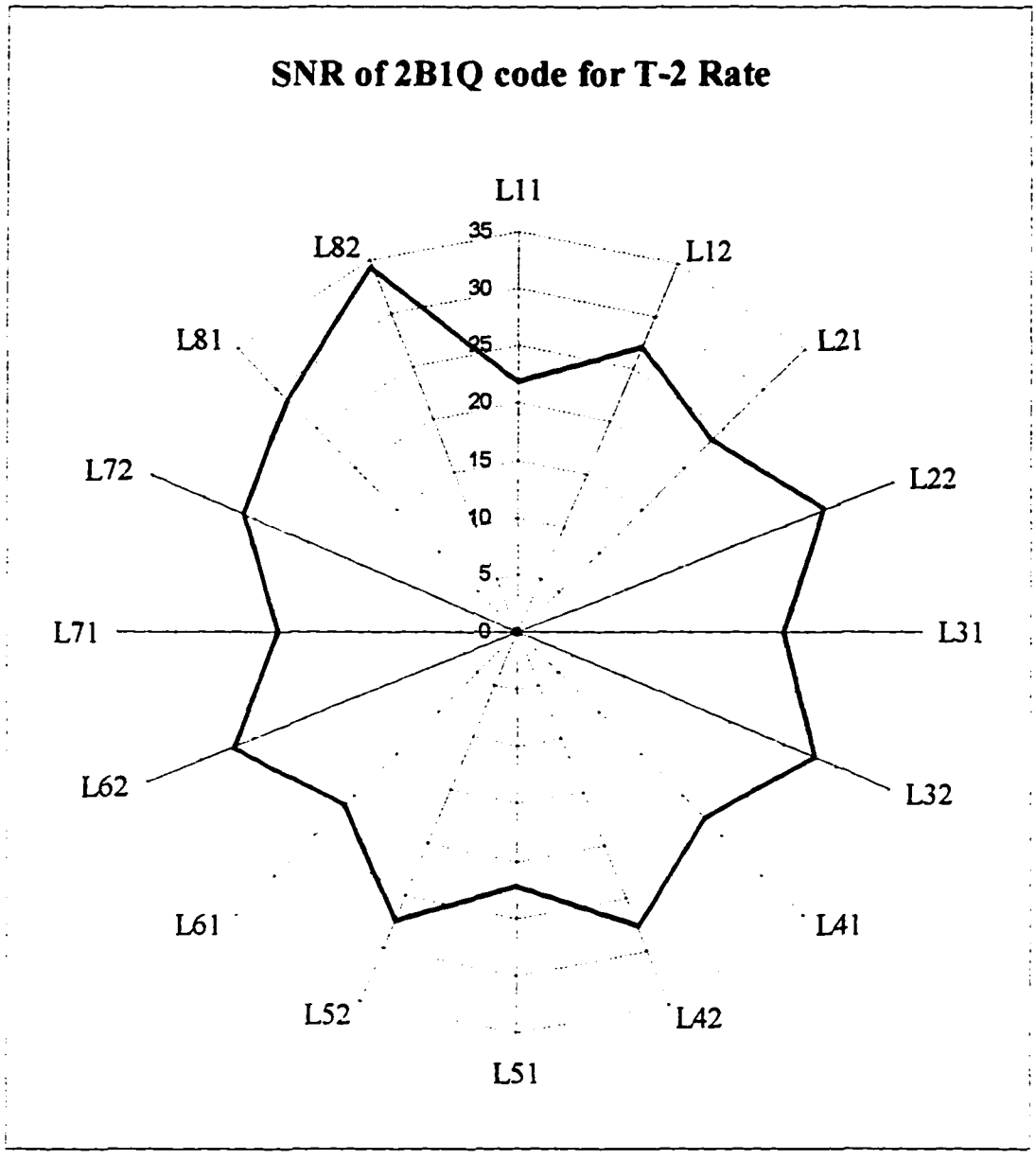

Figure 8.12 Signal-to-noise ratio (SNR, dB) of 2B1Q code for T-2 rate.

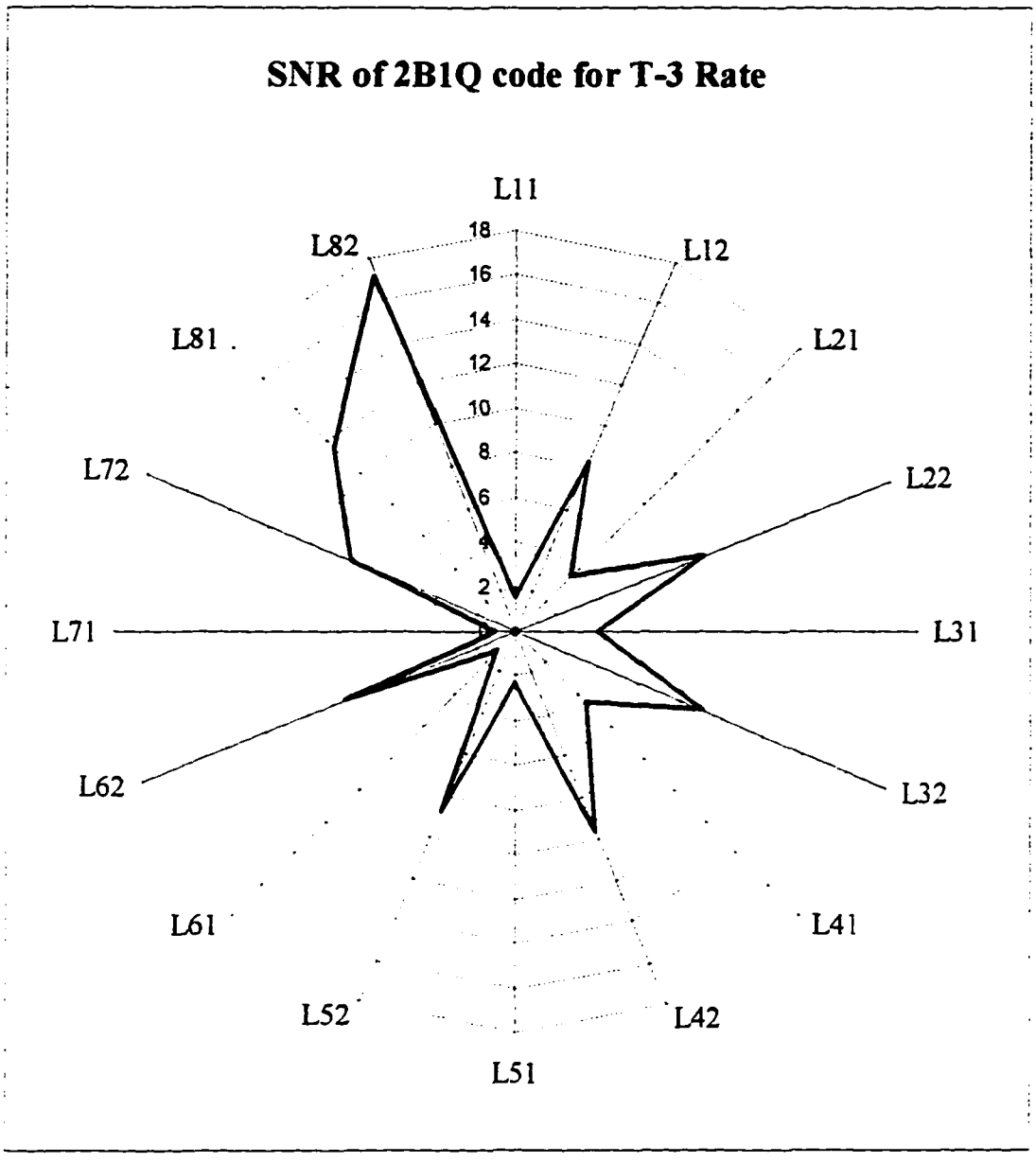

Figure 8.13 Signal-to-noise ratio (SNR, dB) of 2B1Q code for T-3 rate.

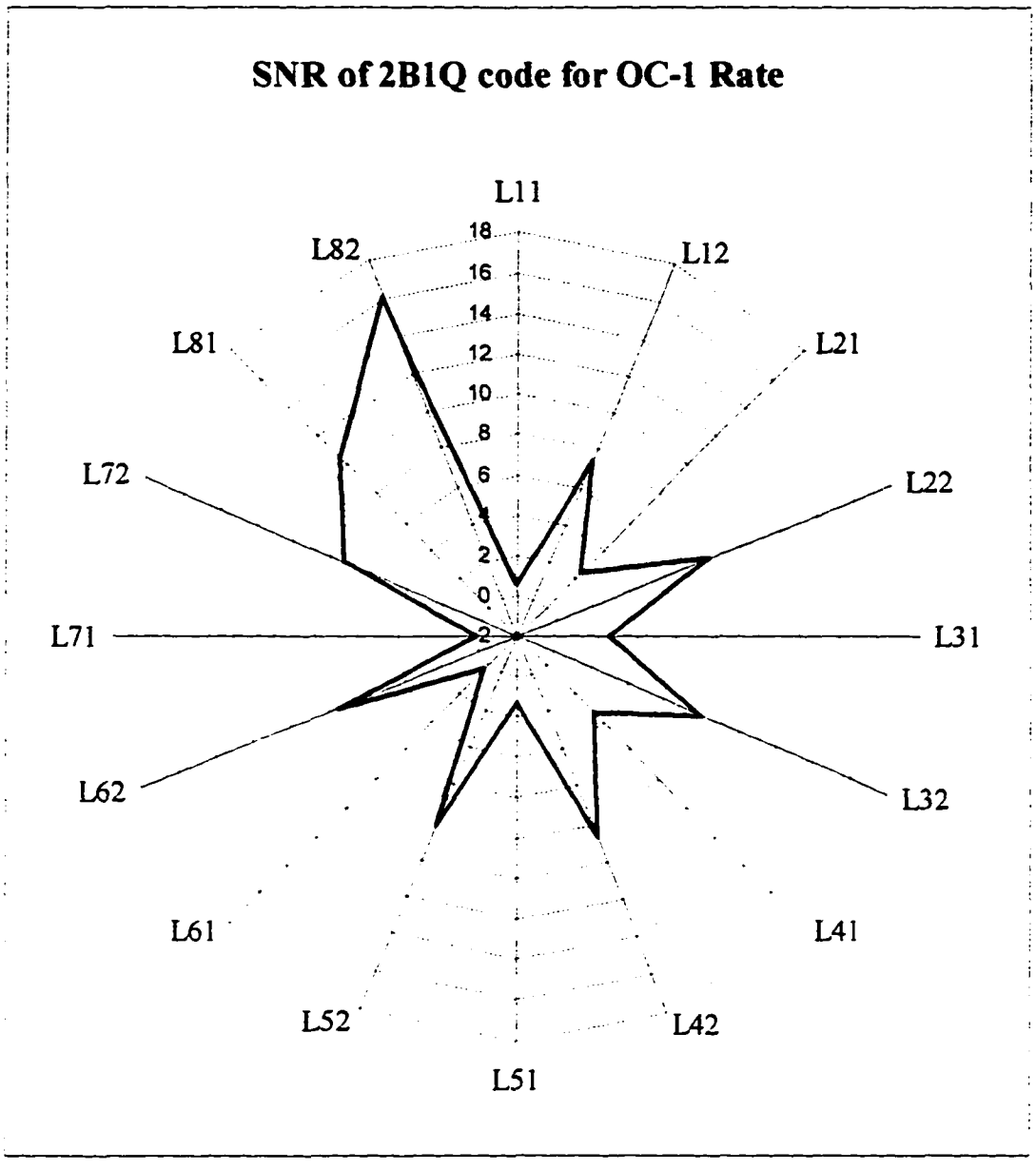

Figure 8.14 Signal-to-noise ratio (SNR, dB) of 2B1Q code for OC-1 rate.

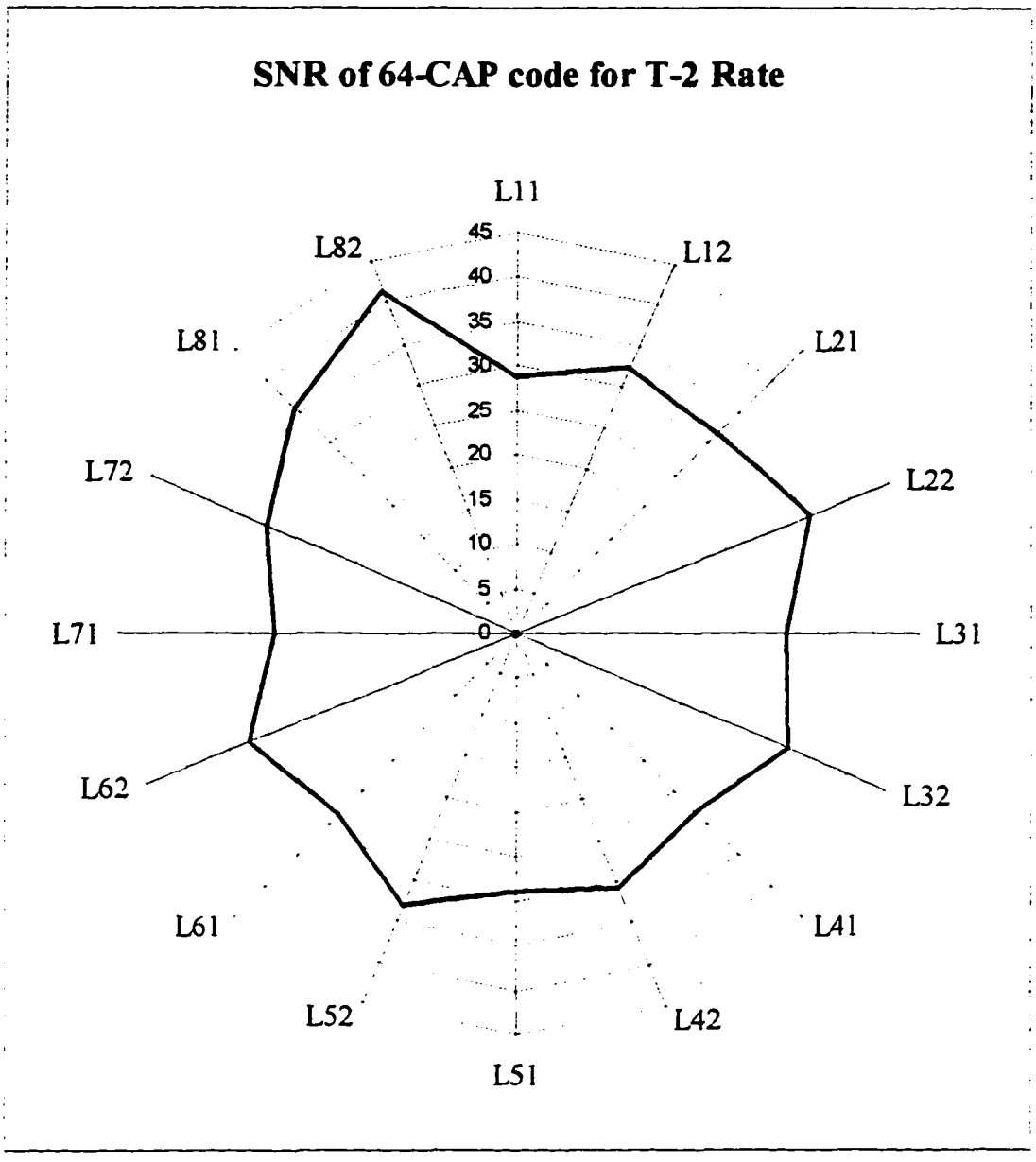

Figure 8.15 Signal-to-noise ratio (SNR, dB) of 64-CAP code for T-2 rate.

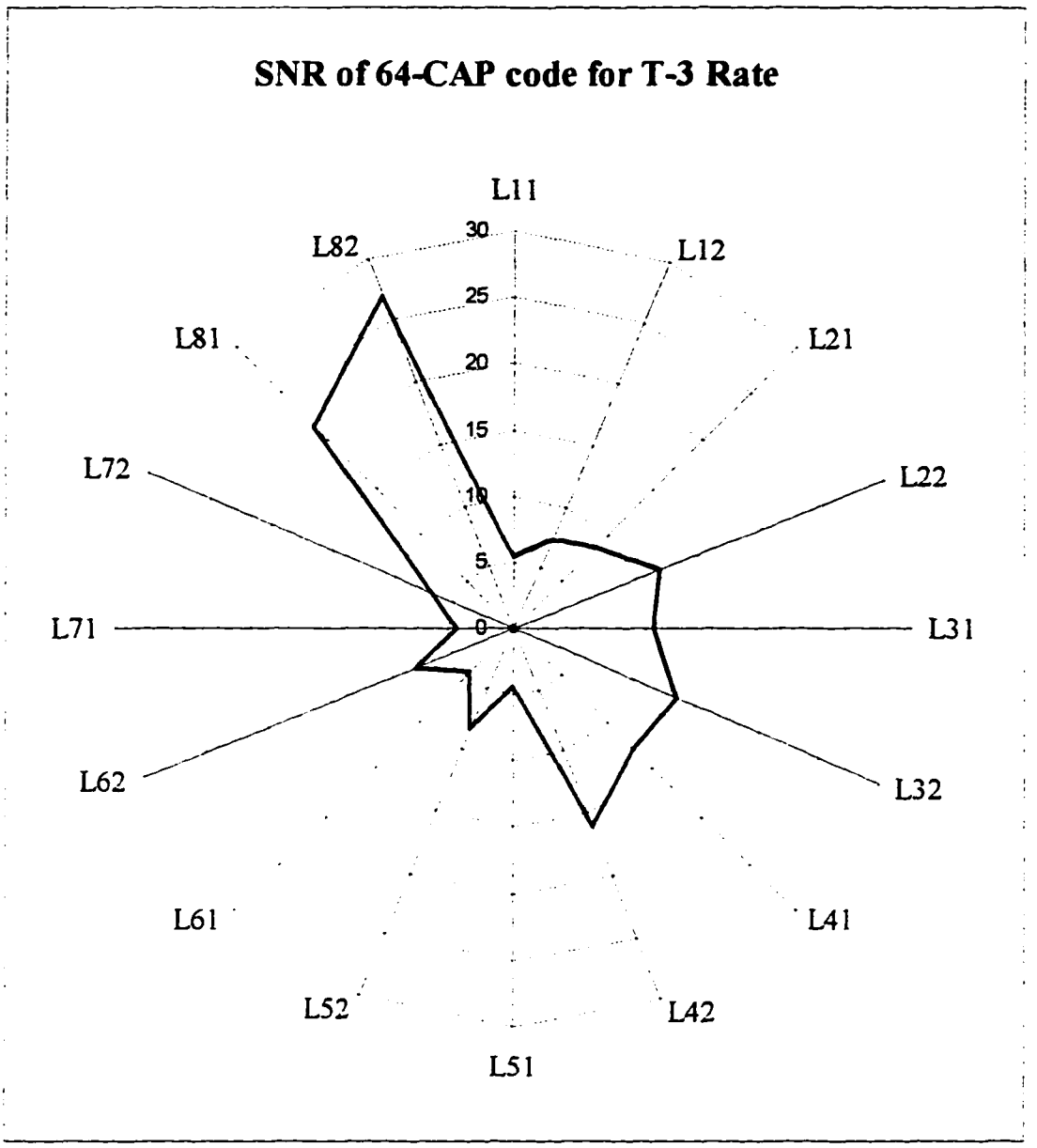

Figure 8.16 Signal-to-noise ratio (SNR, dB) of 64-CAP code for T-3 rate.

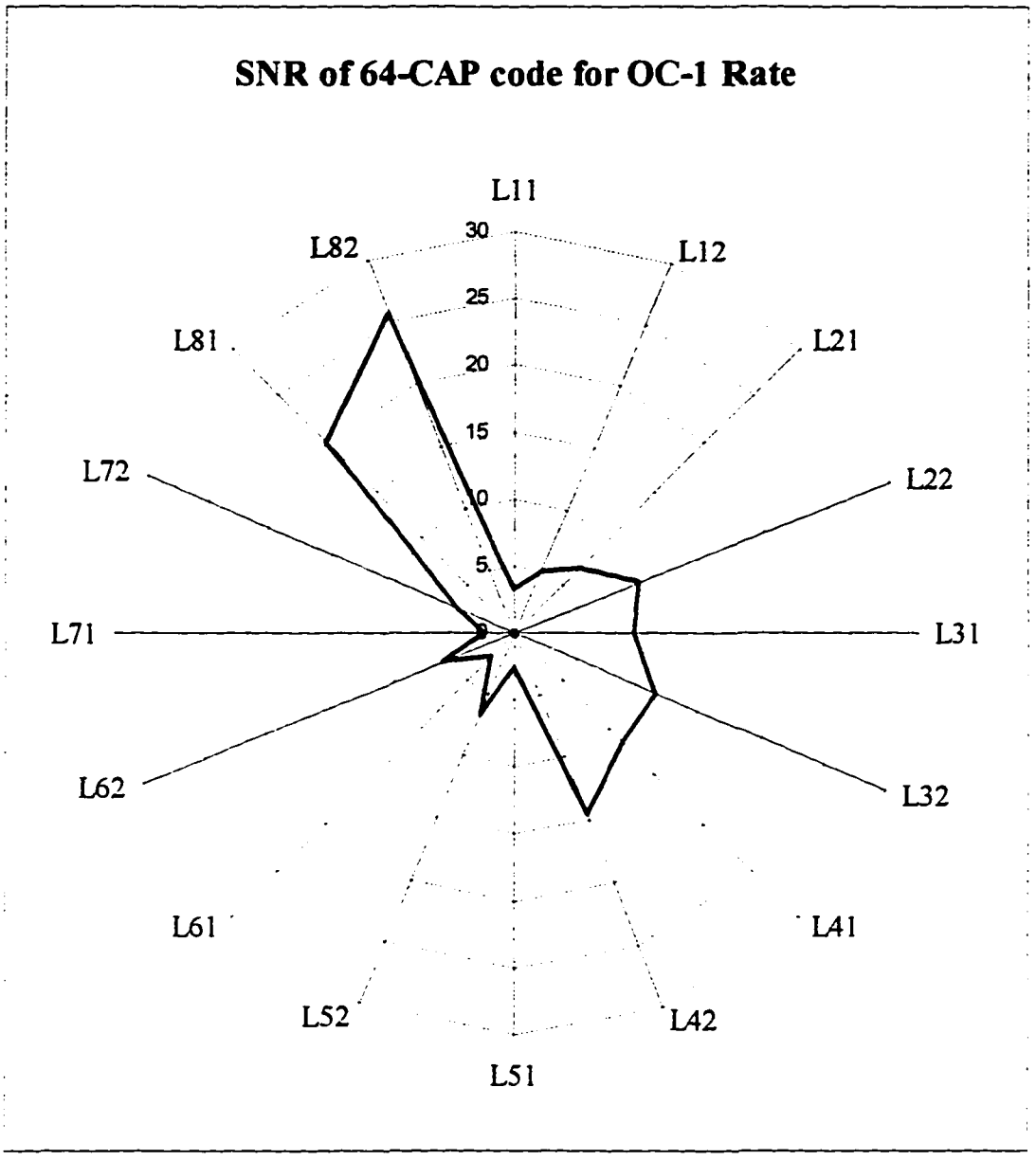

Figure 8.17 Signal-to-noise ratio (SNR, dB) of 64-CAP code for OC-1 rate.

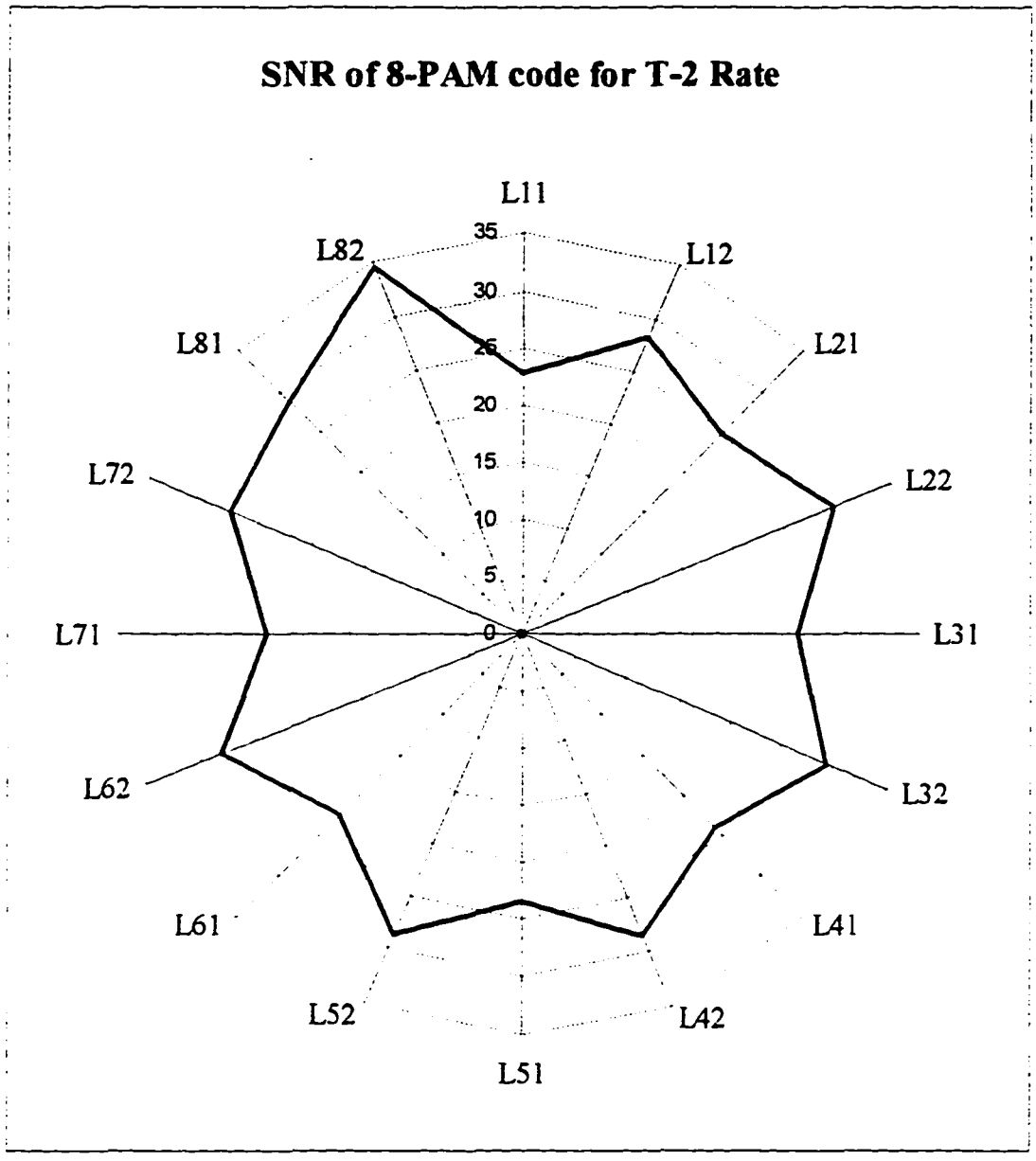

Figure 8.18 Signal-to-noise ratio (SNR, dB) of 8-PAM code for T-2 rate.

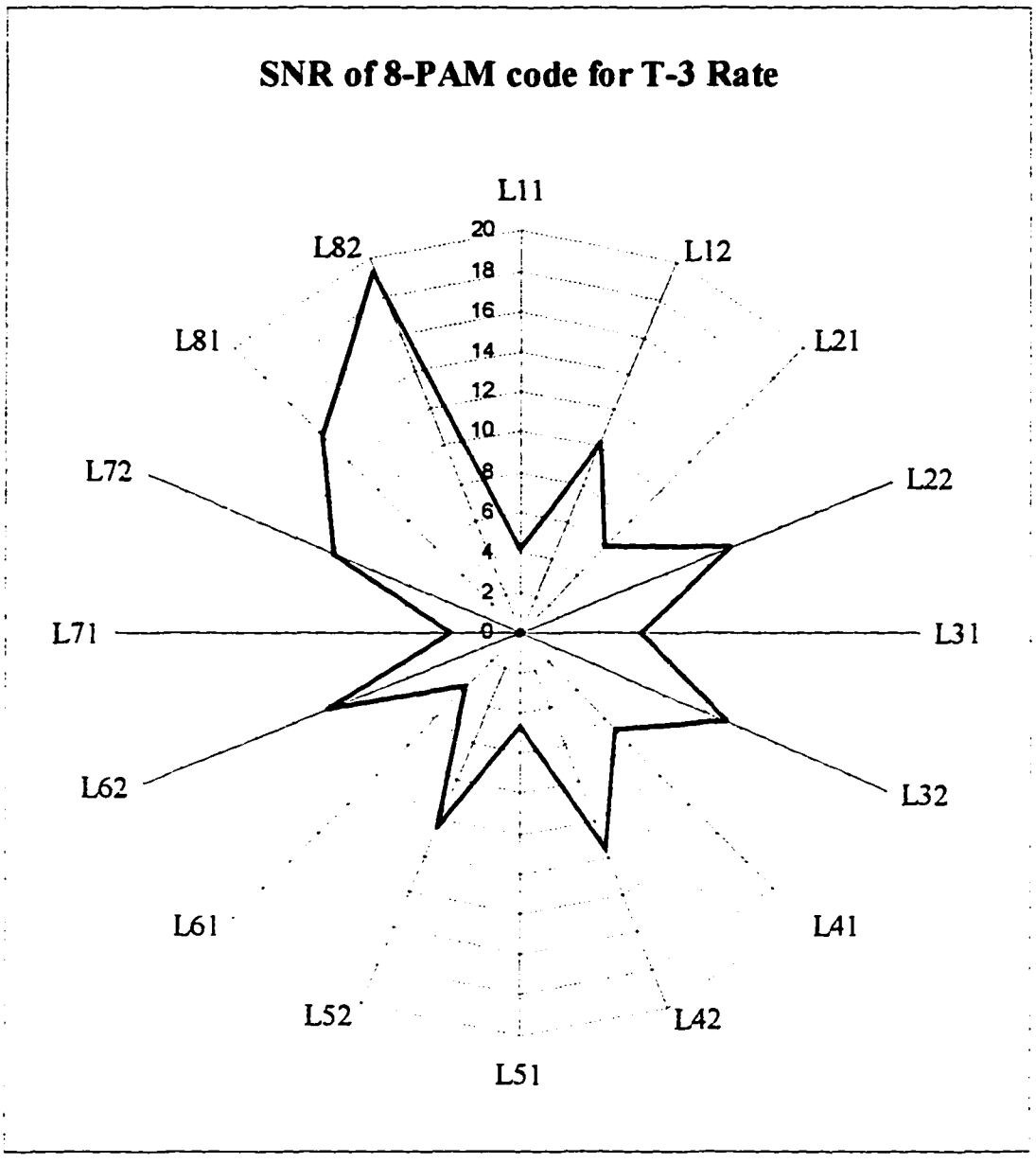

Figure 8.19 Signal-to-noise ratio (SNR, dB) of 8-PAM code for T-3 rate.

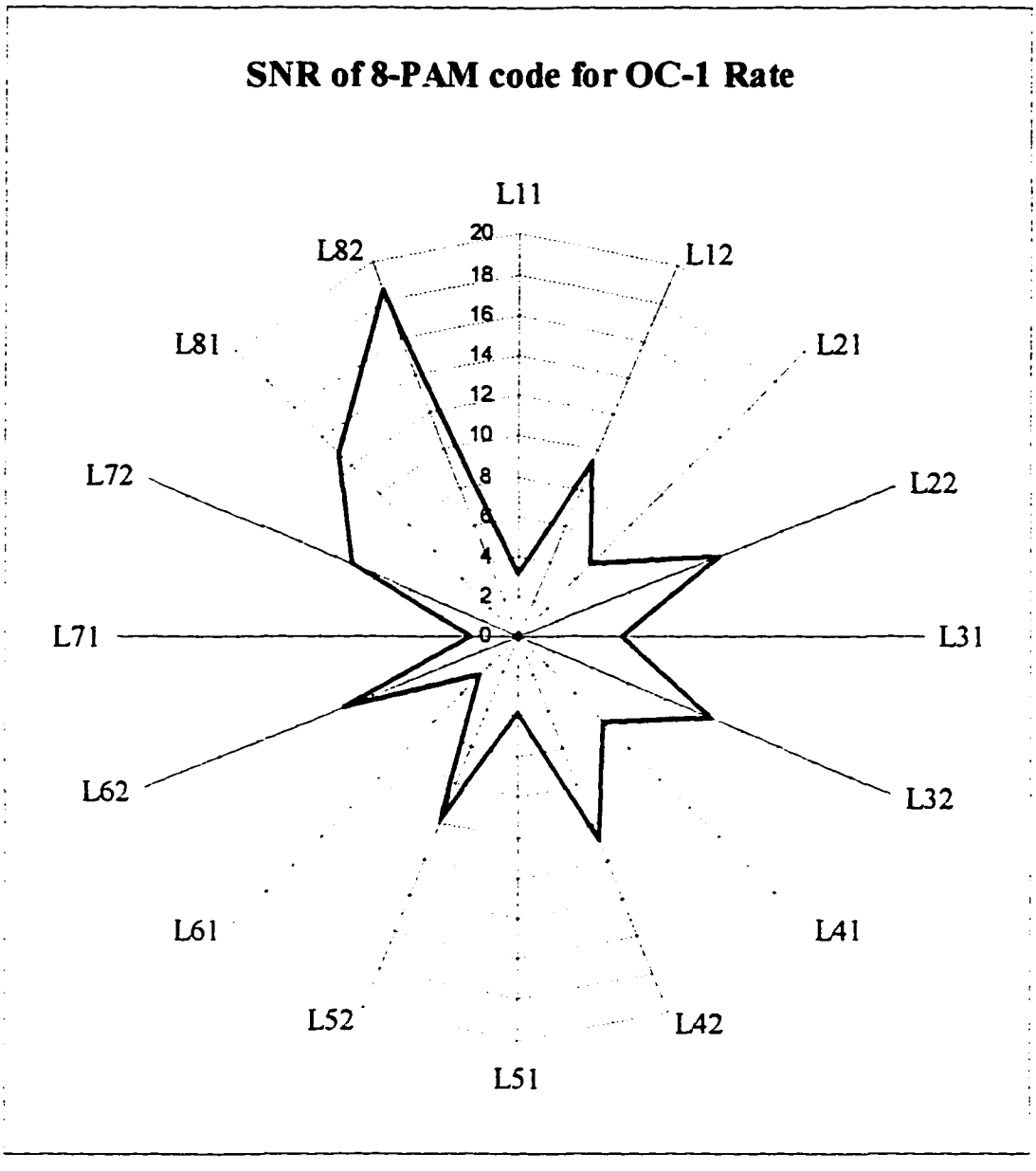

Figure 8.20 Signal-to-noise ratio (SNR, dB) of 8-PAM code for OC-1 rate.

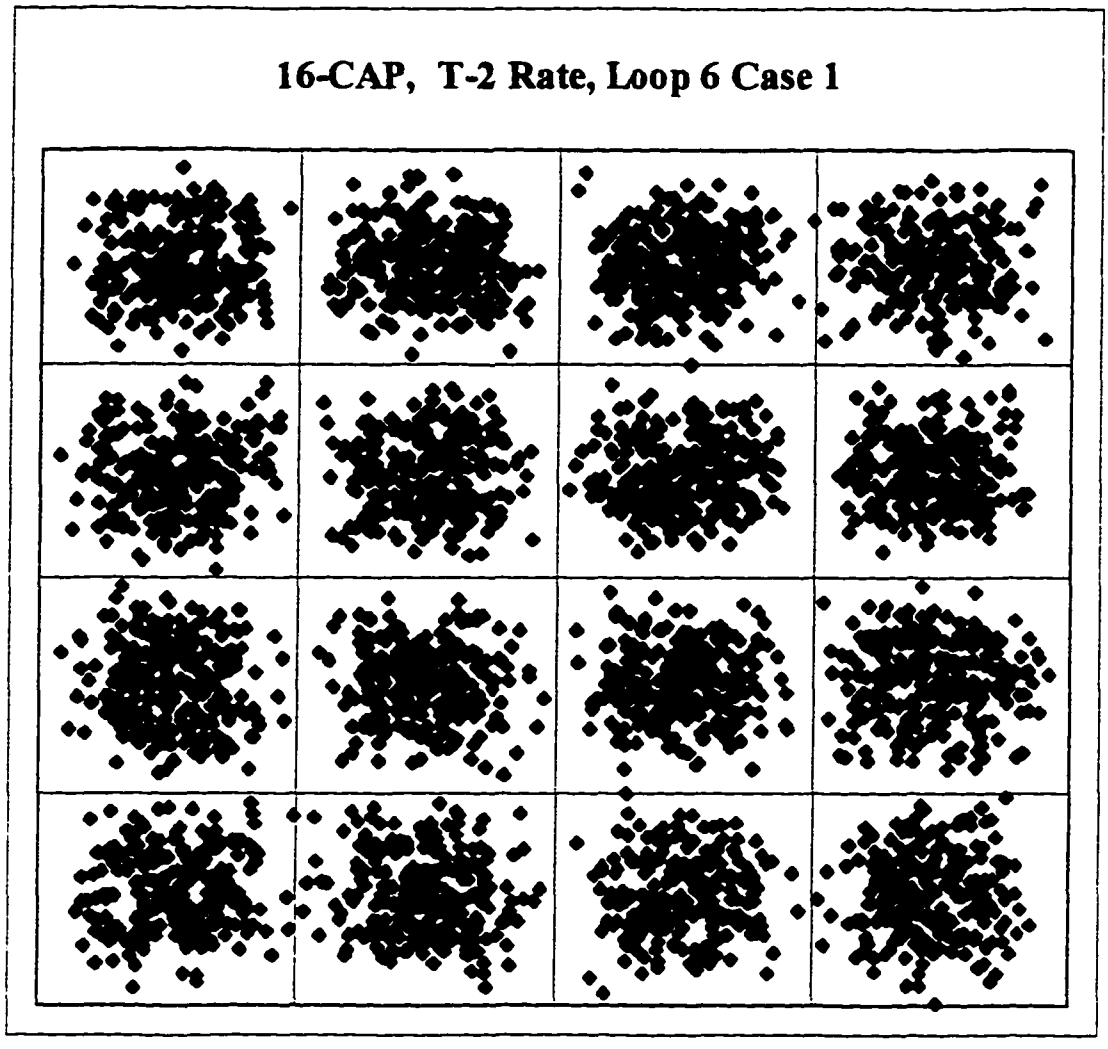

Figure 8.21 16-CAP constellation code for loop 6 case 1 at T-2 rate.

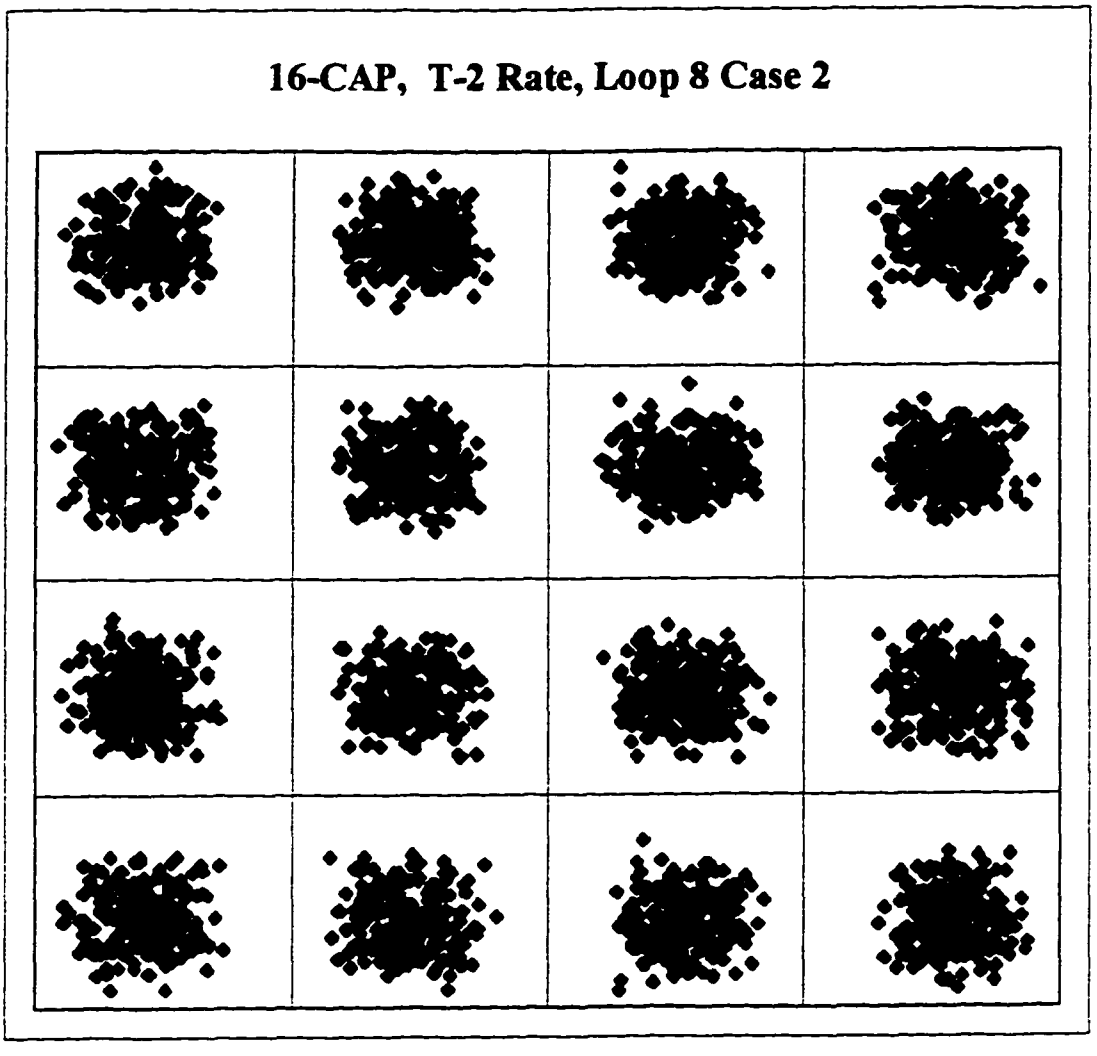

Figure 8.22 16-CAP constellation code for loop 8 case 2 at T-2 rate.

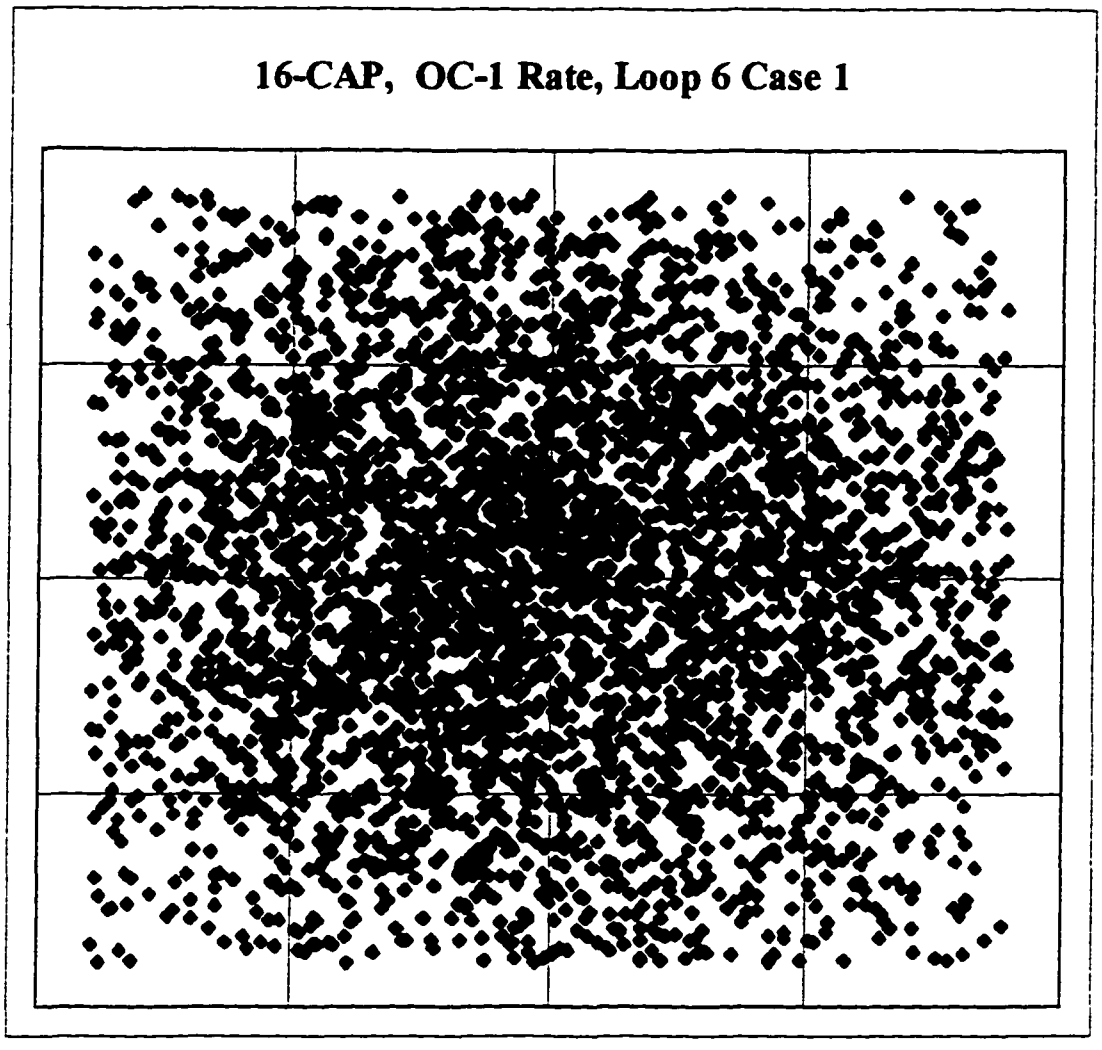

Figure 8.23 16-CAP constellation code for loop 6 case 1 at OC-1 rate.

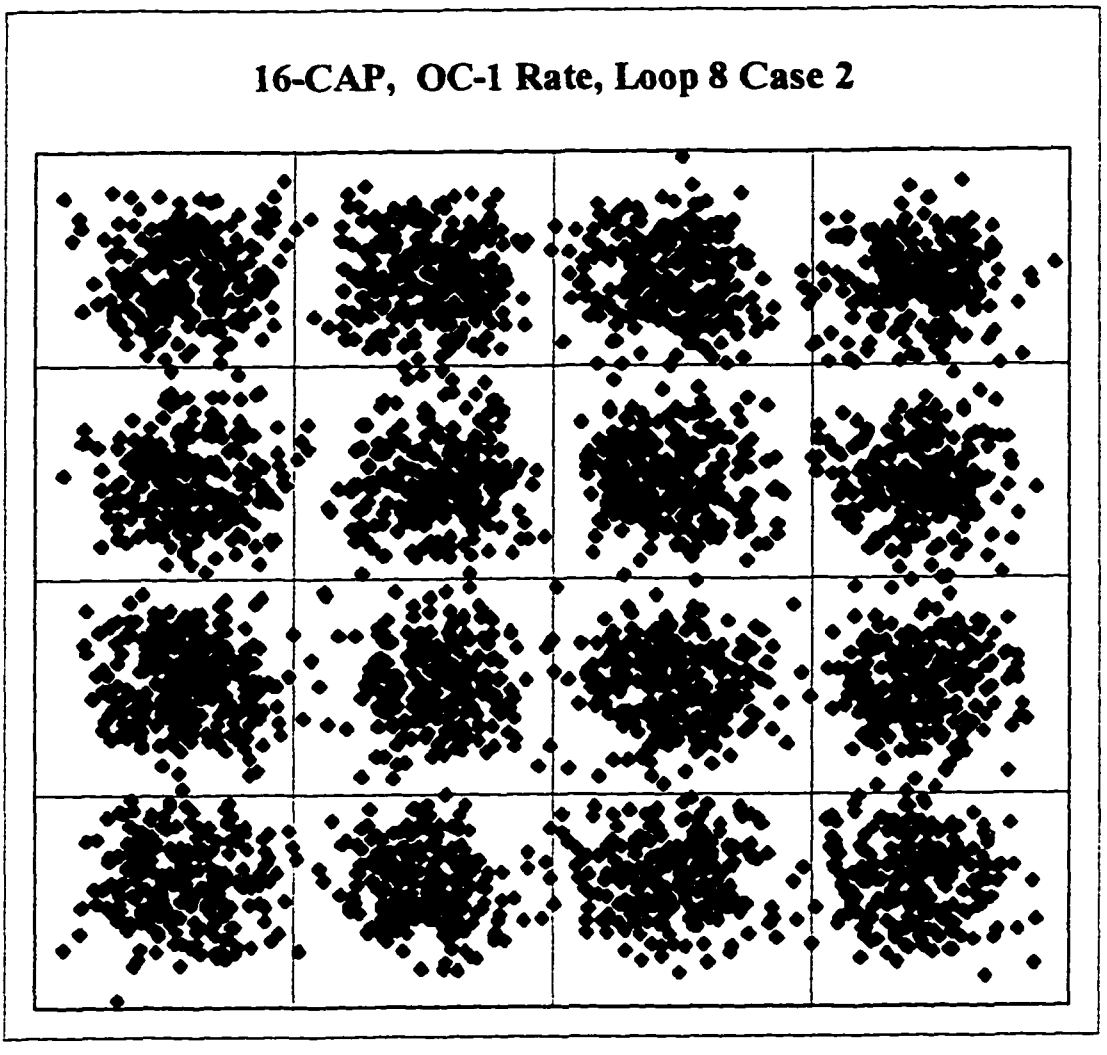

Figure 8.24 16-CAP constellation code for loop 8 case 2 at OC-1 rate.

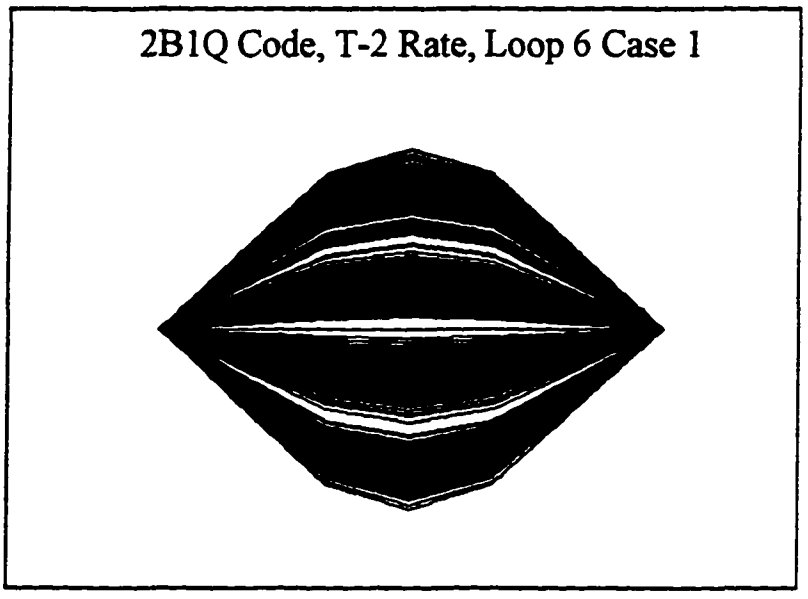

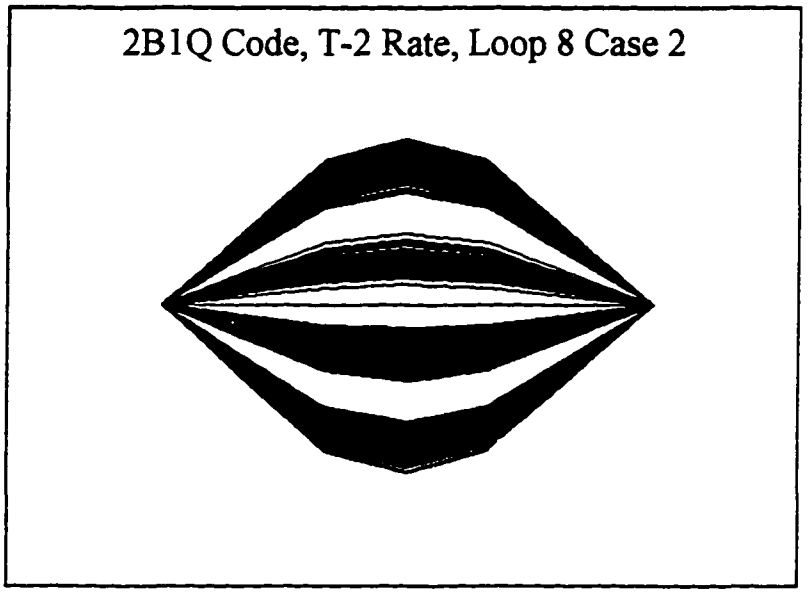

Figure 8.25 2B1Q code eye diagrams for loop 6 case 1 and loop 8 case 2 at T-2 rate.

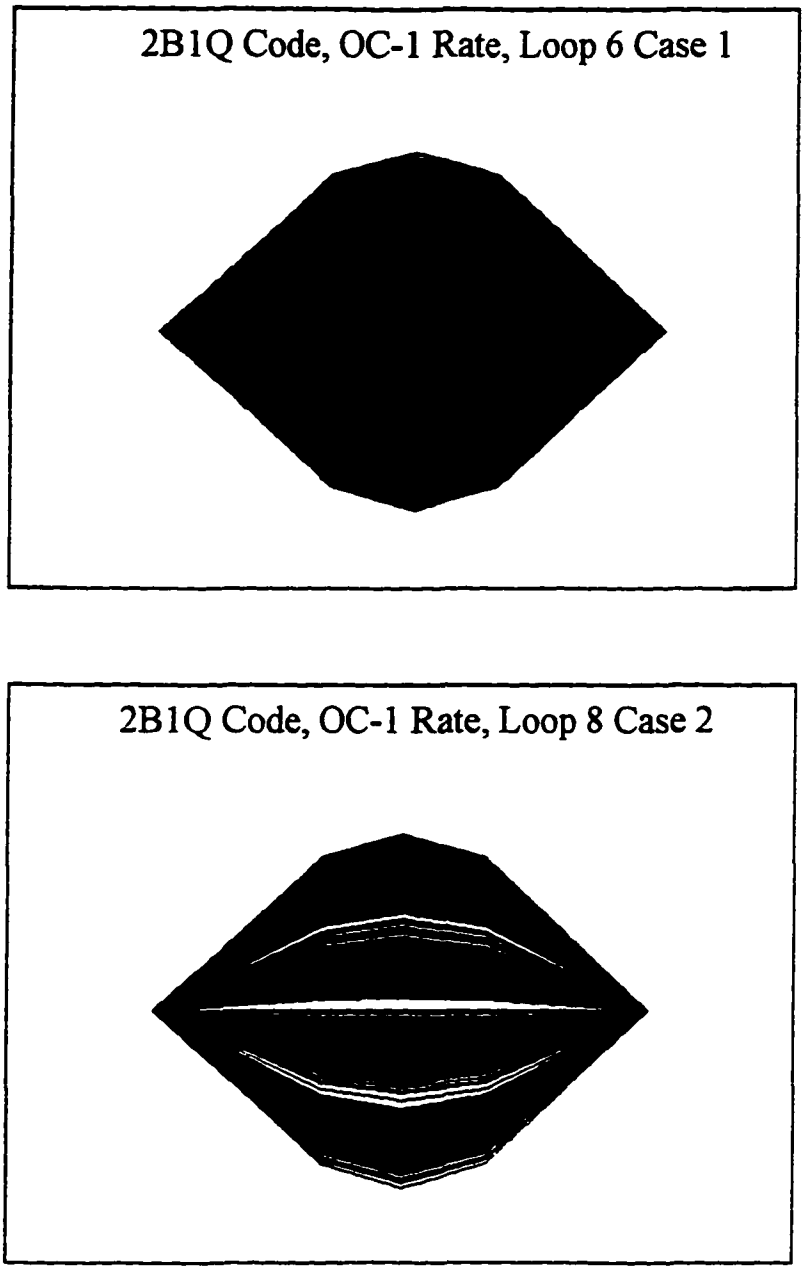

Figure 8.26 2B1Q code eye diagrams for loop 6 case 1 and loop 8 case 2 at OC-1 rate.

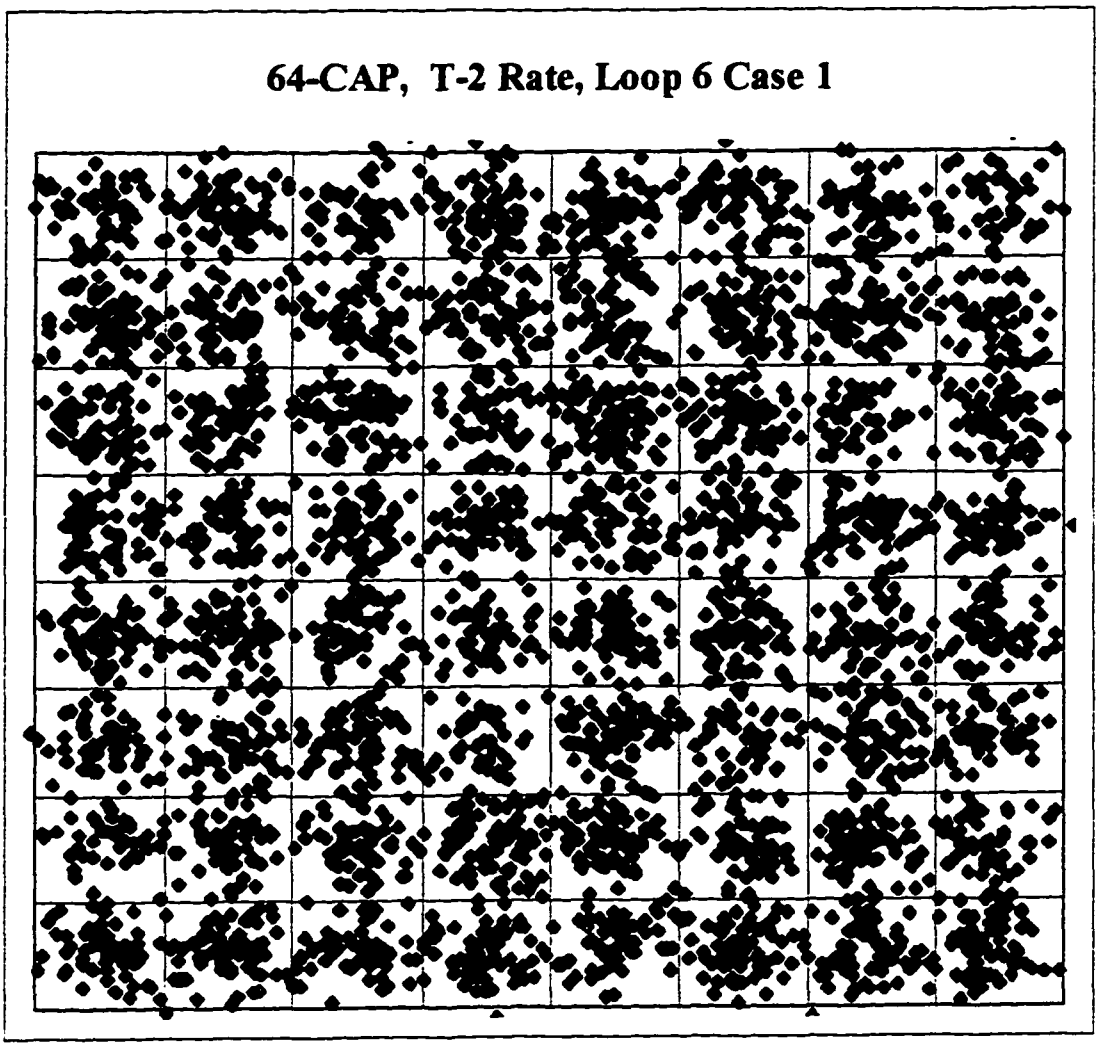

Figure 8.27 64-CAP constellation code for loop 6 case 1 at T-2 rate.

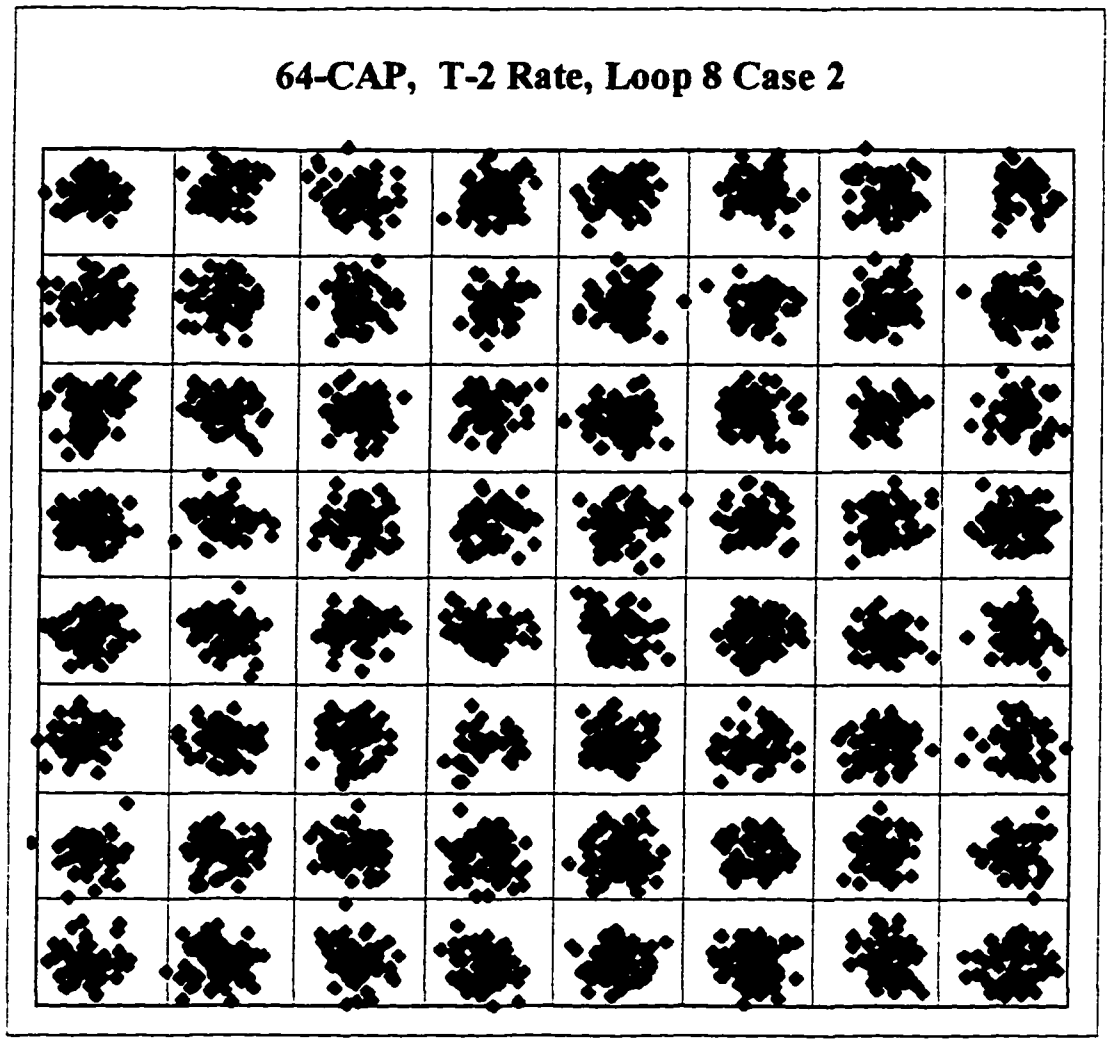

Figure 8.28 64-CAP constellation code for loop 8 case 2 at T-2 rate.

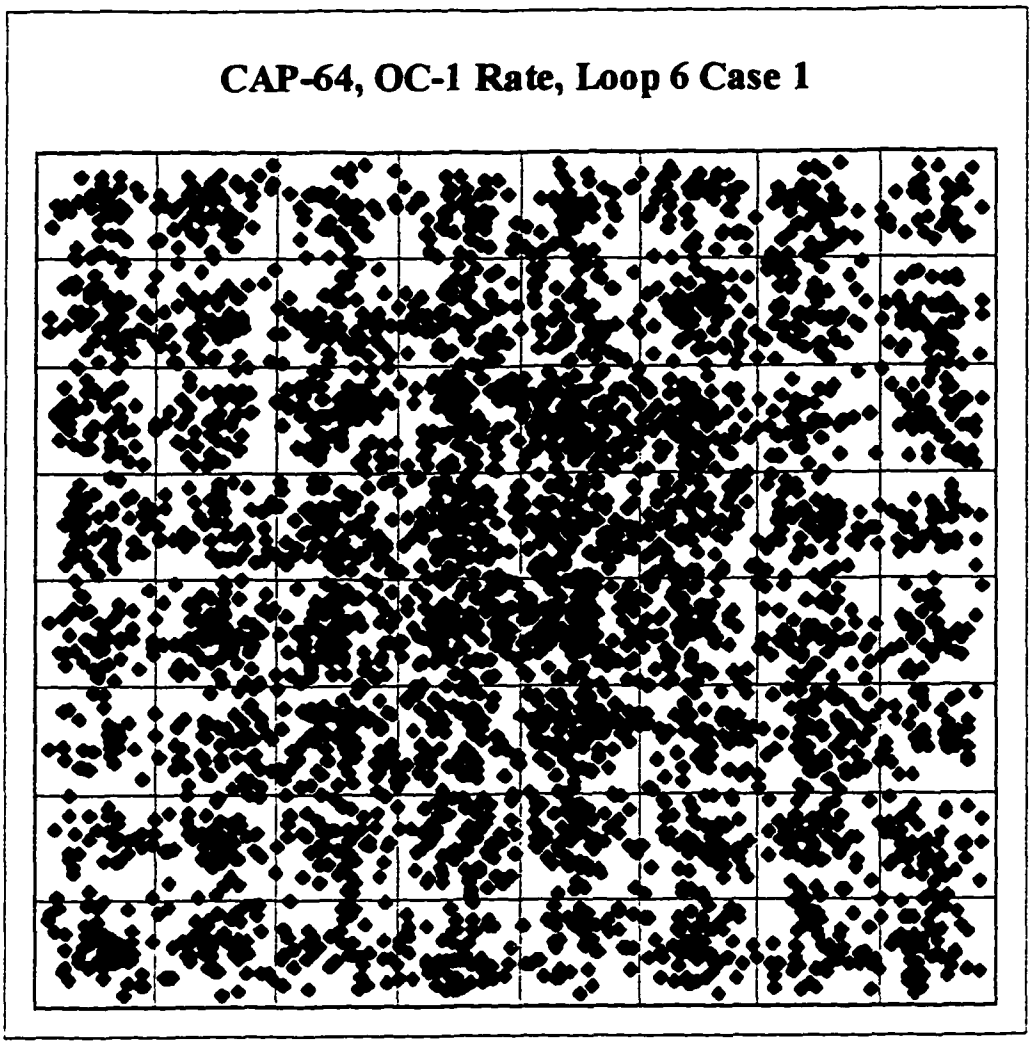

Figure 8.29 64-CAP constellation code for loop 6 case 1 at OC-1 rate.

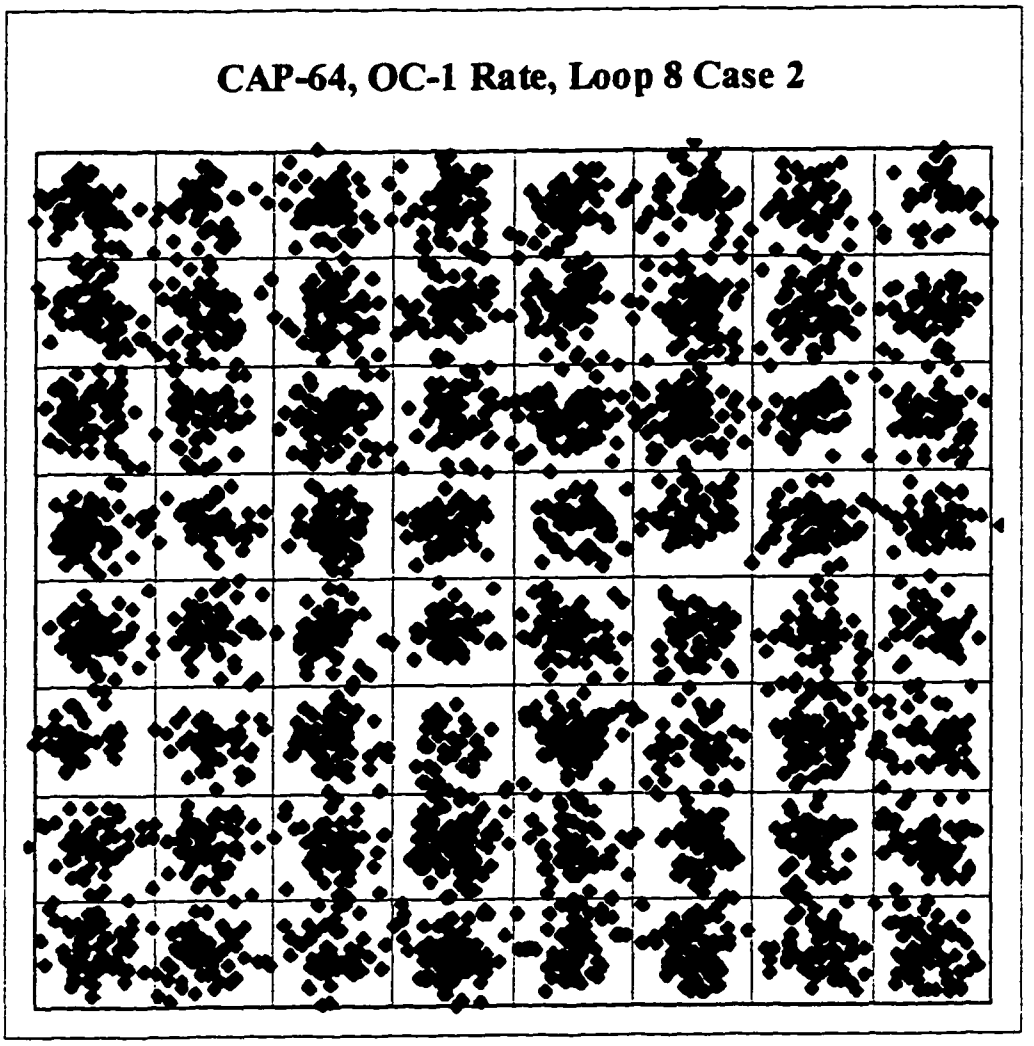

Figure 8.30 64-CAP constellation code for loop 8 case 2 at OC-1 rate.

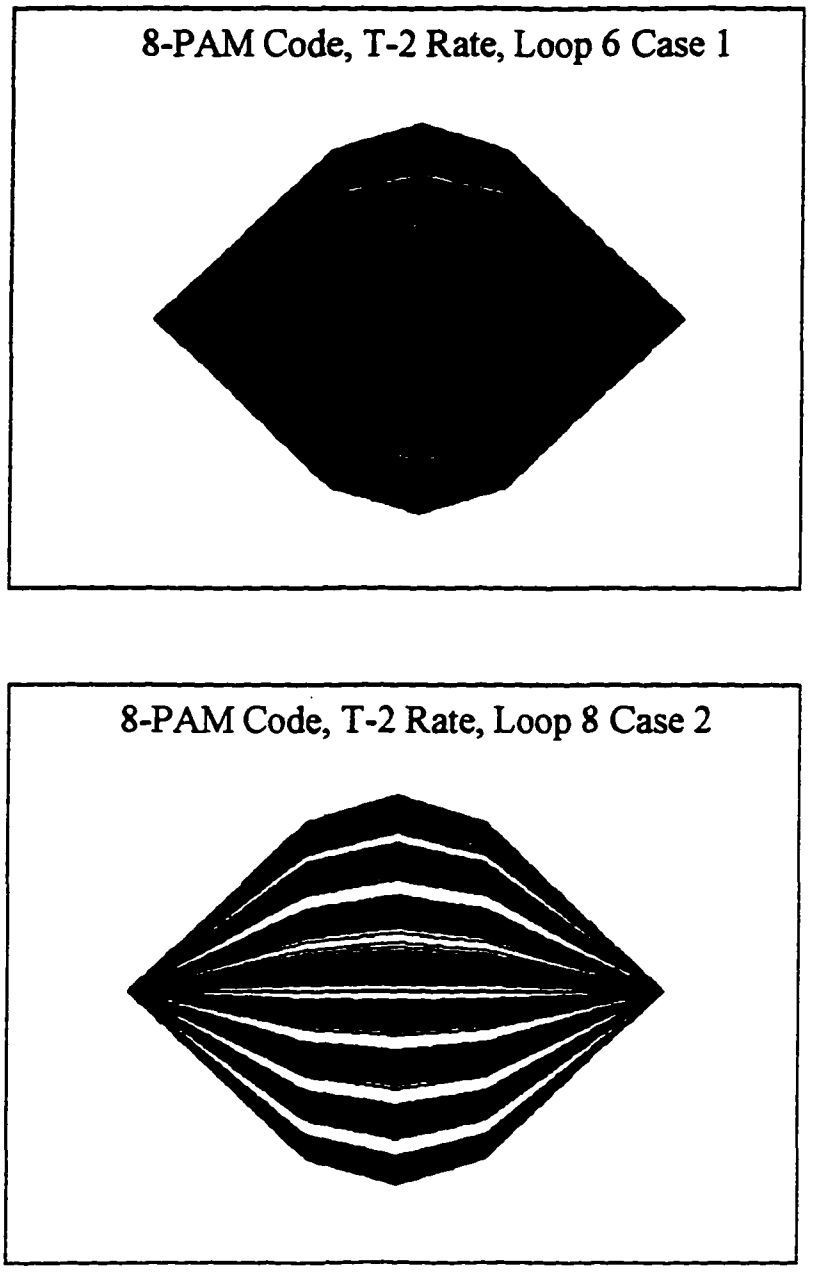

Figure 8.31 8-PAM code eye diagrams for loop 6 case 1 and loop 8 case 2 at T-2 rate.

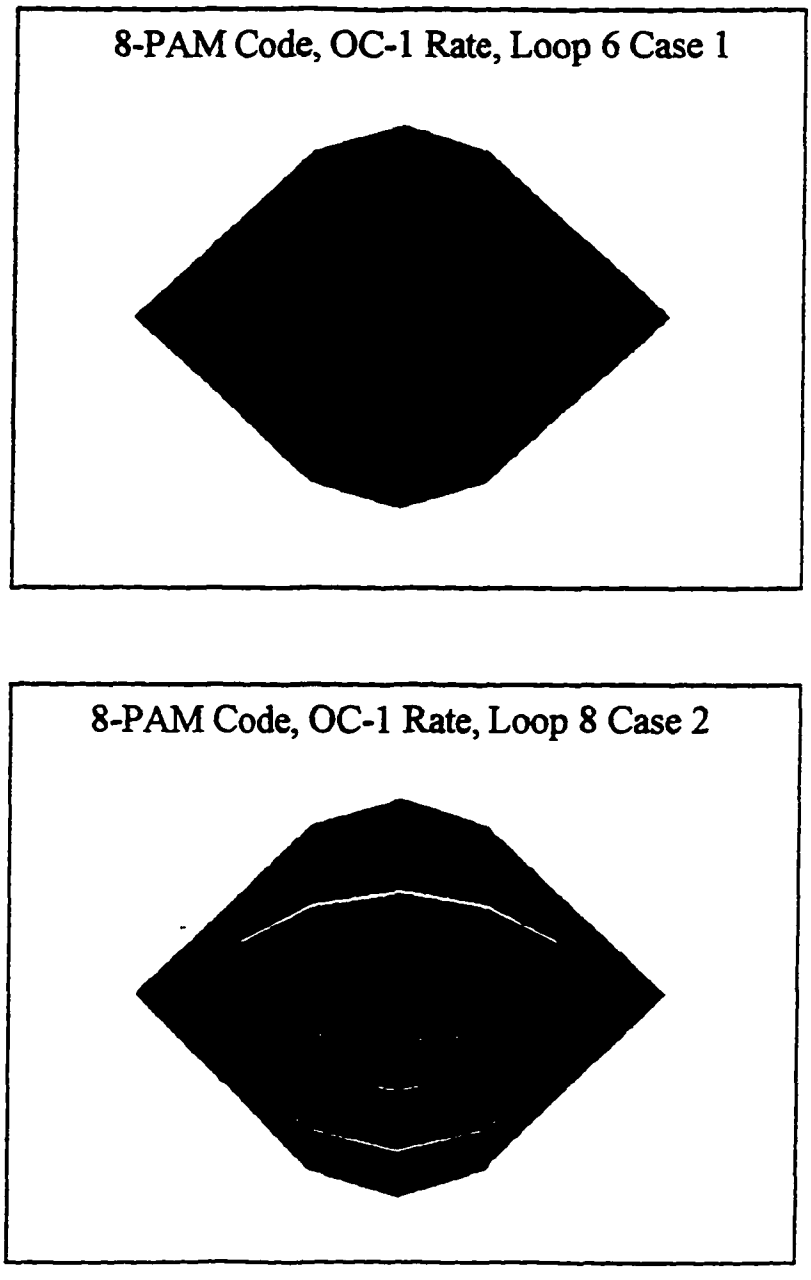

Figure 8.32 8-PAM code eye diagrams for loop 6 case 1 and loop 8 case 2 at OC-1 rate.

CHAPTER 9

9. Concluding Remarks

This research present carrierless amplitude and phase modulation (16-CAP and 64-CAP) and ML coding (2B1Q and 8-PAM) techniques for use with existing wire pair links to transmit data to the premises distribution at rates of T1, E1, T2, E2, E3, T3 and OC-1. Emphasis is given to higher rates since multilevel and multidimensional codes behave well for very high frequencies and regular codes are successfully optimized for lower rates. Simulation results are presented for CAP and ML codes using loop configurations in a basic point to multipoint (bus) passive topology of network environment.

A loop database is created, where all factors are considered, like network termination, bridge taps, loop length, frequency loss relations, loop termination. Old premises distribution topologies are investigated (loop 1-7), where the existence of bridge taps type of networks are dominant factor and have a enormous influence over the signal. In newer topologies (loop 8), these networks have been completely eradicated and therefore enhancing transmission capability of the medium.

The basic impairments studied are due to bridge taps, propagation loss, loop termination and self-NEXT. Impedance mismatches resulting from change in cable gauge are avoided by using uniform cabling (24 AWG) in all the loops. Frequency response of the loops are a major source of study for these impairments. The bandwidth utilized for these responses is typically equal or smaller than the FCC radiation limit of 30 MHz.

Performance of codes is studied by demonstrating usage of smaller bandwidth for fixed data rate or looking into a higher data rate for a fixed bandwidth. Both cases have shown the efficiency of each code and loops considered. Spectral shaping by tweaking filter components (excess bandwidth) has been analyzed and consequently implemented into transmitters. Power spectral density (PSD) plots for steps ranging from transmitter filter output up to receiver input (combined loop and transmitter filter) have been produced.

Another aspect of performance is studied when self-NEXT and Gaussian noise is introduced in the loop. There are two main attributes that affect NEXT performance, insertion loss of the loop and frequency spectrum of self-NEXT. Both attributes are associated to the system bandwidth and the PSD of the line code. Plots of NEXT loss for 49 interferers are produced for all codes of interest.

Time domain results have been produced at the output of the channel in constellation format for 16-CAP and 64-CAP and in eye diagram format for 2B1Q and 8-PAM codes. These diagrams are constructed for T-2 and OC-1 rates since they represent the lower and upper ends of the whole set of rates being studied.

Probability of symbol error is another parameter of performance that has been looked upon, it is characterized as a function of the signal-to-noise (SNR) for a given code and its number of levels. This characterization allows the assessment of total amount of power required on the channel. Radar plots of all codes for data rates of 6.312 Mbits/s (T2), 44.736 Mbits/s (T3) and 51.84 Mbits/s (OC-1) have been made with SNR as a parameter. And viability issue for all loops have been analyzed.

The software package utilized and its construction routines are given in the appendix.

APPENDIX A

A.1 Modeling of Digital Transmission Line through ABCD Matrix Reduction Techniques

Consider a uniform transmission line (figure A.1) carrying data signals from the transmitter to any point that is at a distance x . If the primary constants of the homogeneous line are fixed as R Ohm per unit length, L Henries per unit length, G mhos per unit length and C Farads per unit length, then the voltage and current relationship for the elemental length dx can be derived.

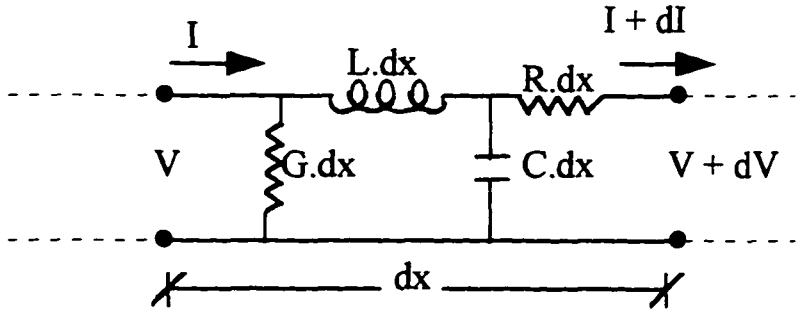

Figure A.1 An infinitely long data transmission line with distributed electrical characteristics R, L, G and C.

Let "dV" and "dI" be the voltage and current for the "dx" cable length (figure A.1). As current changes or reduces because of Admitance (Y) in the line and voltage changes or reduces because of Impedance (Z) in the line, the following relationship will hold,

$$\frac{\partial V}{\partial x} = (R + jwL)\, I \qquad (A.1)$$

Change in the voltage is dependent on impedance when a steady current is maintained.

As of same token,

$$\frac{\partial I}{\partial x} = (G + j\omega C)\, V \qquad (A.2)$$

Where change in the current is dependent on the admitance when a steady voltage is maintained. But, because of transients in the system, I and V vary proportionally to $\partial V/\partial x$ and $\partial I/\partial x$ respectively. Therefore a variation in the voltage results in a variation in the current.

$$\frac{\partial^2 V}{\partial x^2} = (R + j\omega L)\frac{\partial I}{\partial x} \qquad (A.3)$$

Substituting (A.2) into (A.3)

$$\frac{\partial^2 V}{\partial x^2} = (R + j\omega L)(G + j\omega C)\, V \qquad (A.4)$$

Since $(R + j\omega L)(G + j\omega C)$ is a constant, (A.4) can be defined as:

$$\frac{\partial^2 V}{\partial x^2} = \gamma^2 V \qquad (A.5)$$

Which is true, since voltage variation along the line is a constant times a steady V and $\gamma = \sqrt{(R + j\omega L)(G + j\omega C)}$ is a complex quantity called propagation constant. It ascertain reduction of current and voltage in the signal along the transmission path.

As the signal travels along the line it suffers attenuation and phase delay and therefore the complex quantity γ (propagation constant) , can also be defined as

$$\gamma = \alpha + j\beta \qquad (A.6)$$

The real part α in equation A.6 is called the attenuation constant and the imaginary part β is called the phase constant of the signal. These constants in terms of primary constants can be defined as:

$$\gamma^2 = (\alpha + j\beta)^2 = (\alpha^2 - \beta^2) + j\,2\alpha\beta = (R + j\omega L)(G + j\omega C) \qquad (A.7)$$

From (A.7),

$$(\alpha^2 - \beta^2) = (RG - \omega^2 LC) \qquad (A.8)$$

$$2\alpha\beta = \omega(LG + RC) \qquad (A.9)$$

$$(\alpha^2 + \beta^2) = \sqrt{(R^2 + \omega^2 L^2)(G^2 + \omega^2 C^2)} \qquad (A.10)$$

$$\alpha = \sqrt{\frac{(RG - \omega^2 LC) + \sqrt{(R^2 + \omega^2 L^2)(G^2 + \omega^2 C^2)}}{2}} \qquad (A.11)$$

$$\beta = \sqrt{\frac{(\omega^2 LC - RG) + \sqrt{(R^2 + \omega^2 L^2)(G^2 + \omega^2 C^2)}}{2}} \qquad (A.12)$$

For $\omega >> 0$,

$$\beta = \sqrt{\frac{\omega^2 LC + \omega^2 LC}{2}} = \omega \sqrt{LC} \qquad \text{(A.13)}$$

Now assume that the transmission line has length D and is excited with voltage and current, then the voltage and current along the line will be a function of both the frequency ω and the distance x. Therefore voltage and current in time domain can be written as

$$V(x, \omega) = V(x)\ e^{j\omega t} \qquad \text{and} \qquad I(x, \omega) = I(x)\ e^{j\omega t}$$

The voltage and current as a function of distance along the line consists of two propagating waves, one from the source to termination (source wave) and the other from termination to source (reflected wave). The total voltages and currents are the sum of the two waves, where the current of the two waves are flowing in opposite directions. Therefore the total voltage and current can be expressed as,

$$V(x) = V_s\ e^{-\gamma x} + V_r\ e^{\gamma x} \qquad \text{(A.14)}$$

$$I(x) = \frac{1}{Z_0} (V_s e^{-\gamma x} - V_r e^{\gamma x}) \qquad (A.15)$$

where V_s and V_r are the source wave and reflected wave respectively. Z_0 is a complex impedance and is called the characteristic impedance of the transmission line, and it equals the ratio of the voltage to current at any point of the line (independent of x) for either the source or reflected wave.

$$Z_0 = \frac{V_s}{I_s} = \frac{V_r}{I_r} \qquad (A.16)$$

When deriving (A.14) and combining with (A.1) and (A.15), it is obtained,

$$\frac{\partial V}{\partial x} = \gamma[-V_s e^{-\gamma x} + V_r e^{\gamma x}] = [R + j\omega L] I \qquad (A.17)$$

and from (A.17), (A.14) and γ,

$$Z_o = \sqrt{\frac{R + j\omega L}{G + j\omega C}} \qquad (A.18)$$

The characteristic impedance is dependent of length, as the primary constants change with distance, and is expressed in Ohms; it approaches the

value of $Z_0 = \sqrt{\frac{L}{C}}$ as the frequencies are raised and for smaller frequencies it approaches the value of $Z_0 = \sqrt{\frac{R}{G}}$ since there is a dominance of resistence for these frequencies.

As the Balancing of the network is done via characteristic impedance and the termination load, if the line is terminated with a balanced load $Z_0 = Z_L$, there exist a maximum transfer of energy from source to the load. Therefore, with the same token there is no reflection or returned energy and current and voltage are in a phase synchronization.

Now the characteristic impedance can also be represented in term of the propagation constant by combining A.7 and A.18, therefore,

$$Z_0 = \frac{\gamma}{G + j\omega C} = \frac{G\gamma}{G^2 + \omega^2 C^2} - j\frac{\gamma\omega C}{G^2 + \omega^2 C^2} \qquad (A.19)$$

Most of the commmunication links can be modelled by a two port network as given in figure A.2.

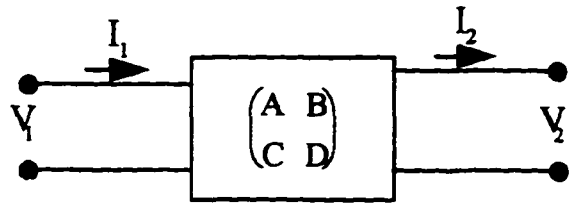

Figure A.2 Two port network.

The transmission matrix with elements A, B, C and D is used in modelling the system. These elements are dependent on the length of the cable, temperature, frequency and the primary constants R, L, G and C. The voltage and current V_1 and I_1 are for the input port (transmitter) and V_2 and I_2 are for the output port (receiver). The A, B, C and D matrix relates to the voltages and currents by the following set of linear equations,

$$\begin{cases} V_1 = AV_2 + BI_2 \\ I_1 = CV_2 + DI_2 \end{cases} \Leftrightarrow \begin{bmatrix} V_1 \\ I_1 \end{bmatrix} = \begin{bmatrix} A & B \\ C & D \end{bmatrix} \begin{bmatrix} V_2 \\ I_2 \end{bmatrix}$$

Let Z_1, V_1 and I_1 be the source impedance, voltage and current. From the source wave and reflected wave,

$$I_1 = I_s - I_r = (V_s - V_r) / Z_0 \qquad (A.20)$$

$$V_1 = V_s + V_r = (I_s + I_r) Z_0 \qquad (A.21)$$

Now combining (A.20) and (A.21) the following results are brought about:

$$I_s = (I_1 + V_1 / Z_0) / 2 \qquad \text{(A.22)}$$

$$I_r = (V_1 / Z_0 + I_1) / 2 \qquad \text{(A.23)}$$

$$V_s = (V_1 + I_1 Z_0) / 2 \qquad \text{(A.24)}$$

$$V_r = (V_1 - I_1 Z_0) / 2 \qquad \text{(A.25)}$$

Taking in consideration (A.22), (A.23), (A.24) and (A.25); V(x) , I(x) and Z(x) for the cable mentioned earlier can be identified as,

$$V(x) = V_s e^{-\gamma x} + V_r e^{\gamma x} = [(V_1 + I_1 Z_0)/2]\ e^{-\gamma x} + [(V_1 - I_1 Z_0)/2]\ e^{\gamma x}$$

$$V(x) = V_1[(e^{-\gamma x} + e^{\gamma x})/2] - I_1 Z_0\,[(e^{\gamma x} - e^{-\gamma x})/2]$$

$$= V_1\cosh(\gamma x) - I_1 Z_0 \sinh(\gamma x) \qquad \text{(A.26)}$$

$$I(x) = I_s e^{-\gamma x} - I_r e^{\gamma x} = I_1\cosh(\gamma x) - V_1 / Z_0 \sinh(\gamma x) \qquad \text{(A.27)}$$

$$Z(x) = Z_0\,[(Z_1 - Z_0 \tanh(\gamma x)) / (Z_0 - Z_1 \tanh(\gamma x))] \qquad \text{(A.28)}$$

From (A.28) the line impedance and the load impedance Z_L are related to each other in form of,

$$Z_1 = Z_0 [(Z_L + Z_0 \tanh(\gamma x)) / (Z_0 + Z_L \tanh(\gamma x))] \quad (A.29)$$

Now at the load or the receiver end the general form for voltage and current is:

$$I_2 = I_r - I_s = (V_s - V_r) / Z_0 \quad (A.30)$$

$$V_2 = V_r + V_s = (I_r + I_s) Z_0 \quad (A.31)$$

Now combining (A.30) and (A.31) the following results are brought about:

$$I_s = (V_2 / Z_0 - I_2) / 2 \quad (A.32)$$

$$I_r = (V_2 / Z_0 + I_2) / 2 \quad (A.33)$$

$$V_s = (V_2 - I_2 Z_0) / 2 \quad (A.34)$$

$$V_r = (V_2 + I_2 Z_0) / 2 \quad (A.35)$$

Now from (A.32), (A.33), (A.34) and (A.35) the voltage and current are:

$$V(x) = V_s\, e^{-\gamma x} + V_r\, e^{\gamma x} = [(V_2 - I_2 Z_0)/2]\; e^{-\gamma x} + [(V_2 + I_2 Z_0)/2]\; e^{\gamma x}$$

$$V(x) = V_2 \cosh(\gamma x) + I_2 Z_0 \sinh(\gamma x) \qquad \text{(A.36)}$$

$$I(x) = I_s\, e^{-\gamma x} - I_r\, e^{\gamma x} = I_2 \cosh(\gamma x) + V_2 / Z_0 \sinh(\gamma x) \qquad \text{(A.37)}$$

The general two port network representation of the transmission line leads to

$$\begin{bmatrix} V_1 \\ I_1 \end{bmatrix} = \begin{bmatrix} A & B \\ C & D \end{bmatrix} \begin{bmatrix} V_2 \\ I_2 \end{bmatrix}$$

Therefore from (A.36) and (A.37) we have,

$$\begin{bmatrix} V_1 \\ I_1 \end{bmatrix} = \begin{bmatrix} \cosh(\gamma x) & Z_0 \sinh(\gamma x) \\ \dfrac{\sinh(\gamma x)}{Z_0} & \cosh(\gamma x) \end{bmatrix} \begin{bmatrix} V_2 \\ I_2 \end{bmatrix} \qquad \text{(A.38)}$$

Equations in (A.38) satisfy interchangeability of input and output ports, since,

$$\cosh^2(\gamma x) - \sinh^2(\gamma x) = 1 \quad \Rightarrow \quad AD - BC = 1$$

Therefore, $\begin{vmatrix} A & \rightarrow & B \\ C & & D \end{vmatrix}$ and $\begin{vmatrix} D & \leftarrow & B \\ C & & A \end{vmatrix}$

APPENDIX B

B.1 The Fast Fourier Transform

When a finite Fourier transform is needed on a data set, the procedure to perform is a DFT (discrete Fourier transform). As the set expands, the effort used in carrying out the computations is exorbitant. A new algorithm for computing the DFT, which substantially reduces the amount of computations was proposed by Cooley and Tukey. The algorithm is known as the Fast Fourier Transform (FFT) algorithm. It converts time domain data into frequency domain data.

The discrete Fourier transform is defined as

$$\bar{X}(n) = \sum_{k=0}^{N-1} x(k)\, e^{-j2\pi nk/N} \qquad n = 0, 1, 2, ..., N-1 \qquad (B.1)$$

Where $\bar{X}(n)$ are the coefficients of N frequency terms and x(k) are the N values of the signal samples in time domain. In equation (B.1), $\bar{X}(n)$ is a vector containing N elements and on the right hand side there is a matrix of

NxN complex elements. A set of N linear equations has to be solved to obtain $\bar{X}(n)$.

To simplify the matter, let $e^{-j2\pi/N} = W_N$, then equation (B.1) becomes

$$\bar{X}(n) = \sum_{k=0}^{N-1} x(k)\, W_N^{nk} \qquad n = 0, 1, 2, ..., N-1 \qquad (B.2)$$

Therefore, taking into account x(k) as a complex term and W_N as a complex exponential, to compute the discrete Fourier transform (DFT) for one value of n will require N complex multiplication and N-1 complex additions. Now to calculate $\bar{X}(n)$, where n = 0, 1, ..., N-1, will require NxN complex multiplications and N(N-1) complex additions. The FFT algorithm will reduce the number of such operations and improve over the direct DFT computations.

To achieve the efficiency described by the FFT algorithm, the same will decompose the DFT computation into successive smaller DFT computations. In the process, the symmetry and the periodicity of W_N will be a essential tool; i.e., $W_N^0 = 1$ and $W_N^k = W_N^{k \bmod N}$.

The decomposition or decimation process is well depicted for vectors whose length N is an integer power of 2, $N = 2^{\epsilon}$. Vectors whose length is not a power of 2 will be augmented with a sequence of zero samples. The FFT algorithm takes advantage of this even arrangement of the sequence and divide it into further half subsequences recursively until the whole set is divided into subsets of two elements.

As seen above, N is an even vector. This can lead to divide $\bar{X}(n)$ into two subsets of N/2 elements, with even and odd number indexing of k.

$$\bar{X}(n) = \sum_{k\ even} x(k)\, W_N^{nk} + \sum_{k\ odd} x(k)\, W_N^{nk} \qquad (B.3)$$

As defined, let k = 2p + 1 when k is odd and k = 2p when k is even. Consequently equation (B.3) can be written as

$$\bar{X}(n) = \sum_{p=0}^{N/2-1} x(2p)\, W_{N/2}^{pn} + W_N^n \sum_{p=0}^{N/2-1} x(2p+1)\, W_{N/2}^{pn} \qquad (B.4)$$

This converges into,

$$\bar{X}(n) = A(n) + W_N^n\, B(n) \qquad n = 0, 1, \ldots, N-1 \qquad (B.5)$$

Although the index n ranges from 0 to N-1 (N values), A(n) and B(n) need only to be computed for n between 0 and (N/2) - 1, since both sums are periodic in n with period of N/2, i.e., $A(n + N/2) = A(n)$ and $B(n + N/2) = B(n)$.

The vector A(n) will perform $(N/2)^2$ complex multiplications and $(N/2 - 1)^2$ complex additions. The vector B(n) will perform N complex multiplications with the complex exponential W_N^n in addition to the same amount of computations as of A(n). Therefore a total of $2(N/2)^2 + N$ complex multiplications and $2(N/2 - 1)^2 + N$ complex additions are performed. As it can be seen here, decomposition of the DFT will require less computations than a direct computation of the DFT ($2(N/2)^2 + N < N^2$, assuming $N > 2$).

Now since N is a power of 2, further decomposition can be achieved. The vectors A(n) and B(n) can be considered as smaller DFT's and can be broken down into more smaller pieces, until N becomes 2. At that point a 2-point DFT is simply computed.

Therefore, as

$$A(n) = \sum_{p=0}^{N/2-1} x(2p)\, W_{N/2}^{pn} \quad \text{and} \quad B(n) = \sum_{p=0}^{N/2-1} x(2p+1)\, W_{N/2}^{pn}$$

are further subdivided into N/4 DFT, thus, would be computed as:

$$A(n) = \sum_{p=0}^{N/2-1} a(p)\, W_{N/2}^{pn} = \sum_{t=0}^{N/4-1} a(2t)\, W_{N/2}^{2tn} + \sum_{t=0}^{N/4-1} a(2t+1)\, W_{N/2}^{(2t+1)n}$$

$$= \sum_{t=0}^{N/4-1} a(2t)\, W_{N/4}^{tn} + W_{N/2}^{n} \sum_{t=0}^{N/4-1} a(2t+1)\, W_{N/4}^{tn} \qquad \text{(B.6)}$$

Similarly,

$$B(n) = \sum_{t=0}^{N/4-1} b(2t)\, W_{N/4}^{tn} + W_{N/2}^{n} \sum_{t=0}^{N/4-1} b(2t+1)\, W_{N/4}^{tn} \qquad \text{(B.7)}$$

The whole process of reaching up to 2-point DFT will require $\varepsilon = \log_2 N$ stages of computations, and as can be noted, each stage has N complex multiplications and N complex additions. Therefore, the total computation required by the FFT algorithm is $N \log_2 N$.

B.2 Algorithm to calculate FFT

- Compute A(n) for n = 0, 1, ... , N/2 - 1, recursively.

- Compute B(n) for n = 0, 1, ... , N/2 - 1, recursively.

- Compute $\overline{X}(n)$ for n = 0, 1, ... , N - 1, where A(n) = A(n mod N/2) and B(n) = B(n mod N/2).

E.g.: $\overline{X}(4) = A(4) + W_8^4 B(4) = A(0) + W_8^4 B(0)$

Since the values of A(0) and B(0) are already calculated, there is no need to calculate them, just fetch them from the memory and calculate $\overline{X}(4)$.

APPENDIX C

C.1. Transfer Functions for 2B1Q Shaping Filters

The transfer function for 2B1Q shaping filter will be derived based on the assumption that when transmitting the pulse, it has the same energy as of the Polar pulse.

$$\text{Energy (E)} = \int_{t_1}^{t_2} |x(t)|^2 \, dt \qquad \text{(C.1)}$$

The 2B1Q code has a pulse duration of 2T, where T is the symbol period of a Polar pulse. Since it is a rectangular pulse, C.1 can be derived into,

$$E = \int_{-T}^{T} K^2 \, dt \qquad \text{(C.2)}$$

Where K is the amplitude of the pulse. Now, for 2B1Q pulse to have same energy as of polar pulse (E_{polar} = T), K must satisfy the following requirement:

$$\int_{-T}^{T} K^2\,dt = T \quad \Rightarrow \quad K = \frac{1}{\sqrt{2}} \tag{C.3}$$

Since the 2B1Q pulse has the same shape as the polar pulse, it can be derived from the latter. Therefore, taking K in consideration the function is,

$$S(f)_{Polar} = \frac{\sin(\pi fT)}{\pi f} \Rightarrow \quad S(f)_{2B1Q} = \frac{\sin(2\pi fT)}{\sqrt{2}\pi f} \tag{C.4}$$

C.2. Transfer Functions for CAP Shaping Filters

The passband pulses s(t) and $\hat{s}(t)$ from equation (4.3) and (4.4) have their f(t) component as

$$f(t) = \frac{\sin[\pi(1-\alpha)\,t/T] + [4\alpha\,(t/T)] \,.\, \cos[\pi(1+\alpha)\,t/T]}{\pi\,[1-(4\alpha\,t/T)^2]\,t/T} \tag{C.5}$$

In C.5, α is called the rolloff parameter or the excess bandwidth. The spectrum or transfer function X(f) for the pulse above, which is also known as square-root raised cosine pulse, is

$$\begin{cases} T & 0 \le |f| \le (1-\alpha)/2T \\ \dfrac{T}{\sqrt{2}}\sqrt{1-\sin\left[\pi T\left(f-\dfrac{1}{2T}\right)/\alpha\right]} & (1-\alpha)/2T \le |f| \le (1+\alpha)/2T \end{cases} \qquad \text{(C.6)}$$

Now for the transfer function of s(t) and $\hat{s}(t)$ the shifting property of the Fourier transform can be used, e.g.,

$$h(t) = x(t)\, e^{j 2\pi f_0 t} \quad \Leftrightarrow \quad H(f) = X(f - f_0) \qquad \text{(C.7)}$$

and from (C.7)

$$h(t) = x(t)\, e^{-j 2\pi f_0 t} \quad \Leftrightarrow \quad H(f) = X(f + f_0) \qquad \text{(C.8)}$$

now s(t) can written as

$$s(t) = f(t)\cos(2\pi f_c t) = f(t)\,\frac{e^{j2\pi f_c t} + e^{-j2\pi f_c t}}{2}$$

$$s(t) = \frac{1}{2} f(t) e^{j 2\pi f_c t} + \frac{1}{2} f(t) e^{-j 2\pi f_c t} \qquad (C.9)$$

combining (C.7), (C.8) and (C.9)

$$S(f) = \frac{1}{2} X(f - f_c) + \frac{1}{2} X(f + f_c) \qquad (C.10)$$

With the same token

$$\hat{s}(t) = f(t) \sin (2\pi f_c t)$$

and

$$\hat{S}(f) = \frac{1}{2j} X(f - f_c) - \frac{1}{2j} X(f + f_c) \qquad (C.11)$$

Now for a completion, (C.10), (C.11) and (C.6) should be combined.

APPENDIX D

D.1. Simulation functions and tools used

General purpose digital signal processing tools were employed for the simulation study. This tools were created on a general purpose UNIX based platform. The main purpose of the tools is to performs DSP and related tasks. Figure D.1 display step by step procedure of simulation performed. The outer portion represent the whole communication system model and the inner portion is a conception of the outer system from the simulation point of view.

At the scrambler bit stream is random as possible and passed to the serial to parallel encoder where 2D-Mapping is done. Now two streams of symbols are handled by the two transmission shaping filters (Sqroot Raised Cosine), which are then added or subtracted and passed to the loop filter. Basically the signal is attenuated at the loop (power level is usually low). At this point white Gaussian noise and crosstalk are added to the signal and handed over to the receiver.

The following functions represent the six points in figure D.1:

(1) "symgen" : Generates CAP symbols. It can produce m-points depending on applications and parameters (e.g., 10,000 - 15,000 symbols).

(2) "sqrracos": Generates square root raise cosine response.

(3) "loopfcn": Generates loop response.

(4) "wgn and crossi" : Generates white gaussian noise and crosstalk.

(5) and (6) is the signal received and analyzed through the function "fftmg".

D.2. Detailed description of functions and commands utilized

af: Performs arithmetic function.

Usage: af "aa-bb"

This function subtracts "bb" from "aa". In same fashion "af" can be used to add, divide and multiply.

conj: Complex conjugate of input vector.

Usage: Let the vector x = [3 4]

$\Rightarrow$ conj x = [3 -4]

fftmag: friendly DFT magnitude response computations.

Usage: fftmag [-c] [-l] [-n N] [-f f_s] [-m] xfile yfile

fftmag writes frequency scale data to "xfile", and FFT magnitude response data to "yfile". The [-n N] option allows specification of FFT frequency resolution (number of output points). N must be greater than or equal to the input data rank, and less than 8192. Default value is 512.

The assumed sampling frequency (Hz) is specified using the [-f f_s] option. Default is 9600 Hz. This affects nothing other than the frequency scale values which are written to "xfile".

Input data type is specified to be complex if the " -c " option is present, and real-valued otherwise. If input is complex, output will extend from DC (null) to $\frac{N-1}{N} f_s$, otherwise it extends from DC to $\frac{N-1}{2N} f_s$.

If " -l " is specified, output is linear, i.e. | H(f) | . If -l is not specified, output is power spectrum in dB, i.e. 20 log (| H(f) |) .

If " -m " is specified, output magnitudes are normalized so that the largest is approximately 0 dB (for log output) or unity (for linear output).

invert: What invert basically does is it inverts sequences on a tuple-by-tuple basis.

Usage: Let the vector y = [1 2 3 4]

⇒ invert y = [4 3 2 1]

⇒ invert 2 y = [3 4 1 2]

loopfcn (loop function): It takes the values of the loop and give the transfer function H(f) for the loop, using ABCD matrices. Then it gives the frequency response for that transfer function for all the frequency that are applied to it (all from zero to 500). H(f) can have any complex values x + jy , for all f's that are used. It is basically a filter.

loopmgn (loop magnitude): It takes the absolute values out of "loopfcn". This function gives the magnitude of the loopfcn in dB. It give values as power (even though it is the loss), therefore basically what it does is:

$$10 \log|H(f)|^2 = 20 \log |H(f)| \text{ , where } |H(f)| = \sqrt{x^2 + y^2}$$

pwr: "pwr" and "energy" compute respectively the power and energy of the vector read from stdin, assumed to be a real valued signal. Energy is computed as $\sum_{1}^{N} X_i^2$, where X_i is a real-valued input vector element, and N is the input vector rank. Power is simply "energy/N".

Usage: Let vectors z1 = [0.2 1 0.4] and z2 = [0.31 1.58 0.63]

⇒ pwr z1 = 0.39

⇒ pwr z2 = 1

The vector z2 can be said to be normalized to unit power.

rank : Gives the number of elements in a vector.

reize: Convert real-valued vector to complex 2-tuples with zero imaginary part.

rtop: Convert rectangular coordinate into polar.

sqracos: Generate square-root raised-cosine impulse response or we may say that it computes N symmetrically sampled points from the "square-root raised-cosine" impulse response.

SYNOPSIS: sqracos α μ N

alpha = excess bandwidth or roloff factor (0 <= alpha <= 1.0)

mu = samples/symbol interval.

N = Number of samples in output impulse response.

An example would be to generate response of a square-root raised-cosine Nyquist passband filter which are FIR transmitter and receiver filters for data transmission over Band-Limited channels. Therefore a typical filter can be:

sqracos 0.2 4 18

The parameters are deciphered as: Let be assumed that symbol rate of 2400 Hz (2400 symbols/s) is used, N=18 is the tap coefficients for the filter, α = 0.2 is the rolloff factor, sampling frequency of 9.6 kHz (9600 samples/s). The sampling ratio is μ = sampling frequency/symbol rate, therefore

9600/2400 = 4 (each symbol is sampled 4 times, meaning 4 samples per symbol are obtained).

- "sqracos" creates the desired baseband filter with real-valued coefficients.
- For small "N" and "α" , truncation effects can result in cascaded impulses with significant ISI.
- The square-root raised cosine spectrum admits a closed-form Fourier transform.

In the example: sqracos 0.2 4 18 | reize | modulate 1900 9600, "reize" converts to a complex vector the input from the square root raised cosine filter and "modulate" multiplies the vector elements by $e^{(n.2\pi 1900)/9600}$ rotating the frequency response counterclockwise by 1900 Hz (with assumed sampling rate of 9600 Hz).

symgen : Generate pseudorandom sequence of 2-D symbols from a given constellation lattice, optionally providing various impairments. The impairments are only added when they are specified in the parameters. Including white Gaussian noise (WGN), phase jitter, and frequency offset.

Synopsis: symgen -ccfile -nN

-ccfile File cfile contains I/Q pairs which define the constellation point set. Currently, the program enforces a limit of 512 points. The first number is taken to be the I coordinate of the first point, the second as the Q coordinate of the first point, the third as the I of the second point, the fourth as Q of the second point, etc.. Constellation points can put in a file in any order; there are no symmetry requirements.

-nN N specifies the number of points to be output.

Output from symgen is 4-tuples to stdout, the first two numbers being the impaired point location [Re,Im], and the last two being the unimpaired point location [Re,Im].

wgn: Generate a white Gaussian, real-valued sequence of length N and variance σ^2. It generates a one-dimensional Gaussian RV w (real-valued w), using the mapping $w = \cos(2\pi r_1)\ln(r_2)$ where r_1 and r_2 are drawn independently from uniform distribution on (0,1].

Synopsis: wgn N σ^2

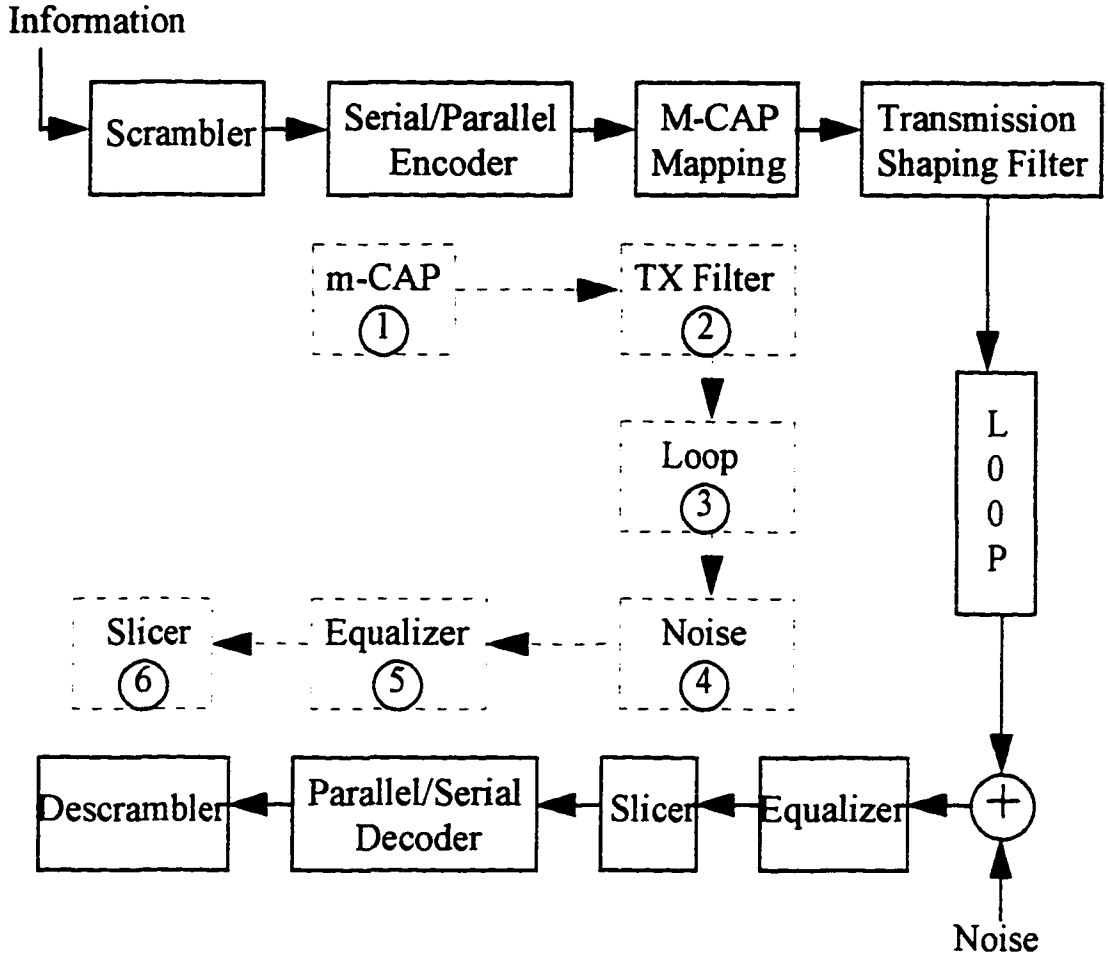

Figure D.1 Communication system model.

REFERENCES

[1] Syed V. Ahamed and Michael J. Miller, "Digital Transmission Systems and Networks", Vol. I, Computer Science Press, Rockville, Maryland, 1988.

[2] Syed V. Ahamed and Michael J. Miller, "Digital Transmission Systems and Networks", Vol. II, Computer Science Press, Rockville, Maryland, 1988.

[3] Syed V. Ahamed and V.B. Lawrence, "Intelligent Communication Systems", Kluwer Academic Publishers, Norwell, MA, to be published.

[4] Victor B. Lawrence, Joseph L. Locicero and Laurence B. Milstein, "IEEE Communications Society's: Tutorials in Modern Communications", Computer Science Press, Rockville, Maryland, 1983.

[5] B. Hancock, "Network Concepts and Architectures", QED Information Sciences, Wellesley, Massachusetts, 1989.

[6] T. C. Bartee, "Digital Communication", Howard W. Sams & Co., Indianapolis, Indiana, 1986.

[7] J. M. Griffiths, "ISDN Explained", John Wiley & Sons, New York, NY, 1990.

[8] M. Harb, "Modern Telephony", Prentice Hall, Englewood Cliffs, New Jersey, 1989.

[9] Peter W. Gofton, "Mastering Serial Communications", Sybex Inc., Alameda, CA, 1986.

[10] W. Stallings, "Data and Computer Communications", Macmillan, New York, NY, 1985.

[11] W. Stallings, "ISDN and Broadband ISDN", Macmillan, New York, NY, 1992.

[12] Edward A. Lee and David G. Messerschmitt, "Digital Communication", Kluwer Academic Publishers, Norwell, MA, 1988.

[13] N.S. Jayant and Peter Noll, "Digital Coding of Waveforms", Prentice Hall, Englewood Cliffs, New Jersey, 1984.

[14] Simon Haykin, "Digital Communications", John Wiley & Sons, New York, NY, 1988.

[15] R.J. Horrocks and R.W.A. Scarr, "Future Trends in Telecommunications", John Wiley & Sons, New York, NY, 1993.

[16] Roger L. Freeman, "Telecommunication Transmission Handbook", John Wiley & Sons, New York, NY, 1981.

[17] C.E. Shannon and W. Weaver, "A Mathematical Theory of Communication", Univ. of Illinois Press, IL, 1949.

[18] Richard W. Hamming, "Coding and Information Theory", Second Edition, Prentice-Hall, Englewood Cliffs, New Jersey, 1986.

[19] Edward P. Cunningham, "Digital Filtering", Houghton Mifflin Company, Princeton, New Jersey, 1992.

[20] S. Benedetto, E. Biglieri and V. Castellani, "Digital Transmission Theory", Prentice-Hall, Englewood Cliffs, New Jersey, 1987.

[21] Bernhard E. Keiser, "Broadband Coding, Modulation, and Transmission Engineering", Prentice-Hall, Englewood Cliffs, New Jersey, 1989.

[22] Sophocles J. Orfanidis, "Introduction to Signal Processing", Prentice-Hall, Englewood Cliffs, New Jersey, 1996.

[23] Alan V. Oppenheim and Ronald W. Schafer, "Digital Signal Processing", Prentice-Hall, Englewood Cliffs, New Jersey, 1975.

[24] Clifford D. Ferris, "Linear Network Theory", Charles E. Merrill Books Inc., 1962.

[25] M.E. Van Valkenberg, "Network Analysis", Prentice-Hall, Englewood Cliffs, New Jersey, 1955.

[26] William H. Middendorf, "Introductory Network Analysis", Allyn and Bacon Inc., Needham Heights, MA, 1965.

[27] Kishan Shenoi, "Digital Signal Processing in Telecommunications", Prentice-Hall, Englewood Cliffs, New Jersey, 1995.

[28] Members of Technical Staff, "Transmission Systems for Communications", Bell Telephone Laboratories, Holmdel, New Jersey, 1982.

[29] Vera Pless, "Introduction to Theory of Error-Correcting Codes", 2nd Edition, John Wiley and Sons, New York, NY, 1989.

[30] Shu Lin and Daniel J. Costello, "Error Control Coding: Fundamentals and Applications", Prentice-Hall, Englewood Cliffs, New Jersey, 1983.

[31] Hong Y. Chung and Massimo Sorbara, "Constellation Time Division Multiplexing for the 6 Mb/s ADSL", Supercomm/ICC '94, Vol. 2, pp. 821-825, May 1994.

[32] M. Robert Aaron, "Digital Communications, The Silent Revolution", IEEE Communications Society Magazine, Vol. 17, No. 1, pp. 16-26, Jan. 1979.

[33] G. David Forney, R.G. Gallager, G.R. Lang, F.M. Longstaff and S.U.Qureshi, "Efficient Modulation for Band-Limited Channels", IEEE J. on Selected Areas in Comm., Vol.2, No.5, pp. 632-646, Sept. 1984.

[34] Syed V. Ahamed, "Simulation and Design Studies of the Digital Subscriber Lines", Bell System Technical Journal, Vol. 61, pp. 1003-1077, 1982.

[35] Syed V. Ahamed and V. B. Lawrence, "Interoperability of Multiple Databases for the Design and Simulation of High-Speed Digital Subscriber Lines", RIDE-IMS '93, pp. 262-267, Apr. 1993.

[36] A. Reddy and S.V. Ahamed, "Simulation Study of CAP in High Bit Rate Asymmetrical Digital Subscriber Line (ADSL) Environment", ICCC '95, Seoul, S. Korea, pp. 729-733, Aug. 1995.

[37] Syed V. Ahamed and V. B. Lawrence, "Intelligent Networks: Architecture and Implications", Encyclopedia of Physical Science and Technology, Vol. 8, Academic Press, pp. 229-262, 1992.

[38] J.J. Werner, "Tutorial on carrierless AM/PM - Part I - Fundamentals and digital CAP transmitter", UTP Development Forum document, Sept. 29, 1991.

[39] J.J. Werner, "Tutorial on carrierless AM/PM - Part II - Performance of Bandwidth-Efficient Line Codes", Contribution to ANSI X3T9.5 TP/PMD Working Group, Austin, Feb. 16, 1993.

[40] J.B. Buchner, "Ternary Line Signals", 1974 Intl. Zurich Seminar on Digital Comm., Zurich, Switz., pp. F1(1) - F1(9), March 12-15, 1974.

[41] A. Croisier, "Introduction to Pseudo-Ternary Transmission Codes", IBM Journal Res. Dev., Vol. 14, pp. 354-367, Jul. 1970.

[42] J.B. Buchner, "Ternary Line Codes", Philips Telecommunications Review, Vol. 34, No. 2, pp. 72-85, Jun. 1976.

[43] N.Q. Duc and B.M. Smith, "Line Coding for Digital Data Transmission", Australian Telecommunication Research, Vol. 11, pp. 343-349, Nov. 1977.

[44] Gi-Hong Im and J.J. Werner, "Bandwidth-Efficient Digital Transmission up to 155 Mb/s over Unshielded Twisted Pair Wiring", ICC '93, Geneva, pp. 523-526, 1993.

[45] The Commercial Building Telecommunications Wiring Standard, EIA/TIA-568 Draft Standard, July 1991.

[46] M. Sorbara, J.J. Werner, and N.A. Zervos, "Carrierless AM/PM", AT&T Contribution T1E1.4/90-154, Sept. 1990.

[47] W.Y. Chen, G.H. Im, and J.J. Werner, "Design of Digital Carrierless AM/PM Transceivers", AT&T/Bellcore Contribution T1E1.4/92-149, Aug. 19, 1992.

[48] L.W. Adriaenssens, "Transmission Characteristic of a Category-3 UTP Cable (DIW)," AT&T Contribution to ANSI X3T9.4 TP/PMD Working Group, Oct. 15, 1991.

[49] D.L.Waring and J.W.Lechleider, "Digital Subscriber Line Technology Facilitates a Graceful Transition from Copper to Fiber," IEEE Commun. Mag., Vol. 29, pp. 96-103, Mar. 1991.

[50] Lower Layer Protocols and Physical Interfaces, DAVIC 1.0 specifications, part 8, June 1995.

[51] Gi-Hong Im and Jean-Jacques Werner, "Bandwidth-Efficient Digital Transmission over Unshielded Twisted-Pair Wiring", IEEE J. on Selected Areas in Comm., Vol. 13, No. 9, pp. 1643-1655, Dec. 1995.

[52] Syed V. Ahamed, Patricia L. Gruber and Jean-Jacques Werner, "Digital Subscriber Line (HDSL and ADSL) Capacity of the Outside Loop Plant", IEEE J. on Selected Areas in Comm., Vol. 13, No. 9, pp. 1540-1549, Dec. 1995.

[53] Werner Henkel, Thomas Kessler and Hong Y. Chung, "Coded 64-CAP ADSL in an Impulse-Noise Environment - Modeling of Impulse Noise and First Simulation Results", IEEE J. on Selected Areas in Comm., Vol. 13, No. 9, pp. 1611-1621, Dec. 1995.

[54] Walter Y. Chen, "Broadcast Digital Subscriber Lines", IEEE J. on Selected Areas in Comm., Vol. 13, No. 9, pp. 1550-1557, Dec. 1995.

[55] Babak Daneshrad and Henry Samueli, "A 1.6 Mbps Digital QAM System for DSL Transmission", IEEE J. on Selected Areas in Comm., Vol. 13, No. 9, pp. 1600-1610, Dec. 1995.

[56] Allen Gersho and Victor B. Lawrence, "Multidimensional Signal Constellations for Voiceband Data Transmission", IEEE J. on Selected Areas in Comm., Vol. 2, No. 5, pp. 687-702, Sept. 1984.

[57] Technical Reference TA-NWT-001210, "Generic Requirements for High-Bit-Rate Digital Subscriber Lines", Bellcore, Issue 1, October 1991.

[58] R.A. McDonald and C.F. Valenti, "Assumptions for Bellcore HDSL Studies", T1E1.4/89-066, Mar. 13, 1989.

GLOSSARY

19 AWG American Wire Gauge cable with a diameter of 0.9119 mm.
22 AWG American Wire Gauge cable with a diameter of 0.6426 mm.
24 AWG American Wire Gauge cable with a diameter of 0.5105 mm.
26 AWG American Wire Gauge cable with a diameter of 0.4039 mm.
2B1Q Two Binary in One Quaternary. A 4-level multilevel code standardized for basic rate ISDN.
2B+D Two B channels and one D channel. A standard for basic rate ISDN. Each B channel carries voice or data at 64 kbits/s and the D channel carries signaling and overhead at 16 kbits/s.
23B+D Twenty-three B channels and one D channel. A standard for primary rate ISDN.
3B2T 3 Binary and 2 ternary code.
4B3T 4 Binary and 3 ternary code.

A

Access Network Public Switched Network portion that connects premises distribution to the feeder network.
ADSL Asymmetric Digital Subscriber Line. A twisted pair access scheme, for transmission ranging from T-1 to DS-2 rates downstream or to the subscriber end and approximately half T-1 rate for upstream or to the CO. The maximum reach is approximately 18,000 feet for a 24 AWG cable pair.
AMI Alternate Mark Inversion code. It is standardized for T-1 transmission.
ATM Asynchronous Transfer Mode. Transport and switching of voice, data, image and video is done on the same network.

B

B6ZS Bipolar Six-Zero Substitution. Resembling to the high density bipolar code, it works like AMI code with the exception being, long string of zeroes. Substitutes six consecutive zeroes for the code word "A0VA0V", where A is non-zero symbol which adhere to the AMI constraint (polarities of consecutive non-zero symbols are opposite) and V signifies violation to the AMI rule. An example would be that a long string of 6 zeroes is encoded as "+0+-0-" or "-0-+0+" depending on the last non-zero symbol transmitted.
Bandwidth 1. **Total** - Bandwith achieved Theoretically.
2. **Effective** - Bandwidth achieved when cutoff points are applied to the filter responses.

BER Bit error rate. A ratio of error bits to the signal transmitted.
Bearer (B) Channel Information bearing channel for ISDN that provides digital path to a customer. It is standardized at 64 kbits/s.
B-ISDN Broadband ISDN. Digital network operating with ATM switching and very high data rates.

C

m-CAP Carrierless Amplitude and Phase Modulation with m constellation points.
CCITT Consultative Committee for International Telegraphy and Telephony. One of the four bodies that makes the International Telecommunications Union (ITU) which is a body of the United Nations.
CDDI Copper Distributed Data Interface. High speed Lan protocol (100 Mbps). Uses twisted pair cable as the physical medium for connections. It is used basically to form larger networks or backbones.
CO Central Office.
CSA Carrier Serving Area guidelines. Determine the limits of a DLC system, based on how far a 64 kbits/s service can reach based on non-loaded and non-repeatered UTP wires.

D

DAVIC Digital Audio-Visual Council.
dB Decibel. Logarithmic measure between the ratio of two powers. $dB = 10 \log(P_1/P_2)$.
dBm Decibel referenced with a power of one milliwatt.
Delta (D) Channel Generally a separate out-of-band maintenance channel. For basic rate ISDN it has a capacity of 16 kbits/s and for PRISDN the capacity is 64 kbits/s.
DFE Decision Feedback Equalizer.
DFT Discrete Fourier Transform.
Distribution Cable Cable plant that connects the feeder cable to drop wires or to the customer's premises.
DLC Digital Carrier Loop.
DS0 Digital Signal level Zero. A 64 kbits/s digital signal carrying voice.
DS1 Digital Signal level One. Twenty-four voice channels are packed in a 193 bit frame and transmitted at a 1.544 Mbits/s speed. The unframed version, also known as the payload is transmitted at 1.536 Mbits/s and uses 192 bits.
DSn Digital Signal level n . It carries multiples of DS0 signal.
DSL Digital Subscriber Line. End-to-End digital line.
DSP Digital Signal Processing.
DSV Digital Sum Variation. It is the difference between the largest and smallest RDS of all possible code words in a code.
Duty Cycle Ratio of operating time to total elapsed time for a system that operates at irregular intervals. Also the ratio of a scheme where it shows some characteristics in relation to the whole set of possible attributes

(e.g., the one's that appear in a code can have 75% duty cycle, meaning that out of every 4 bits 3 are ones.

E

EIA Electronic Industries Association.
ETHERNET (IEEE 802.3) Most popular LAN protocol in use today. Other LAN types include Token Ring, Arcnet, AppleTalk, FDDI, and CDDI. Basically four types of media are used today for Ethernet: Thin coax, Thick-Wire, Unshielded Twisted Pair and Fiber Optic. Ethernet media uses two main topologies: Star and Bus.
ETSI European Telecommunications Standards Institute.

F

FCC Federal Communications Commission. Regulatory body for telecommunications in the United States. One of its main objective is to govern the public radio frequency spectrum.
FDDI Fiber Distributed Data Interface. High speed (100 Mbps) LAN protocol that uses fiber as medium of transmission. Essentially it is used for creating large networks or backbone networks.
Feeder Network Part of WAN that connects the CO to the boundaries of the customer premises.
FEXT Far End Crosstalk.
FFT Fast Fourier Transform. Algorithms that have the tendency to reduce the computational complexity of a DFT.
FIR Finite Impulse Response filter.
FITL Fiber In The Loop. Employment of fiber equipment and cables in the distribution network.
FSLE Fractionally Spaced Linear Equalizer.
FTTC Fiber To The Curb.

G

Guard Band Band allocated between adjacent channels, which reduces interference from each other, e.g., crosstalk, ISI, etc.. Basically it is used in FDM type of multiplexing. TDM does not require such technique.

H

HDBk High Density Bipolar Codes.
HDSL High bit rate Digital Subscriber Line. It uses ISDN transport technology to carry DS1 signals.
HFC Hibrid Fiber to Coaxial.

I

IEEE Institute of Electrical and Electronic Engineers.
Impulse Noise It is generated by mechanical closing and opening of mechanical switches (these devices

generate an impulse). Other sources are thunder-storms, which carries heavy loads of electrons.
ISI Intersymbol Interference. If a pulse is transmitted down the loop, the phase nonlinearity will cause the pulse to spread out in time. In a pulse train, the smeared out pulses will overlap with each other causing ISI.
IIR Infinite Impulse Response filter.
IN Intelligent Network.
ISDN Integrated Services Digital Network.
ISO International Standards Organization.
ITU-T International Telecommunication Union. Telecommunication standardization division.

L

LAN Local Area Network.
LEC Local Exchange Carrier.
Low Pass Filter A specific frequency below which a filter will allow all frequencies to pass.

M

MAN Metropolitan Area Network.
mBnT Codes that map blocks of "m" binary bits into blocks of "n" ternary symbols.

N

NEXT Near-End Crosstalk.
N-ISDN Narroband ISDN. Comprises of basic rate ISDN and PRISDN.

O

ONU Optical Network Unit. Optical signals are converted to electrical format, such that they can be transmitted over coaxial or twisted pair lines. Usually it is used in a HFC type of network at the customer's premises.
OSI Open Systems Interconnection.

P

PAM Pulse Amplitude Modulation.
PCM Pulse Code Modulation.
PIC Polyethylene Insulated Conductor.
POTS Plain Old Telephone System. Basic analog telephone service, with 4 kHz of bandwidth. For new services to access same line as the POTS, should use a different spectrum.
PR-4 Partial Response Class-4 Code.
PRISDN Primary Rate ISDN (see 23B + D).
PSD Power Spectral Density.

Q

QAM Quadrature Amplitude Modulation.
QPSK Quadrature Phase Shift Keying.